AN ISOTOPIC ASSESSMENT OF OIL SANDS MINE SITE WATERS TO IMPROVE WATER MANAGEMENT PRACTICES

A Thesis Submitted to the
College of Graduate and Postdoctoral Studies
In Partial Fulfillment of the Requirements
For the Degree of Master of Science
In the Department of Civil, Geological, and Environmental Engineering
University of Saskatchewan
Saskatoon

By

Spencer Joseph Chad

PERMISSION TO USE

In presenting this thesis/dissertation in partial fulfillment of the requirements for a Postgraduate degree from the University of Saskatchewan, I agree that the Libraries of this University may make it freely available for inspection. I further agree that permission for copying of this thesis/dissertation in any manner, in whole or in part, for scholarly purposes may be granted by the professor or professors who supervised my thesis/dissertation work or, in their absence, by the Head of the Department or the Dean of the College in which my thesis work was done. It is understood that any copying or publication or use of this thesis/dissertation or parts thereof for financial gain shall not be allowed without my written permission. It is also understood that due recognition shall be given to me and to the University of Saskatchewan in any scholarly use which may be made of any material in my thesis/dissertation.

DISCLAIMER

Reference in this thesis/dissertation to any specific commercial products, process, or service by trade name, trademark, manufacturer, or otherwise, does not constitute or imply its endorsement, recommendation, or favoring by the University of Saskatchewan. The views and opinions of the author expressed herein do not state or reflect those of the University of Saskatchewan, and shall not be used for advertising or product endorsement purposes.

Requests for permission to copy or to make other uses of materials in this thesis/dissertation in whole or part should be addressed to:

Head of the Department of Civil, Geological, and Environmental Engineering
University of Saskatchewan
3B48 Engineering Building, 57 Campus Drive
Saskatoon, Saskatchewan S7N 5A9 Canada

OR

Dean
College of Graduate and Postdoctoral Studies
University of Saskatchewan
116 Thorvaldson Building, 110 Science Place
Saskatoon, Saskatchewan S7N 5C9 Canada

ACKNOWLEDGEMENTS

I would like to begin by thanking my supervisors Dr. S. Lee Barbour and Dr. Jeffrey McDonnell, without whom none of this work would have ever been possible. I have been so incredibly lucky to have had such well-established and respected individuals in their fields to guide me along this journey. I have learned so much from both you, of which has gone far beyond the world of academia and carried over into both my professional and personal life.

Lee – I cannot fully express how grateful I am of you and your efforts to get me to the finish line of my M.Sc. I am not sure what convinced you to take me on as a graduate student when we first met in your office, or how you never gave up on me after all these years, but thank you for taking a chance on me and sticking with me to the end. Your involvement over the final few months of this process, despite a few curve balls, has been such a testament to your strength as a person and dedication to your students.

Jeff – thank you for agreeing to co-supervise me with Lee and welcoming me into your lab group. Your experience and insight as a researcher, teacher, scientist, and author has been invaluable in the creation of this thesis. I deeply appreciate you agreeing to step into the role you did without hesitation over the past few months and see me to the end of my M.Sc journey.

Thank you to Syncrude Canada Ltd. for making this project possible and all those that contributed in various forms such as Dallas Heisler, Warren Zubot, Jessica Piercey, Richard Kao, and Mohamed Salem to name a few.

Thank you, Dr. John Gibson, for sharing you Athabasca River isotope data with me as part of this work and for being willing to answer questions relating to how “isotopes work” as I learned along the way.

Thank you, Dr. Sean Carey for sharing your Base Mine Lake water balance data to be included in this study. This work would not have been nearly as solid without it.

Thank you to my family and friends for their support over the years and for always asking how the thesis is going – despite my curt or cringe worthy responses.

And finally, thank you to my wife Stephanie. I think I started my M.Sc while we were still just dating and here we are now three years married. Your patience and support over all these years has been incredible. You have always been there with the right words of encouragement despite many periods of self-doubt and frustration.

ABSTRACT

Current oil sands mining technology requires approximately 2 m^3 in the production of 1 m^3 of crude oil. This water demand has resulted in massive volumes of process-affected waters being stored on-site – a volume that is currently not well quantified, though estimated to be in in the order of billions of m^3. A site wide water balance must be closed at each mine in order to effectively manage the on-site storage and reuse of process-affected waters, in addition to planning for future remediation and release of this water following site closure. Oil sands mining operators have identified the constantly evolving nature of both operational water demands and the tailings management infrastructure as key challenges preventing accurate closure of a site wide water balance.

Stable isotopes of oxygen and hydrogen (^{18}O and ^{2}H) have been widely used as tracers to close water balances of natural reservoirs. To date, their application to mine water containment systems, such as tailings management facilities, has not yet been implemented. This study demonstrates the use of ^{18}O and ^{2}H as tools to track key components of the water balance associated with the Mildred Lake mine, operated by Syncrude Canada Ltd in Northern Alberta. There, process affected waters are stored in interconnected tailings ponds referred to as the recycle water (RCW) circuit, with approximately 200 million m^3 of water accessible for reuse in the extraction and transport of bitumen. This thesis characterizes the primary mechanisms of each water balance component contributing to the seasonal and inter-annual evolution of isotopic signatures of the RCW circuit and an end pit lake located at Mildred Lake mine. The thesis uses isotopic "finger-printing" of contributing water sources to characterize each part of the system. Isotope mass balance techniques were implemented to estimate evaporative loss from these systems and are compared to traditional methods of estimating evaporation (*e.g.,* Penman combination equation and eddy covariance towers).

This study found that isotopic seasonality of both the RCW circuit and the end pit lake were muted compared to natural systems within the region due to the contribution of large volumes of highly enriched pore water to tailings pond water stores as a result of tailings settlement. Samples collected from tailings ponds showed a systematic shift

towards greater isotopic depletion during the ice-on period. I hypothesized that this shift occurred as a result of fractionation during ice formation in addition to mixing with process water released from tailings. Such mechanisms appeared to contribute to the observable spring depletion of the RCW circuit in addition to depleted snowmelt during the spring freshet.

The seasonal variations in the isotopic signatures of individual tailings ponds were consistent with differences in water management between ponds. I then used an integrated isotopic signature as a proxy for the entire RCW circuit in isotope mass balance modelling scenarios. The proportion of inflow lost to evaporation from the RCW circuit was calculated as a decimal ratio using isotope mass balance modelling. The evaporation/inflow ranged from 0.11 to 0.22 over a five-year period, consistent with a high through-flow system with low residence time. These ratios correspond to 67–133 mm yr^{-1} of inflow water lost to evaporation from the RCW circuit based on estimated volumes of the water balance inputs.

A simplified isotope mass balance model of the RCW circuit was used to estimate evaporative losses based on observable temporal isotopic enrichment during the open water period and assuming all other outflows of the water balance were zero. Using this model evaporation rates were found to range from 418 to 931 mm yr^{-1}, while evaporation rates measured on-site using eddy covariance ranged from 350-520 mm yr^{-1}. The difference between the isotope mass balance and eddy covariance results suggest a contribution of highly enriched tailings pore water to the overall enrichment of the RCW circuit in addition to open water evaporation.

The isotope mass balance model was also used to simulate the evolution of the daily isotopic signature of a highly monitored demonstration end pit lake. The simulated pattern of isotope evolution was used to obtain an optimized estimate of lake evaporation. This estimate was then compared to a measured water balance over a four-year period. The model showed good agreement when ^{18}O was used as the tracer; however, when ^{2}H was used as the tracer the model consistently under predicted open water enrichment - likely due to evaporative fractionation effects.

This thesis represents the first study that we are aware of that applies isotope mass balance techniques to an engineered system within the Alberta oil sands region. Our

results highlight the potential value of using stable isotope tracers to aid in on-site water management of tailings ponds as well as helping to improve our understanding of the transport and distribution of water moving through mine closure landscapes.

DEDICATION

In one drop of water are found the secrets of all the endless oceans — Khalil Gibran

To my wife Steph. I did it!

TABLE OF CONTENTS

LIST OF TABLES

LIST OF FIGURES

Chapter 1: Introduction

The oil sands region of Northern Alberta, Canada, contains the world's third-largest proven crude oil reserve at roughly 168 billion barrels (27 billion m^3 crude oil) (Sauchyn et al., 2015). Oil sands extraction has been a highly controversial topic over the past few decades due to potential environmental impacts from operations and uncertainty regarding future mine closure. A key aspect of these impacts is the potential legacy associated with large stores of oil sands process affected waters (OSPW) on site. For example, the Mildred Lake Mine site operated by Syncrude Canada Ltd. (SCL) currently requires approximately 2 m^3 of fresh or "raw" water to be imported from the Athabasca River for every 1 m^3 of crude oil produced. Currently, SCL operates as a zero discharge facility, as no policy exists for the release of water to the surrounding environment. This lack of discharge has led to an OSPW inventory of approximately 1.7 Gm^3 stored on-site since operations began over 40 years ago. This volume grows each day that production continues. Of this OSPW inventory, about 200 Mm^3 is free water with the remainder contained as tailings pore water (W. Zubot, personal communication. 2019).

This large inventory of OSPW highlights the importance of tracking and managing large volumes of water during both operations, as well as following mine closure. Imported water that is not evaporated from ponds or chemically consumed or released as steam within the extraction process is added to the existing inventory of OSPW. In addition to these extraction-derived waters there is also the issue of accumulation of site-wide water from dewatering operations and precipitation. Together, these waters are referred to as the recycle water (RCW) circuit, in which water released from extraction operations is eventually recycled back to bitumen production facilities. This recycling of OSPW is essential to operations, as it limits the amount of imported water required from the Athabasca River.

Accounting of on-site water storage and transport is difficult without accurately quantifying key water balance components of the RCW circuit water balance. Mining operators have identified evaporation and meteoric water input as two water balance components that require better quantification methods in order to improve the accuracy of the RCW Cicuit. Mines will also eventually be responsible for the remediation of OSPW

and its return to the natural environment. Closure strategies such as the re-establishment of site-wide drainage and the release of water to the Athabasca river will require an understanding of the rates, pathways, and distribution of water moving through the closure landscape. This study assesses the feasibility of isotope tracers as an additional tool to improve water balance knowledge for both the RCW circuit and an end pit lake.

The only water currently released from the RCW circuit to the environment is through evaporation. While many methods of estimating evaporation from reservoirs exist, they may not be directly applicable to tailings facilities storing OSPW. This is because traditional methods of estimating evaporation rely primarily on climatic parameters such as temperature, humidity gradients, and wind speed. These methods for estimating evaporation fail to incorporate parameters of engineered oil sands tailings facilities such as the chemical makeup of process water and surficial bitumen mats that may affect evaporation flux.

Studies involving stable isotopes of oxygen and hydrogen as water tracers have primarily been used in gauged watersheds for hydrograph separation (see Buttle, 1994; Klaus and McDonnell, 2013 for review), transit time modelling (Harman and Kim, 2014; Jasechko et al., 2016; Tetzlaff et al., 2018) and more recently vegetation source partitioning (Evaristo et al., 2015). Traditional methods have long been established for isotope tracer studies to investigate specific lake parameters (Dincer, 1968; Zimmerman and Ehhalt, 1970; Gonfiantini, 1986). More recently, stable isotopes have been used in ungauged basins for estimates of water balance studies when hydrometric data is limited (see Gibson et al., 2016a, Gibson et al., 2016b for a comprehensive review of methods).

The progress in isotope hydrology within natural systems has been substantial; however, to date, the adaption of these approaches to mine-affected waters has been minimal. There have been some previous studies that have applied isotope tracer methods at mine sites (Huang et al., 2015; Barbour et al., 2016; Dompierre and Barbour, 2016; Baer et al., 2016). These recent studies have focused on the chemical transport through waste rock piles and reclamation covers, the influence of tailings settlement within an end-pit lake, and isotopic fingerprinting mine site waters.

No studies that I am aware of have yet attempted to apply an isotope tracer method directly to an operating recycle water circuit water balance at an oil sands mine

site. If it were possible, such tracing could provide crucial estimates of imported water losses to improve the efficiency of water usage and management in an industry where production and extraction processes are directly linked to the import and recycling of water.

1.1 Research objective

This study attempts to characterize meteoric water input and evaporative loss contributing to the RCW circuit water balance through the use of the stable isotopes of oxygen and hydrogen (^{18}O and ^{2}H) as water tracers. The purpose of this work is to provide new techniques with the potential to improve the accuracy of site-wide water balances at an oil sands mine site. Stable isotope tracers provide an "in situ" tracer method for quantifying the contribution of various water sources and estimating evaporative losses of a reservoir by measuring the ratio of heavy to light isotopes making up the water molecules themselves. This isotope ratio is controlled mainly by the mixing of isotopically distinct water sources and phase changes of water resulting in fractionation through the water circuit.

I explore the primary controls on the unique isotopic signature of OSPW derived from cooling tower blowdown water in addition to the contributions from river import, meteoric water input, tailings dewatering, and open water evaporation. Water samples were collected at varying timescales in the period 2012 to 2018 to establish an inventory of isotopic signatures of site wide waters at this oil sands mine site. Isotope mass balance modelling was then implemented based on observable seasonal and inter-annual patterns of spring depletion and summer/ fall enrichment of the isotopic composition of the RCW circuit. Isotope mass balance modelling was also applied to the first demonstration end pit lake within the oil sands region, to investigate how isotope tracers may be used to track the hydrological evolution of reclaimed tailings landscapes as they evolve from OSPW signatures to freshwater chemical compositions.

The specific research objectives of the study were to:

1. Characterize the temporal evolution of ^{18}O and ^{2}H within the RCW circuit at Syncrude's Mildred Lake and Aurora mine sites;

2. Develop an interpretation of the controls on the isotopic signature associated with fresh input water or extraction waters as well as evaporation;
3. Develop and test various isotope mass balance models to estimate evaporative losses as applied to the overall RCW circuit as well as a demonstration end pit lake; and
4. Provide insight on future development of isotope tracer techniques to be applied at the industry level.

The overarching goal was to determine how isotope tracer techniques may be further developed and applied by the oil sands industry. This work was aimed further at providing insight on techniques that may improve water management and usage on-site, as well as planning for future mine closure involving the development of reclamation landscapes at operational oil sands mine sites.

1.2 Layout of thesis

This thesis contains a total of five chapters. Chapter 2 is a literature review to provide an introduction to oil sands mining operations, critical concepts in isotope hydrology relevant to this study, a summary of recent studies applying isotope tracers at mine sites, and a review of contemporary studies implementing isotope tracer techniques used to develop isotope mass balance techniques within this study.

Chapters 3 and 4 have been written as stand-alone papers, which will be further developed for possible journal submission following the completion of this thesis. Chapter 3 is a continuation of the work initiated by Baer et al. (2016). The chapter focuses on quantifying the seasonal and inter-annual patterns of the RCW circuit based on a high-frequency water-sampling program building on the initial isotope characterization of site-wide waters undertaken by Baer et al. (2016). The work investigates the effects of meteoric water inputs, evolution and impacts of cooling tower blowdown released to the RCW circuit, evaporative enrichment during the open water period, and input of tailings pore water released during settlement.

Chapter 4 builds upon the results of Chapter 3 by implementing isotope mass balance techniques to quantify evaporative losses from the RCW circuit and an end pit lake (Base Mine Lake) at Mildred Lake mine. Evaporation rates for the Mildred Lake

mine are initially estimated based on the Penman combination equation (Penman, 1948) used to estimate evaporation from a reservoir, as well as eddy covariance tower measurements undertaken by Professor Sean Carey of McMaster University. These evaporation rates are compared to rates calculated using several forms of the isotope mass balance equation. A separate model of daily evaporation and the associated seasonal evolution of the isotopic signature of water from Base Mine Lake (an end pit lake) was also developed and used to compare with a measured water balance for the lake.

Chapter 5 summarizes the overall conclusions from Chapters 3 and 4 and provides future recommendations for the development of stable isotopes of water as tracers to improve water management at oil sands mine sites.

1.3 References

Baer, T., Barbour, S. L., & Gibson, J. J. (2016). The stable isotopes of site-wide waters at an oil sands mine in northern Alberta, Canada. *Journal of Hydrology*, *541*, 1155-1164.

Barbour, S. L., Hendry, M. J., & Carey, S. K. (2016). High-resolution profiling of the stable isotopes of water in unsaturated coal waste rock. *Journal of Hydrology*, *534*, 616-629.

Buttle, J. M. (1994). Isotope hydrograph separations and rapid delivery of pre-event water from drainage basins. *Progress in Physical Geography*, *18*(1), 16-41.

Dincer, T. (1968). The use of oxygen 18 and deuterium concentrations in the water balance of lakes. *Water Resources Research*, *4*(6), 1289-1306.

Dompierre, K. A., & Barbour, S. L. (2016). Characterization of physical mass transport through oil sands fluid fine tailings in an end pit lake: a multi-tracer study. *Journal of contaminant hydrology*, *189*, 12-26.

Evaristo, J., Jasechko, S., & McDonnell, J. J. (2015). Global separation of plant transpiration from groundwater and streamflow. *Nature*, *525*(7567), 91.

Gibson, J. J., Birks, S. J., Yi, Y., Moncur, M. C., & McEachern, P. M. (2016a). Stable isotope mass balance of fifty lakes in central Alberta: Assessing the role of water balance parameters in determining trophic status and lake level. *Journal of Hydrology: Regional Studies*, *6*, 13-25.

Gibson, J. J., Birks, S. J., & Yi, Y. (2016b). Stable isotope mass balance of lakes: a contemporary perspective. *Quaternary Science Reviews*, *131*, 316-328.

Gonfiantini, R. (1986). Environmental isotopes in lake studies. *Handbook of environmental isotope geochemistry*, *2*, 113-168.

Harman, C. J., & Kim, M. (2014). An efficient tracer test for time-variable transit time distributions in periodic hydrodynamic systems. *Geophysical Research Letters*, *41*(5), 1567-1575.

Huang, M., Hilderman, J. N., & Barbour, L. (2015). Transport of stable isotopes of water and sulphate within reclaimed oil sands saline–sodic mine overburden. *Journal of Hydrology*, *529*, 1550-1561.

Jasechko, S. (2016). Partitioning young and old groundwater with geochemical tracers. *Chemical Geology*, *427*, 35-42.

Klaus, J., & McDonnell, J. J. (2013). Hydrograph separation using stable isotopes: Review and evaluation. *Journal of Hydrology*, *505*, 47-64.

Sauchyn, D. J., St-Jacques, J. M., & Luckman, B. H. (2015). Long-term reliability of the Athabasca River (Alberta, Canada) as the water source for oil sands mining. *Proceedings of the National Academy of Sciences*, *112*(41), 12621-12626.

Tetzlaff, D., Piovano, T., Ala-Aho, P., Smith, A., Carey, S., Marsh, P., . . . Soulsby, C. (2018). Using stable isotopes to estimate travel times in a data-sparse Arctic catchment: Challenges and possible solutions. *Hydrological Processes*, *32*(12), 1936-1952.

Zimmermann, U., & Ehhalt, D. H. (1970). Stable isotopes in study of water balance of Lake Neusiedl, Austria. *Isotope hydrology*, 129-138.

Chapter 2: Literature Review

This chapter introduces oil sands mining operations, a review of key concepts relating to isotope hydrology necessary for this study, and key literature used for the development of this study. It ends with an overview of the research gap this study attempts to fill.

2.1 Mine site overview

The purpose of this section is to provide a foundational understanding of oil sands mining operations in Northern Alberta. A brief summary of the main aspects of oil sands mining is provided, including regional geology, extraction and upgrading of bitumen, tailings management, and water import, usage, and management on site. These details have been provided to aid the reader in understanding the crucial role that water, both imported and recycled, plays in the recovery of bitumen. It also provides a context for the difficulties of managing and storing such massive volumes of water associated with oil sands mining.

2.1.1 Mine site geology

Oil sands are found within the McMurray Formation of Northern Alberta, itself composed of shale, sandstone, and the bitumen-impregnated sand (Baer, 2014). The McMurray Formation is overlain by shale and sandstones from the Cretaceous Clearwater Formation and a thin layer of sandstone from the Grand Rapids Formation. The surficial soils overlying the bedrock include glacial deposits overlain by organic and muskeg layers (Isaac et al., 1982).

The ore itself contains an average percent composition of 12 % bitumen; 3 to 6 % water; and 84-86% solids, made up of quartz, silts, and clay. The major clay components are composed of 40-70% kaolinite, 28-45 % illite, and 1-15 % montmorillonite (Chalaturnyk et al., 2002). Chemical properties of the clays play an important role in the formation of gel-like structures necessary for the hot water extraction process discussed further in the following section.

2.1.2 Mining and extraction

Mining of the oil sands involves the removal of muskeg and overburden material to reach the oil sands deposit approximately 40-60 m below the surface (Scales, 1999). Once excavated, the ore is transported to extraction facilities through a combination of large shovel excavators, haul trucks, and hydrotransport technology (Syncrude Canada Ltd., 2007).

Separation of bitumen from mineral solids involves a hot water extraction process involving conditioning, separation, and treatment of the recovered froth. Oil sands are delivered to crushers and then conveyed to a cyclofeeder, which converts the ore to slurry through the addition of hot water and sodium hydroxide. This slurry is then transported to the extraction plant by pipeline. This hydrotransport method allows for the conditioning of the oil sands within the pipeline before bitumen extraction (McDonell et al., 1995).

Conditioning within the pipeline results in the initiation of bitumen froth. The pipeline then feeds into tumblers and primary settling vessels producing bitumen froth — operating temperatures of water range from 35°C during hydrotransport to 75°C in the tumblers (Zubot, 2010).

The final step of the extraction is the treatment of the bitumen froth. Bitumen froth contains bitumen, water, and solids and treatment is required to remove as much water and solids as possible before upgrading. Bitumen froth is diluted with naptha to reduce the viscosity of bitumen and to enhance the difference in density between water and bitumen (Zubot, 2010). The diluted bitumen then goes through a series of centrifugation and settling steps. Finally, the diluted bitumen is distilled for naptha recovery and reuse, and the dried naptha-free bitumen is sent to the upgrading plant.

The high demand for water necessary in hydrotransport and extraction is only feasible through the use of recycled water. Without the conservation and reuse of recycled water within the system, production would be limited due to source- and containment issues.

2.1.3 Upgrading and cooling towers

Raw bitumen is converted to synthetic crude oil for processing in downstream refineries. Upgrading of bitumen involves separating bitumen into various hydrocarbon fractions through distillation, conversion of distilled bottoms into lighter molecular weight materials by fluid coking (carbon rejection) and LC Fining® hydroprocessing (hydrogen addition), and hydrotreating the distillates to remove nitrogen and sulphur species present (Zubot, 2010).

Natural gas fired boilers are used to generate the steam required for the production of hydrogen. The hot water used in extraction is produced indirectly from the heat generated during steam production. In an effort to conserve water, open circulating cooling towers are employed to reduce the water temperatures allowing for reuse in the cooling circuit. Hot water is piped into the cooling tower unit and dispersed onto fill media providing maximum surface area for the water to collect. Evaporative cooling is used to reduce water temperatures. As the hot water interacts with circulating warm air within the cooling tower, a portion of the water evaporates, removing heat from the water. The cooled water is collected in a basin at the base of the cooling tower and subsequently passed through process units or vessels requiring cooling. This reheated water is then returned back to the cooling tower to be cooled and recirculated.

The make-up water within the cooling tower circuit contains dissolved impurities, which continue to concentrate in repeated cycles through the cooling towers. If the concentrations become too high, it can lead to scaling and corrosion of equipment, negatively affecting the efficiency of the upgrading process. In order to mitigate this increased concentration, a portion of water from the cooling basin is replaced with fresh water. Freshwater addition also balances the losses from evaporation. The removed water is referred to as the blowdown water stream. This blowdown water joins the recycle water circuit, supplying water demand for extraction purposes.

The efficiency of cooling towers is evaluated by the ratio of the concentration of a dissolved species in the blowdown water to the make-up (fresh) water. This ratio is referred to as the cycles of concentration (COC). If the COC is ten or greater, performance is rated as high, and if it is two or less, it is rated as very poor (Zubot, 2010). The amount of water released as blowdown and thus how many cycles make-up water makes in the circuit to maintain low levels of dissolved impurities is related to the COC.

The upgrader requires freshwater, also known as raw water, for steam generation and to provide make up water for the cooling towers. The raw water requirement is met by diverting freshwater from the Athabasca River. This river import makes up the remaining fraction of water used in the mining process that cannot be utilized from recycled water.

2.1.4 Tailings management

The extraction of bitumen results in the accumulation of sand, silt, and clay particles, as well as a small amount of unrecovered bitumen referred to as tailings (Zubot, 2010). The tailings are hydraulically transported to containment facilities following extraction using recycled water — also referred to as oil sands process affected water (OSPW). Tailings on site are classified based on the composition of particles and water content. Sand tailings refer to those that are composed primarily of sand composite and will settle out from fluid tailings resulting in quick dewatering. Sand tailings are stored primarily in the tailings facility referred to as Southwest Sand Storage (SWSS).

Fluid fine tailings (FFT) are those composed of fine-grained materials (silts and clays) that have recently been discharged to tailings ponds. FFT generally has high water content, resulting in fluid-like properties and long settling times due to its small particle size. The water content of these tailings gradually decreases over several years, after which they are referred to as mature fine tailings. Mature fine tailings still have water contents around 65-70 % by weight resulting in a thick “yogurt” type consistency (Zubot, 2010). Tailings ponds referenced further in this study are generally composed of both FFT and mature fine tailings. Composite tailings refer to tailings created by mixing sand tailings, mature fine tailings, and a dewatering coagulant. The coagulant allows for the development of structurally stable material that can be used in construction on-site (Zubot, 2010).

Recycled water is used for the hydraulic transport and deposition of tailings to the above-ground tailings management facilities. During the deposition of tailings, coarser solids settle out quickly, forming the perimeter dykes and sand beaches. Oil sands process-affected water and finer particle fractions enter the tailings basin and begin to settle. During the consolidation of the FFT, water is released from the pore space,

forming a clarified layer of OSPW at the surface available for reuse in extraction, upgrading, and transport.

2.1.5 Recycle water circuit

The RCW circuit is crucial to Syncrude's water management, as no policy exists to release current OSPW stores to the environment. The RCW circuit is used to limit the need to import additional water to the site for tailings management. Currently, 80-85% of the water associated with oil sands mining processes is made up of recycled water.

The collection and return of OSPW from tailings ponds is a primary activity for managing tailings and improving water use efficiency. Appropriate management involves the collection and pumping of OSPW to a centralized location — the recycle water pond — from which the extraction plant is supplied. Water is recycled from tailings ponds through the collection of OSPW from the free water within the tailings containment structures.

A conceptual model for the RCW circuit is shown in *Fig. 2.1*. The recycling of OSPW throughout the RCW circuit should result in mixing across the various tailings basins, creating similar water chemistry and isotopic composition in all basins. However, slight variations of isotopic composition between tailings ponds may arise due to varying atmospheric conditions (humidity and temperature) affecting fractionation.

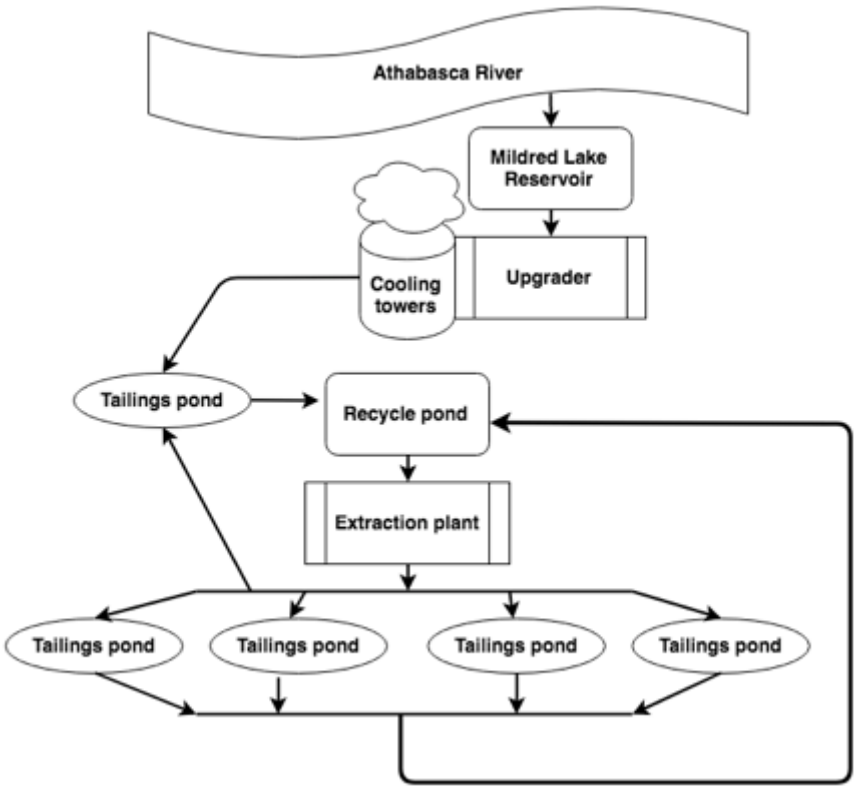

Figure 2.1 Conceptual model of import water and circulation between interconnected tailings ponds comprising the recycle water circuit.

2.1.6 Athabasca River "raw" water import

The Athabasca River basin is one of seven major river basins in Alberta. Originating within the Columbia ice fields of the Rocky Mountains, the Athabasca River flows over 1400 km in a northeasterly direction before ending at Lake Athabasca. It is the longest river in North America that is unencumbered by dam structures (Jasechko et al., 2012).

Discharge rates of the Athabasca River vary seasonally, with average weekly flows ranging from 88 to over 3500 $m^3 s^{-1}$. Lower flows occur from January to March (90 – 250 $m^3 s^{-1}$) with the highest flows associated with spring melt (1000-3500 $m^3 s^{-1}$), which persist through summer and decline to an average of 500 $m^3 s^{-1}$ by October (AEP, 2015).

Estimated average withdrawal based on oil sands licenses from the Athabasca River is 103 million $m^3 yr^{-1}$, of which SCL draws an average of 40 million $m^3 yr^{-1}$. The oil sands withdrawal licenses make up approximately 71% of the total water withdrawal in

the Athabasca River Basin (AEP, 2015). Imported water for oil sands production has never exceeded the licensed allocation volume of 430 million m^3 yr^{-1} (AEP, 2015) and the demand for water by the oil sands is constant regardless of the discharge rates of the river. It is important that oil sands water demands do not alter seasonal flow rates of the Athabasca River as First Nations and Metis communities rely on the Athabasca River and the surrounding area for traditional activities. The river is an important navigational route, and altering flow rates can affect the ability to operate small watercrafts; particularly in fall, when low flows can persist for weeks or months.

One goal of sustainable mining is to limit the effects on the surrounding environment. Therefore, studies to improve knowledge surrounding mine site water management and usage efficiency are essential in managing or reducing the water import demands from the Athabasca River in the oil sands region. No water withdrawn from the Athabasca River for oil sands mining processes is returned to the river. Therefore, all water extraction for mining is a net loss for the river basin water balance.

2.1.7 End pit lakes

End pit lakes are a mine closure strategy in which mined out pits are used for water storage, passive water treatment and, in some cases, for tailings storage when constructing a closure landscape. End pit lake design involves adding a surface water cap of freshwater to be placed over the stored tailings. The intent of the water cap is to allow for the development of natural biogeochemical processes associated with aquatic ecosystems to break down the contaminants associated with process-affected waters over time (COSIA, 2012). The advantages of the end pit lake strategy are that it addresses tailings storage issues, reclamation of the in-pit, as well as reintegration of process-affected water with the surrounding landscape. Once capped, the end pit lake will be an artificial lake intended to evolve to resemble a natural lake over time through naturally occuring biogeochemical processes.

Base Mine Lake (BML) is the first demonstration end pit lake within the oil sands region and is located on Syncrude's Mildred Lake mine site. The purpose of the BML demonstration project is to improve industry understanding of end pit lake design and operation — specifically, the hydrological and biochemical evolution of these end pit

lakes from OSPW dominated chemical signatures to those consistent with natural freshwater lakes within the region.

The tailings placed within BML prior to capping consisted of fluid fine tailings that were dredged from the Mildred Lake Settling Basin from 1994 to 2012. A total volume of 1.9 Gm^3 of fluid fine tailings was deposited at the in-pit to a maximum depth of 45 m (Dompierre, 2016). Freshwater was pumped from Beaver Creek Reservoir to provide the freshwater cap for BML at rates of 6.7 to 7.7 $Mm^3\ yr^{-1}$. Over time, water liberated from tailings settlement adds to the overall storage of the water cap - as fluid fine tailings are expected to settle from 45 to 35 m (Syncrude, 2013).

2.2 Stable isotope tracing of water

This section provides an introduction to aspects of isotope hydrology relevant to the work performed within this study. Governing equations and definitions of relevant parameters relating to the isotopic assessment and isotope mass balance models in each study are outlined within their respective chapters.

Throughout this thesis, the term "stable isotope tracers" or "stable isotopes" refers specifically to the stable isotopes of oxygen ^{18}O, and hydrogen ^{2}H. Unless noted otherwise, ^{18}O and ^{2}H will be referred to succinctly as isotopes. These isotopes are considered near ideal tracers of the hydrologic cycle based on their natural distribution within the water cycle, conservative nature, and that they are found directly within the water molecule (Edwards et al., 2004). The physical behaviour of water molecules containing the less abundant, or also commonly referred to as "heavier" or "rare" isotopes (*e.g.* $^{1}H^{1}H^{18}O$, $^{1}H^{2}H^{18}O$) results in systematic isotopic variations of observable waters throughout the hydrologic cycle when compared to the more abundant (*i.e.* “light” or “common”) species ($^{1}H^{1}H^{16}O$).

Stable isotope species do not decay over time. As a result, the abundance patterns of rare isotopes versus common isotopes are governed by physiochemical processes (Criss, 1999). Again, these governing factors demonstrate the power of stable isotopes as tracers within the hydrologic cycle as the isotopic abundance ratios found within waters are governed by either mixing or phase change processes, and do not require quantification of natural isotopic decay rates (Mook, 2006).

2.2.1 Delta Notation

Natural variations in the abundance of the stable isotopes are normally quite small and are therefore not useful for comparative analysis (Criss, 1999). It is general practice to report a measured difference in the isotopic composition of a sample (*x*) and an accepted standard (*std*) in terms of dimensionless δ-values (delta-values), defined by:

$$\delta_x = 1000 \frac{R_x - R_{std}}{R_{std}} \qquad (Eq.\,2.1)$$

where *R* represents the ratio of the rare to abundant isotope species within a sample (*e.g.* ${}^{18}R = \frac{{}^{18}O}{{}^{16}O}$).

The primary reference measurement standard is VSMOW (Vienna Standard Mean Ocean Water), as defined by Craig (1961) and Gonfiantini (1978).

Therefore δ-values within this study are reported based on the following relationships:

$$\delta\,{}^{2}H = 1000\left[\frac{\left(\frac{{}^{2}H}{{}^{1}H}\right)_x}{\left(\frac{{}^{2}H}{{}^{1}H}\right)_{VSMOW}} - 1\right] \qquad (Eq.\,2.2)$$

and

$$\delta\,{}^{18}O = 1000\left[\frac{\left(\frac{{}^{18}O}{{}^{16}O}\right)_x}{\left(\frac{{}^{18}O}{{}^{16}O}\right)_{VSMOW}} - 1\right] \qquad (Eq.\,2.3)$$

The factor of 1000 is used to convert the δ-values to per mil (‰).

2.2.2 Isotope fractionation of evaporating waters

Isotopic fractionation refers to the separation of a sample into parts that have different ratios of "heavy" (higher mass) and "light" (lower mass) isotopes than the original ratio. *Figure 2.2* is an example of fractionation occurring during evaporation

from a body of water resulting from the phase change of water from liquid to vapour. The lighter part is referred to as being depleted, whereas the heavier fraction is referred to as enriched. This partitioning results in the differences of physical and chemical behaviours associated with individual isotopic compositions of the same molecule.

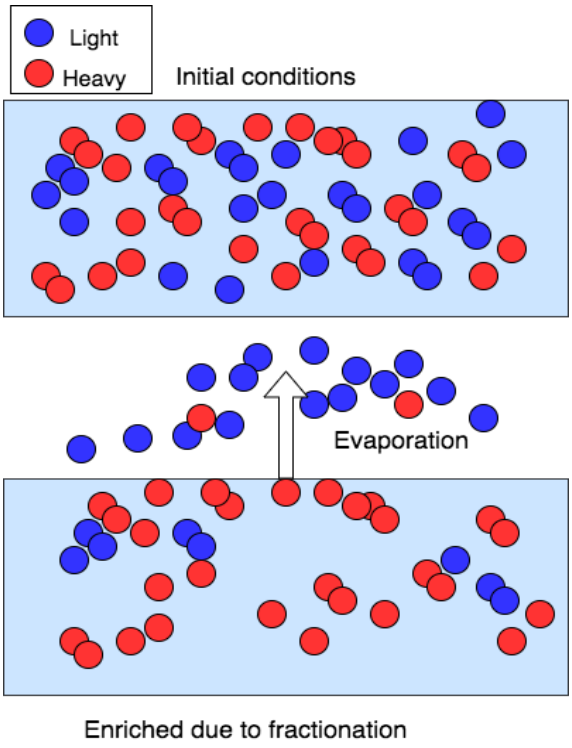

Figure 2.2 Process of evaporation enrichment for a water body as a result of isotopic fractionation.

There are three types of fractionation processes: equilibrium fractionation (or thermodynamic fractionation), kinetic (or transport fractionation), and non-equilibrium fractionation (Mook, 2006; Gat, 2010). Fractionating processes are mass dependent based on a quantitative difference in the degree of isotopic fractionation directly related to the mass difference of atoms or molecules involved. This mass dependency is exhibited with regards to hydrogen isotopes where fractionation effects are larger by almost an order of magnitude compared to oxygen isotopes based on an isotopic species mass ratio of 2:1 for hydrogen compared to 18:16 for oxygen.

Kinetic fractionation is the result of an irreversible or one way physical or chemical mass transport process. Absorption or diffusion of gases is an example that will result in kinetic fractionation. The binding energies of the original compound largely determine the effects of kinetic fractionation. For a physical process, the lighter isotopes

have a higher velocity and lower binding energy, and in chemical processes, lighter isotopes will react more rapidly than the heavy isotopes (Criss, 1999).

Equilibrium fractionation is the result of the isotope effect arising from a reversible (thermodynamic) equilibrium reaction. In this case, the total mass and isotope transport will be equal in both directions. This process can be observed when liquid water and water vapour become equilibrated within a closed volume (Mook, 2006; Gat, 2010).

In nature isotopic fractionation processes are often not entirely kinetic (one-way process) or equilibrium (no net mass transport) processes; therefore, the process of non-equilibrium fractionation arises (Mook, 2006). Evaporation from a lake is an example of non-equilibrium fractionation, as water vapour will condense (two-way mass transfer) and equilibration between the lake and atmosphere is not reached based on net evaporation.

2.2.3 Meteoric water line

The Global Meteoric Water Line (GMWL) is the linear relationship between the global isotopic compositions of precipitation when plotted in dual-isotope space ($\delta^{18}O$ versus $\delta^{2}H$) and can be expressed by the following equation developed by Craig (1961):

$$\boldsymbol{\delta^{2}H} = 8 \cdot \delta^{18}O + 10 \quad (‰\ SMOW) \text{ (Eq. 2.4)}$$

This relationship is based on the similarities in isotopic fractionation of the isotopes of hydrogen and oxygen, and thus their behaviour in the hydrologic cycle is similar (Ingraham, 1998). The equation for the GMWL is only applicable on a global scale. However, the importance of Craig's observations is that the isotopic composition of meteoric waters behaves predictably. Therefore, the relationship can be estimated using the Rayleigh model (Craig, 1961). One key observation from the survey of global meteoric waters is that isotopically depleted waters are associated with cold regions and enriched waters with warm regions (Clark and Fritz, 1997).

2.2.4 Seasonality effects and the local meteoric water line

The development of a Local Meteoric Water Line (LMWL) for precipitation is more useful in undertaking isotopic interpretations of the hydrological cycle at specific sites (compared to the GMWL) since the LMWL reflects local climatic seasonality. Differential fractionation occurring during primary evaporation of water vapour is a function of humidity, whereas secondary evaporation as rain or snow falls from a cloud is a function of temperature (Benjamin et al., 2005). Therefore, climates that experience strong seasonality in temperature and humidity will display varying isotopic compositions throughout the changing seasons. The LMWL is affected by these two factors resulting in a unique slope and intercept for differing locations. Differences in the fractionation of ^{18}O and ^{2}H during evaporation of rain or sublimation of snow will affect the slope of the LMWL. If ^{2}H experiences greater enrichment than ^{18}O, the slope will steepen in comparison to the GMWL.

Baer et al. (2016) developed a LMWL for Mildred Lake mine site based on precipitation data collected for the years 2009 and 2012 based on techniques from Peng et al. (2004) and Wassenaar et al. (2011). The weighted equation was calculated using a weighted least squares regression technique and reported as:

$$\delta^2 H = 7.20 \cdot \delta^{18} O - 10.3 \text{ ‰} \qquad \text{(Eq. 2.5)}$$

Deviations of the isotopic composition of water samples from the precipitation derived LMWL will occur as the result of natural evaporative processes acting on surface water or as a result of artificially created evaporation or condensation associated with anthropomorphic processes (e.g. oil sands extraction). Baer et al. (2016) suggested that there are two main enrichment factors causing deviation of the isotopic composition of OSPW from the LMWL. The first is a result of operational conditions involving high humidity and temperature found within the cooling towers allowing for near-equilibrium enrichment. The second is a result of open water evaporation occurring at the surface of the tailings ponds to the ambient atmosphere.

Baer et al. (2016) also observed seasonal variations in the isotopic composition of precipitation. Highly enriched precipitation values were found to occur during mid-summer large rain storm events, and depleted precipitation was associated with late-season events and cooler temperatures close to 0°C. Isotopic composition of snow was also found to be the most depleted of all precipitation since snowpack accumulation occurs when the air temperature is below 0°C. Engineered barriers do not exist to prevent the addition of meteoric waters to the RCW circuit. Therefore, the isotopic signature of the RCW circuit may reflect the seasonal patterns of meteoric waters within the region based on the addition of precipitation to the overall inventory of OSPW on site.

2.2.5 Evaporation line

The GMWL or LMWL is the initial starting point for tracking the movement of surface waters throughout the hydrologic cycle. However, to begin investigating the water balance for a specific surface water body, an evaporative line should also be established.

Temporal samples of isotopic composition from an evaporating body of water will follow a linear trend defining an evaporative pattern of enrichment often termed the local evaporation line (LEL). The slope of the LEL is controlled mainly by the ambient atmospheric parameters (i.e. humidity and δ-atmospheric water vapour), as well as the isotopic fractionation factor controlled by temperature (Gat, 1995; Gibson et al., 2008). Therefore surface waters within a region generally exhibit LELs with a similar slope as they experience similar atmospheric conditions. Observed LEL slopes generally range from 4.0 to 7.0 depending on local conditions (Gibson et al., 2016c). However, a systematic steepening of LEL slopes towards the GMWL at high latitudes has been observed corresponding to climatic seasonality (Gibson et al., 2005). This steepening is likely due to a decrease in evaporation relating to shorter evaporative seasons and less available energy to drive evaporation as latitude increases. The evaporation line is easily developed through regression analysis of surface water samples when collected over several seasons. The slope of the LEL can also be estimated by modelling the effects of isotopic fractionation using observed atmospheric parameters.

Two important interpretations can be drawn from the LEL in regards to the water balance. The first important water balance interpretation is the isotopic influence of source waters to a water body. Often the intersection of the LEL and the LMWL is used to estimate the total weighted isotopic composition of source water to regional water bodies based on the assumption that the water bodies are fed primarily by local precipitation (Gibson et al., 1993; Yi et al., 2008).

When samples from a specific site are plotted along a regional evaporative line, the degree of offset from the evaporative line can be used to interpret the influence of different source waters on the overall composition of the water body. For instance, if samples are trending below the evaporative line, this may indicate that the estimated input based on the LMWL and LEL intersection is underestimating the volume of snow or spring melt for that specific system. Work by Yi et al. (2008) was able to identify the contribution of spring snowmelt, summer rains, and river flooding inputs to lakes located in the Peace-Athabasca Delta due to the distinct ranges of the isotopic composition of each input. The study was able to provide evidence of summer rainfall replenishing shallow basins across the delta following below-average snow accumulation from the previous winter, as well as identify a year when snowmelt and river flooding played a more significant role in the contribution to lakes following high winter snow accumulation.

The second important water balance interpretation of the LEL is the ability to provide approximations of evaporative loss experienced by a water body based on isotopic enrichment. This enrichment is represented by the degree of offset along the evaporative line and away from the LMWL, proceeding proportionately to the fraction of water lost by evaporation (Gibson and Reid, 2014). The relationship between evaporative fractionation and atmospheric conditions governing the fractionation are well known (Gonfiantini 1986; Gibson et al., 1993). This relationship makes it possible to model the evaporation line based on measurements of atmospheric parameters in conjunction with isotope mass balance theory. Therefore, first-order approximations of evaporative loss can be attained based on the position of water samples collected from a reservoir when plotted in dual-isotope space and referenced to the LMWL and modelled evaporation line.

2.2.6 Craig and Gordon model

Early surveys of surface waters displayed temporal isotopic enrichment of heavy isotopes among the isotopic compositions of lakes and evaporative basins (Gat, 2010). Originally Rayleigh fractionation of an open-system was thought to explain this enrichment; where the Rayleigh distillation equation for an open-system is defined as (Kendall & Doctor, 2003):

$$R = R_0 f^{(a-1)} \qquad (Eq. 2.6)$$

where a is the fractionation factor, f is the fraction of the remaining volume of the decreasing reservoir, R_0 is the isotope ratio of the original reservoir, and R is the isotope ratio of the reservoir at f.

Surveys of highly evaporative systems did not result in extreme isotopic enrichment predicted by the Rayleigh process. Based on a series of experimental studies in both the laboratory and field (Dansgaard, 1954; Friedmann et al., 1956; Craig et al., 1963, Lloyd, 1966) it was realized that isotopic enrichment of a body of water could not be a one-way Rayleigh process, but rather, limited by the back-diffusion of atmospheric water molecules with the water body surface. Another unique observation on the behaviour of evaporating water bodies was that the temporal isotopic composition of the water body plotted systematically away and to the right of the meteoric water line as volume decreased and enrichment progressed (Craig, 1961b; Gat, 2008). Based on these observations, a need for a quantitative understanding of fractionation effects at the water-vapour interface of an evaporating body of water arose (Horita et al., 2008). Craig and Gordon (1965) put forth a one-dimensional linear resistance evaporative model to describe the fractionation that occurs as water is transferred across the water surface-atmospheric boundary.

The Craig and Gordon (C-G) model represents the isotopic composition of evaporative flux based upon subdividing the whole evaporation process into steps (as described by Craig and Gordon, 1965; Gonfiantini, 1986):

1. A well-mixed sublayer of saturated water vapour exists above a well-mixed reservoir. The liquid surface of the reservoir is trying to reach isotopic equilibrium with this sublayer through equilibrium fractionation.

2. Water vapour is then transported to a diffusion layer existing above the saturated sublayer where molecular diffusion results in kinetic fractionation.
3. The water vapour then reaches a turbulent layer where isotopic fractionation does not occur during transport. The vapour mixes with vapour derived from other sources already present in the atmosphere.
4. This water vapour within the turbulent atmospheric region also penetrates the diffusion layer and may condensate on the liquid surface.

These steps can qualitatively explain the isotopic behaviour of water bodies evaporating in natural conditions based on the evaporation and vapour migration mechanisms (Gionfantini, 1986). The non-equilibrium fractionation (molecular diffusion) can explain the deviation in water bodies from the meteoric water line while the remixing of depleted atmospheric vapour can explain the limiting enrichment a water body may experience during evaporation. This phenomenon was observed by Craig et al. (1963) and Gonfiantini (1965) where water bodies with differing initial isotopic compositions, but undergoing evaporation under similar atmospheric conditions, reached the same composition in the final stages of desiccation. The C-G model explains this observation based on the isotopic exchange with atmospheric water vapour limiting the overall enrichment of the reservoir.

Characterizing the isotopic composition of the water lost from surface water bodies as a result of evaporation (δ_E) is central to the isotope mass balance methodology for water balance studies. Direct sampling of the δ_E of water vapour above evaporating water bodies is generally not feasible, and consequently, there is a reliance on the theoretical predictions of the C-G model (Craig and Gordon, 1965; Horita et al., 2008). C-G model has become a cornerstone of isotope studies of the hydrological cycle, both at regional and global scales (Horita et al., 2008), as the role of evaporation is a pivotal link in any study of the hydrological cycle (Gat, 2008).

2.3 Stable isotopes as tracers

The purpose of this section is to provide an introduction to contemporary studies utilizing isotope tracer techniques and contextualize the research gap this study attempts

to fill. First, a review of isotope mass balance studies of natural systems is presented to demonstrate traditional isotope mass balance techniques this study has adapted for application at an oil sands mine site. Following this section, a review of the use of isotope tracers within mining applications is provided to demonstrate the limited work within the literature conducted to date using stables isotopes as tracers for hydrological assessments at operating mine sites.

2.3.1 Isotope mass balance applications to natural systems

There have been a number of studies that have utilized isotope mass balance techniques to estimate evaporation fluxes from natural bodies of water or to predict the isotopic evolution of a water body as a result of evaporation (Gonfiantini, 1986; Gibson et al., 1993; Gibson and Reid, 2014; Jasechko et al., 2014; Gibson et al., 2016a). Many of these studies have been performed in similar seasonal climates to that of Mildred Lake mine and in close proximity to mine sites (Gibson et al., 1998; Gibson, 2002; Gibson et al., 2016a). However, based on a review of current literature, there have been no studies explicitly utilizing the isotope mass balance techniques directly on operational tailings circuits or mine closure surface water bodies to quantify evaporation for closing a water balance of an operational mining water circuit.

So what *has* been done? Gibson et al. (1996) tested the validity of the isotopic method for estimating evaporation on a small tundra lake in the Canadian Arctic. This site was chosen to demonstrate the sensitivity of small lakes in a continental setting to evaporation during the ice-free period due to potentially large variations in atmospheric conditions controlling evaporation. The isotope mass balance technique was tested against a standard mass balance, energy balance, aerodynamic profile, and class A evaporation pan methods for estimating evaporation. Multiple models were ran using a "time step", or non-steady state approach, of varying time intervals, for the isotope mass balance model - while assuming steady-state conditions over short periods. For the ^{18}O balance, good agreement was found between the standard methods if time intervals were set to be just over one week. However, the ^{2}H balance was found to be less accurate in comparison for short time periods, and it was recommended that it should not be used for time intervals less than 50 days in this setting.

Studies performed within similar climates as SCL's mine site can be used as a reference point for this study. Some studies measure evaporation as a percent ratio (%) between evaporation (E) and inflow (I) fluxes. Based on a study of fifty lakes throughout central Alberta during 2008 and 2009 (including the Athabasca River Basin), Gibson et al. (2016a) reported a range of E/I values of 18 to 136% with overall lake evaporation exceeding precipitation input by 6% on average and accounting for approximately 72% of water loss within the region. This indication of evaporation as the dominant process for water loss within the water balance further exemplifies the necessity of quantifying evaporation within the water balance for mining purposes. Only lake water samples were collected for actual isotopic analysis, with all other parameters being modelled. Isotopic composition for precipitation was modelled based on empirically derived relationships with latitude and elevation. It is important to note that this study was performed using a steady-state mass balance approach for an annual water mass balance. The steady-state assumption assumes that evaporation is the only outflow and is equal to inflow. Without actual inflow measurements, a volume or rate cannot be calculated for evaporation.

In an effort to understand the role of evaporation associated with tailings ponds within a mine site in Yellowknife, NWT, Gibson et al., (1998) utilized a non-steady state isotope mass balance model at a reference lake located 1 km from the north-west tailings pond at the Giant Yellowknife Mine. The mean annual evaporation was reported as 387 mm during the open water period, based on the isotope mass balance technique performed over six years utilizing ^{18}O as the tracer. This estimation was compared to both the Penman combination method for evaporation and a standard water balance and found to agree within 20% for both cases.

Gibson (2002) performed an intensive analysis based on a non-steady state isotope mass balance model using both a fraction-dependent model and a time-dependent model to perform short-term evaporation and water budget prediction for several shallow Arctic lakes. A small lake (surface area of 6 ha and an average depth of 0.65 m) was selected as well as five nearby lakes (4.4 - 30.2 ha) and two mine-tailings ponds (20.5 and 79.3 ha) located in Lupin, Yellowknife. All inputs were sampled for isotopic analysis at regular intervals for June, July and August of 1992 and 1993 as well as lake samples. Isotopic composition of the atmosphere (δ_A) was estimated using evaporative pans based

on a method from Gibson et al., (1999). A nest of shallow wells was used to collect lateral inflow samples to the main study lake with the inclusion of the snowpack signature in the overall isotopic composition. The study found that evaporation losses were the dominant factor controlling isotopic enrichment of the bodies of water and could, therefore, be used to estimate the evaporation losses for highly transient systems. Mean lake evaporation was estimated at 1.6 mm day^{-1} for the study period with mid-summer evaporation ranging from 1.3 to 1.9 mm day^{-1} during 1993 and 3.8 to 4.5 mm day^{-1} in 1992. These results were able to identify subdued evaporative fluxes during a wet season (1993) versus a dry season (1992).

2.3.2 Mining related applications of isotope tracer methods

This section provides an overview of isotope tracer studies as applied to mine sites. Although stable isotopes of water have been used to investigate hydrologic systems in nature as early as the 1960s (Dincer, 1968), there have been few studies involving ^{18}O and ^{2}H as tracers at mine-affected landscapes or engineered hydrologic systems. Stable isotopes of water are unaffected by geochemical or biological processes, making them ideal candidates for transport or pollutant transport associated with hydrological pathways through complex systems (Kendall and McDonnell, 1998). Fractionation of varying source waters also allows for fingerprinting specific isotopic signatures to their respective sources aiding in understanding the effects of anthropomorphic activities on hydrologic pathways.

A study performed by Gammons et al. (2010) of abandoned coal mines across central Montana used stable isotopes of water to further understanding of water sources contributing to the effects of acid mine drainage. Based on the isotopic signatures of shallow groundwater the study was able to determine that agricultural practices in the region play a large role in the amount of water available for acid mine drainage production and that changes in land use promoting storage and evapotranspiration could limit the number of contributions to acidic water discharge from abandoned mines. A comparison of ^{18}O and ^{34}S within the mine drainage and the underlying Madison aquifer

was also able to support the theory that acid mine drainage may be leaking into the Madison groundwater based on their distinct isotopic compositions.

Barbour et al., (2016) performed a study in an effort to understand further the rate of water migration through unsaturated mine waste rock dumps using high-resolution isotopic depth profiles. The study outlined two particular challenges for applying stable isotopes of water as tracers to estimate net percolation through waste rock piles for deep profiles due to the effect of evaporative fractionation that occurred during field sampling and the potential dampening of seasonal isotopic signatures through the unsaturated soil profile as a result of transport processes. The study was able to identify seasonal oscillations of meteoric water present within the unsaturated waste rock and use these oscillations to estimate the recharge rates through the waste piles.

Removal of saline-sodic shale is required to access underlying bitumen ore within the Northern Alberta oil sands region. This shale is then used in the manufacturing of reclamation cover systems as overburden dumps recontoured with a layer of salvaged peat and glacial mineral soil (Boese, 2003). The purpose of these cover systems is to incorporate disturbed surficial material into reclaimed landscapes that will support the growth of vegetation through sufficient nutrient and water availability while preventing the root zone from the effects of salinity and sodicity in the underlying shale layers. Salt transport from the shale to the cover layer is controlled by molecular diffusion when concentration gradients are large and by advective transport, which is downward as a result of net percolation (*i.e.*, recharge) into the dumps or upward as a result of evapotranspiration from the reclamation covers.

Huang et al. (2015) developed transport models of the observed ^{2}H profiles into the overburden shale to estimate recharge rates through the reclaimed shale overburden dumps at SCL. These models could then be used to simulate the observed profiles of salinity produced as a result of pyrite oxidation to help quantify the rates of salt production occurring within the shale. Net percolation rates were estimated to be 20.8 x 10^{-5} m day^{-1} at plateau locations to 2.2 x 10^{-5} m day^{-1} at the slope locations, demonstrating a relationship with topography. This study demonstrates the opportunity for stable isotopes of water to model complex geochemical systems based on their conservative nature.

One of the complications with the end pit lake reclamation strategy discussed in *Sec. 2.2.7* is understanding the evolution of FFT settlement and the resulting transport of high concentrations of dissolved constituents, naphthenic acids, petroleum hydrocarbons, and unrecovered bitumen. Dompierre et al. (2016) identified two main transport processes influencing the transport of chemical constituents within the FFT adjacent to the overlying lake. These were advective-diffusive mass transport associated with the upward migration of OSPW expelled by FFT self-weight consolidation and mixing created by unstable density profiles through the end pit lake and upper portion of FFT. Stable isotopes were used as tracers in the study in an effort to further constraint the transport processes based on their conservative nature and representation of the water molecule by the isotopic composition. Simulating both heat and stable isotope transport further supported this interpretation. Dompierre et al., (2016) was able to demonstrate that advection is the most dominant transport mechanism through the FFT at BML as well as suggest the occurrence of seasonal mixing with the upper portion of FFT and lake water. The flux associated with the dewatering of FFT was determined to be 0.004 m^3 day^{-1} m^{-2} with an approximate mixing depth of 1.1 m below the mud line due to lake turnover.

Baer et al. (2016) developed a catalogue of stable water isotope signatures collected from various water and soil locations at Mildred Lake mine and provides the foundation for our study. They were able to publish the first LMWL developed for Mildred Lake mine (discussed in *Sec. 3.4*). Seasonality was observed in the Athabasca River water collected by Gibson et al. (2016b), but river samples remained close to the LMWL, representing the large influence of groundwater and meteoric water on the Athabasca River, which could be carried over to the RCW circuit within our study. The isotopic composition of water imported from the river and stored in Mildred Lake Reservoir plotted mainly within the cluster of river import samples, although some evaporative enrichment was observed. This observation will be explored in-depth in *Chapter 3* of this study. OSPW was found to be more isotopically enriched than the import waters with evaporative slopes plotting above the natural observed evaporative slope for the region (Gibson et al., 2015); however, the slopes are shallower (OSPW slopes range from 3.7 to 4.9 whereas the natural lake slope is 5.2). The pore water of

mature fine tailings dredged from the MLSB and deposited in West in-pit (now BML) had a similar isotopic composition to that of the clarified water sampled from tailings ponds, although it exhibited a larger range suggesting a retained isotopic memory from past water management practices. The study also suggests that the OSPW signatures can be largely explained by equilibrium fractionation of the imported raw river water during its usage in cooling towers and released as blowdown to the RCW circuit, due to internal operating conditions of ~100% humidity. This hypothesis will be explored in-depth in *Chapter 3.*

2.4 References

AEP. (2015) Surface Water Quantity Management Framework for the Lower Athabasca River: Alberta Environment and Parks. 2015; p. 80.

Baer, T. (2014). An evaluation of the use of natural stable isotopes of water to track water movement through oil sands mine closure landforms. (Master's thesis). University of Saskatchewan, College of Graduate Studies Research.

Baer, T., Barbour, S. L., & Gibson, J. J. (2016). The stable isotopes of site-wide waters at an oil sands mine in northern Alberta, Canada. *Journal of Hydrology*, *541*, 1155-1164.

Benjamin, L., Knobel, L. L., Hall, L. F., Cecil, L. D., & Green, J. R. (2005). Development of a local meteoric water line for southeastern Idaho, western Wyoming, and south-central Montana. US Geological Survey (No. 2004-5126).

Boese, C. D. (2003). The design and installation of a field instrumentation program for the evaluation of soil-atmosphere water fluxes in a vegetated cover over saline/sodic shale overburden. (Master's thesis). University of Saskatchewan, College of Graduate Studies Research.

Chalaturnyk, R., Don Scott, J., & Özüm, B. (2002). Management of oil sands tailings. Petroleum Science and Technology, 20(9-10), 1025-1046.

COSIA (Canada's Oil Sands Innovation Alliance Inc.) (2012) Pit Lake Research [online]. Available at: http://www.cosia.ca/pit-lake-research [accessed 12 Oct 2018].

Craig, H. (1961). Isotopic Variations in Meteoric Waters. Science,133(3465), 1702-1703.

Clark, I., & Fritz, P. (1997). Environmental isotopes in hydrogeology. Boca Raton, FL: CRC Press/Lewis.

Craig, H., Gordon, L., Horibe, Y., & Scripps Institution of Oceanography, L. (1963). Isotopic exchange effects in the evaporation of water: 1. Low-temperature experimental results. Journal of Geophysical Research, 68(17), 5079-5087.

Craig, H. & Gordon, L.I. (1965). Deuterium and oxygen-18 variations in the ocean and marine atmosphere. Stable Isotopes in Oceanographic Studies and Paleotemperatures (E. Tongiorgi, edtr) Lab. di Geologia Nucleare, Pisa. pp.9-130.

Criss, R. (1999). Principles of stable isotope distribution. Oxford, NY: Oxford University Press.

Dansgaard, W. (1954). Oxygen-18 Abundance in Fresh Water. Nature,174(4422), 234-235.

Dincer, T. (1968). The use of oxygen 18 and deuterium concentrations in the water balance of lakes. Water Resources Research, 4(6), 1289-1306.

Dompierre, K. (2017). Controls on Mass and Thermal Loading to an Oil Sands End Pit Lake from Underlying Fluid Fine Tailings. (Ph.D. Dissertation). University of Saskatchewan, College of Graduate Studies Research.

Edwards, T. W., Wolfe, B. B., Gibson, J. J., & Hammarlund, D. (2004). Use of water isotope tracers in high latitude hydrology and paleohydrology. In Long-term environmental change in Arctic and Antarctic lakes (pp. 187-207). Springer, Dordrecht.

Friedman, I., Norton, D., Carter, D., & Redfield, A. (1956). The Deuterium Balance of Lake Maracaibo. Limnology and Oceanography, 1(4), 239-246.

Gammons, C. H., Duaime, T. E., Parker, S. R., Poulson, S. R., & Kennelly, P. (2010). Geochemistry and stable isotope investigation of acid mine drainage associated with abandoned coal mines in central Montana, USA. Chemical Geology, 269(1-2), 100-112.

Gat, J. R. (1995). Stable isotopes of fresh and saline lakes. In Physics and chemistry of lakes (pp. 139-165). Springer, Berlin, Heidelberg.

Gat, J. R. (2008). The isotopic composition of evaporating waters–review of the historical evolution leading up to the Craig–Gordon model. Isotopes in environmental and health studies, 44(1), 5-9.

Gat, J. (2010). Isotope hydrology: A study of the water cycle (Series on environmental science and management; v. 6). London: Imperial College Press.

Gibson, J., Edwards, T., Bursey, G., & Prowse, T. (1993). Estimating evaporation using stable isotopes; quantitative results and sensitivity analysis for two catchments in northern Canada. Nordic Hydrology, 24(2), 79-94.

Gibson, J, Edwards, TWD, & Prowse, T. (1996). Development and validation of an isotopic method for estimating lake evaporation. Hydrological Processes, 10(10), 1369-1382.

Gibson, J. J., Reid, R., & Spence, C. (1998). A six-year isotopic record of lake evaporation at a mine site in the Canadian subarctic: results and validation. Hydrological Processes, 12(10-11), 1779-1792.

Gibson, J. J., Edwards, T. W. D., & Prowse, T. D. (1999). Pan-derived isotopic composition of atmospheric water vapour and its variability in northern Canada. Journal of Hydrology, 217(1), 55-74.

Gibson, J. (2002). Short-term evaporation and water budget comparisons in shallow Arctic lakes using non-steady isotope mass balance. Journal of Hydrology, 264(1), 242-261.

Gibson, J., Edwards, T., Birks, S., St Amour, N., Buhay, W., McEachern, P., . . . Pomeroy, John. (2005). Progress in isotope tracer hydrology in Canada. Hydrological Processes, 19(1), 303-327.

Gibson, J. J., Birks, S. J., & Edwards, T. W. D. (2008). Global prediction of δA and δ2H-δ18O evaporation slopes for lakes and soil water accounting for seasonality. Global Biogeochemical Cycles, 22(2).

Gibson, J. J., & Reid, R. (2014). Water balance along a chain of tundra lakes: A 20-year isotopic perspective. Journal of Hydrology, 519, 2148-2164.

Gibson, J. J., Birks, S. J., Yi, Y., & Vitt, D. H. (2015). Runoff to boreal lakes linked to land cover, watershed morphology and permafrost thaw: a 9-year isotope mass balance assessment. Hydrological Processes, 29(18), 3848-3861.

Gibson, J. J., Birks, S. J., Yi, Y., Moncur, M. C., & McEachern, P. M. (2016a). Stable isotope mass balance of fifty lakes in central Alberta: Assessing the role of water balance parameters in determining trophic status and lake level. Journal of Hydrology: Regional Studies, 6, 13-25.

Gibson, J. J., Yi, Y., & Birks, S. J. (2016b). Isotope-based partitioning of streamflow in the oil sands region, northern Alberta: Towards a monitoring strategy for assessing flow sources and water quality controls. Journal of Hydrology: Regional Studies, 5, 131-148.

Gibson, J. J., Birks, S. J., & Yi, Y. (2016b). Stable isotope mass balance of lakes: a contemporary perspective. *Quaternary Science Reviews*, *131*, 316-328.

Gonfiantini, R. (1965). Effeti isotopici nell evaporazione di acque salate (Isotope effects in salt water evaporation). Attidella Societa Toscana di Scienza Naturali, sierie A72: 550-569.

Gonfiantini, R. (1978). Standards for stable isotope measurements in natural compounds. Nature, 271(5645), 534-536.

Gonfiantini, R. (1986). Environmental isotopes in lake studies. Handbook of environmental isotope geochemistry, 2, 113-168.

Horita, J., Rozanski, K., & Cohen, S. (2008). Isotope effects in the evaporation of water: a status report of the Craig–Gordon model. Isotopes in environmental and health studies, 44(1), 23-49.

Huang, M., Hilderman, J. N., & Barbour, L. (2015). Transport of stable isotopes of water and sulphate within reclaimed oil sands saline–sodic mine overburden. Journal of Hydrology, 529, 1550-1561.

Ingraham, N. L., & Criss, R. E. (1998). The effect of vapor pressure on the rate of isotopic exchange between water and water vapor. Chemical Geology, 150(3-4), 287-292.

Isaac, B.A., Dusseault, G.D., Lobb, J.D., & Root, J.D. (1982). Characterization of the lower cretaceous overburden for oil sands surface mining within Syncrude Canada Ltd. leases northeast Alberta, Canada. In Proceedings of the IV International Association of Engineering Geology II, New Delhi, India. A.A. Balkema, Rotterdam, Netherlands.

Jasechko, S., Gibson, J. J., Birks, S. J., & Yi, Y. (2012). Quantifying saline groundwater seepage to surface waters in the Athabasca oil sands region. Applied Geochemistry, 27(10), 2068-2076.

Kendall, C., & Doctor, D. H. (2003). Stable isotope applications in hydrologic studies. *Treatise on geochemistry*, *5*, 605.

Lloyd, R. (1966). Oxygen isotope enrichment of sea water by evaporation. Geochimica Et Cosmochimica Acta, 30(8), 801-814.

McDonell, B., Holmes, G., Mushey, N., Maciejewski, W., & Oxenford, J. (1995). Extraction enabling technologies: Past successes and future challenges. In SPE International Heavy Oil Symposium. Society of Petroleum Engineers.

Mook, W. (2006). Introduction to isotope hydrology: Stable and radioactive isotopes of hydrogen, oxygen and carbon (International contributions to hydrogeology; v. 25). London; New York: Taylor & Francis.

Peng, H., Mayer, B., Harris, S., & Roy Krouse, H. (2004). A 10-yr record of stable isotope ratios of hydrogen and oxygen in precipitation at Calgary, Alberta, Canada. Tellus B, 56(2), 147-159.

Scales, M. (1999) Sweet success. Canadian Mining Journal. 120 (4), 24-29.

Syncrude Canada Ltd. (2007). Syncrude Fact Book. Fort McMurray: Syncrude Canada Ltd. p.21.

Syncrude. (2013). Base Mine Lake Monitoring Plan. Syncrude Canada Ltd., Calgary, AB. Report, 1-38.

Wassenaar, L. I., Athanasopoulos, P., & Hendry, M. J. (2011). Isotope hydrology of precipitation, surface and ground waters in the Okanagan Valley, British Columbia, Canada. Journal of Hydrology, 411(1), 37-48.

Yi, Y., Brock, B. E., Falcone, M. D., Wolfe, B. B., & Edwards, T. W. (2008). A coupled isotope tracer method to characterize input water to lakes. Journal of Hydrology, 350(1-2), 1-13.

Zubot, W. (2010). Removal of Naphthenic Acids from Oil Sands Process Water Using Petroleum Coke (Master's thesis, University of Alberta, Calgary, AB).

Chapter 3: Isotopic characterization of the temporal evolution of oil sands process-affected waters

i. Preface

The following chapter has been written as a stand-alone body of work intended for submission to an academic journal (likely Mine Water and the Environment or Journal of Hydrology: Regional Studies) following the completion of this thesis. The purpose of this study is to provide a characterization of the stable isotope signatures of oxygen and hydrogen (^{18}O and ^{2}H) found within the source and make-up waters of the recycle water (RCW) circuit at an oil sands mine located in Northern Alberta. Here I present a multi-year dataset of isotopic signatures collected bi-weekly from the RCW circuit to characterize observable seasonality. I assess the mixing and fractionating processes contributing to the unique isotopic signature of oil sands process-affected waters. This work provides foundational data for future water balance studies using isotope tracer techniques within the oil sands region. The work also presents key data for future studies relating to the movement of process-affected waters through both the natural surrounding landscape and future closure landscapes within the oil sands region.

To date, portions of this study have been presented in the following formats:

- Chad, S.J. Applications of stable water isotopes (^{18}O and ^{2}H) for assessing operational site water management and performance of closure landscapes. Poster presented at: COSIA: 2019 Oil Sands Innovation Summit; 2019 June 3-4; Calgary, AB.
- Chad, S.J. Controls on the evolution of stable isotopes of oil sands mine site waters. Technical presentation at: Saskatchewan Mining Association Biennial Environmental Forum; 2018 October 17-18; Saskatoon, SK.
- Chad, S.J., Barbour, S.L, McDonnell, J.J. Controls on the evolution of stable isotopes of oil sands mine site waters. Poster presented at: Resources for Future Generations; 2018 June 16-21; Vancouver, BC.

ii. Abstract

Water use and management within the Alberta oil sands region has been an ongoing environmental concern since oil sands mining began more than 50 years ago. Currently over 1.7 billion m^3 of oil sands process-affected water (OSPW) is stored on site at Syncrude Canada Ltd's Mildred Lake mine in Northern Alberta, with an estimated 112,000 m^3 of tailings water added each day. These volumes—together with the aridity of the region—highlight the importance of closing a site-wide water balance for an operational oil sands mine. But the physical water balance components, such as evaporation or meteoric water input, are exceptionally difficult to quantify using standard hydrometric techniques. Therefore, the purpose of this study is to assess the use of stable isotopes of oxygen and hydrogen (^{18}O and ^{2}H) as tracers to understand the main factors contributing to the water balance of the recycle water (RCW) circuit. This study presents the first stable isotope dataset characterizing the seasonal and interannual evolution of source and make up waters of a RCW circuit operating within the Alberta oil sands region.

Water samples were collected at varying timescales over an eight-year period to establish an inventory of site wide water signatures at this oil sands mine site. These samples were used to characterize the seasonal and interannual isotopic evolution of source waters to the RCW circuit. I used them to also assess the degree to which the connected individual tailings ponds are mixed within the circuit.

Previous work indicated that the primary mechanisms contributing to the enriched isotopic signature of the RCW circuit were highly enriched cooling tower water (so-called blowdown water) and open water evaporation from tailings ponds. Our results showed that mixing of cooling tower blowdown at current operational volumes had minimal effect on the overall signature of the RCW circuit. However, it is likely to have contributed to the current isotopic signatures, which evolved since the start of operations. The patterns of seasonal depletion and enrichment are consistent of a system in isotopic steady state at an annual time scale – an important observation for future isotope mass balance modelling. Samples collected during the ice-on period demonstrated that isotopic depletion was occurring as a result of fractionation during ice formation and release of tailings pore water release. This study also demonstrated the opportunity for isotopic

tracers to be used as an additional tool for monitoring cooling tower efficiency based on a closed-system Rayleigh model.

This research will assist in industry attempts to optimize the use of imported freshwater and recycle water in extraction. In future, the method can also be utilized to track the evolution of mine closure landscapes as they evolve from OSPW signatures to freshwater chemical compositions.

3.1 Introduction

The global mining industry is under continuous pressure by public and governmental agencies to improve the sustainability of its operations (Tost *et. al*., 2018). Foremost amongst sustainability issues is mine water demand and management due to high water consumption rates and the potential risk for contaminants to easily be transported off-site by water. In the Alberta Oil Sands Region, these issues are acute. One example of a mine that requires large volumes of freshwater to be imported on-site is the Mildred Lake mine operated by Syncrude Canada Ltd (SCL) located north of Fort McMurray, Alberta, Canada. The Mildred Lake mine imports approximately 2 m^3 of freshwater from the Athabasca River for every cubic meter of recovered bitumen. Based on the current crude oil production of 56,000 m^3 day^{-1} this equals a daily import of 112,000 m^3. Following use in the upgrader, imported water that is not evaporated or chemically consumed contributes to the existing inventory of oil sands process-affected waters. As of 2017, there was about 1.7 Gm^3 of process water stored on-site in engineered tailings management facilities (commonly referred to as tailings ponds) accumulated since the start of operations over 40 years ago. Of this, about 200 Mm^3 is free water with the remainder contained as tailings porewater (W. Zubot, personal communication. 2019).

To minimize freshwater import from the Athabasca River, SCL recycles approximately 80% of the process water stored. The recycled water is oil sands process water (OSPW) defined as any water associated with mining processes. This OSPW is drawn from the stores of clarified water in tailings ponds following settlement of the discharged tailings slurry (Zubot, 2010). The storage, supply, and recirculation of OSPW from tailings ponds through upgrading and extraction facilities is referred to as the recycle water (RCW) circuit and is a vital process in minimizing the demand of

freshwater import on site. The immensity of these stores and the critical stress on water for mine operations in this region highlight the importance of accurately tracking the water balance of site wide waters.

The infrastructure of tailings management facilities and operational water demand at an oil sands mine are constantly evolving relative to mining operations. As a result, measurements of water balance parameters are difficult to directly measure and must be modelled or estimated. Canada's Oil Sands Innovation Alliance (COSIA) conducted a review of five oil sands operator's water flow sheets and found many differences in how operators track site wide water balances and that each mine presented a unique set of challenges (COSIA, 2019).

Two specific areas where water balance information is critically needed that could improve water management during operations, as well as following mine closure, are the quantification of meteoric water inputs and evaporative losses contributing to the site wide water balance. The enormous volume of OSPW storage on-site also highlights future issues associated with the remediation of OSPW and its reintegration to the natural environment through various closure strategies. Developing new and efficient tools for tracking the rates, pathways, and distribution of water moving through closure landscapes is a major research challenge.

Here I explore and evaluate the feasibility of using the stable isotopes of oxygen and hydrogen (^{18}O, ^{2}H) to track hydrological processes at an operating oil sands mine site, and in particular characterize the addition of make-up waters and evaporative losses to/from the RCW circuit are contributing to the unique isotopic signature of OSPW for ultimate water balance analysis.

Past studies involving ^{18}O and ^{2}H as tracers have been used primarily in gauged watersheds for hydrograph separation (see Buttle, 1994; Klaus and McDonnell, 2013 for review), transit time modeling (Harman and Kim, 2014; Jasechko et al., 2016; Tetzlaff et al., 2018) and vegetation water source partitioning (Evaristo et al., 2015). The theory and methods are long established for isotope tracer studies to investigate water balances parameters of surficial waters (Dincer, 1968; Zimmerman and Ehhalt, 1970; Zuber, 1983; Gonfiantini, 1986). More recently, stable isotopes have been used in ungauged basins for estimates of water balance studies when hydrometric data is limited (see Gibson et al,

2016a, Gibson et al., 2016b for a comprehensive review of methods; Gibson and Reid, 2014; Tondu et al., 2013; Turner et al., 2014l Turner, Wolfe, & Edwards, 2010). While much progress has been made in basic research and applications to natural systems, the application of isotope tracing in mining has been minimal.

A small number of studies have used stable isotopes to trace and characterize the rates of recharge or water movement through mine waste and to identify the presence of waters affected by mining processes in adjacent off site water. For instance, Barbour et al., (2016) developed high-resolution depth profiles of ^{18}O and ^{2}H through unsaturated coal mine waste rock dumps to quantify recharge rates associated with spring snowmelt and summer rain. A similar study was undertaken by Huang et al., (2015) who utilized ^{2}H as a tracer to model recharge rates through reclamation covers placed over a shale overburden dump at SCL. They were able to constrain a cover water balance model using the observed $\delta^{2}H$ profiles within the shale and characterize the variation in net percolation with topographic location. Dompierre et al., (2016) used a multi tracer approach involving ^{18}O and ^{2}H within the pore water of fluid fine tailings (FFT) stored in an end pit lake at SCL to demonstrate the rates of water release from self-weight consolidation of the tailings.

Gammons et al., (2010) also used ^{18}O and ^{2}H to quantify the contribution of acid drainage to shallow groundwater from abandoned coal mines across central Montana. Similarly, Allen and Voormeij (2002) showed how ^{18}O and ^{2}H together with dissolved sulphate (SO_4) could be used to assess the percentages of tailings effluent and groundwater in tailings pond seepage.

To date, there has been limited research conducted on why mine waters display their unique isotopic signatures and how these signatures have progressively evolved in response to mining operations. To our knowledge, this is the first study to publish a multi-year dataset of isotopic signatures collected from an engineered and operational mine water circuit — such as the RCW circuit — to quantify the mechanisms contributing to the evolution of the unique OSPW signature, both seasonally and interannually.

Here I build on this past work and especially recent work at the SCL mine site by Baer et al., (2016) to produce “high-resolution” (*i.e.*, bi-weekly) datasets of the isotopic

signatures of site wide waters at the Mildred Lake and Aurora North mine sites for the development of a conceptual model of water cycling and mixing processes. Baer et al., (2016) were able to define a local meteoric water line (LMWL; $\delta^2H = 7.2 \cdot \delta^{18}O\text{-}10.3$ [‰]) based on 2 years of precipitation sampling. They were also able to identify unique signatures for surface freshwater, shale overburden pore water, as well as OSPW held within the tailings circuit. OSPW waters were particularly enriched due in large part to the evaporative fractionation associated with the use of cooling towers within the bitumen upgrading process. Baer et al. (2016) concluded that that the contributions of cooling tower blowdown to the recycle water circuit and open water evaporation from tailings ponds were the primary controls on the isotopic signatures of OSPW.

Process-affected waters display a unique isotopic signature differing from naturally occurring waters of the Alberta Oil Sands Region; from which the water is sourced (Baer et al., 2016). Stable isotopes of ^{18}O and ^{2}H provide the opportunity for an "in-situ" tracer method for quantifying the contribution of hydrological processes such as pond evaporation and surface runoff by measuring the ratio of heavy to light isotopes making up the water molecules themselves. Therefore, isotope tracers may be used to characterize the complex hydrological processes associated with mining operations contributing to the unique OSPW signature.

Characterization of the temporal and seasonal isotopic evolution of site wide waters will further the understanding of how naturally occurring waters (*e.g.* meteoric waters and river import) mix with current process water inventory, as well as provide the opportunity to quantify isotopically fractionating processes - such as evaporative losses. This information can also be used to monitor the potential off-site migration of OSPW, and better aid in future design and monitoring of closure landscapes as they evolve from process-affected to freshwater chemical compositions.

The specific research objectives for this study are as follows:

1. Characterize seasonal and interannual temporal trends of ^{2}H and ^{18}O signatures within the source waters and OSPW stores of the recycle water circuit; and

2. Develop a conceptual model characterizing the relative effects of operational and hydrological processes contributing to the isotopic evolution of the recycle water circuit

3.2 Study site

The Mildred Lake Mine, located 35 km North of Fort McMurray, is operated by Syncrude Canada Ltd. (SCL). The Alberta Oil Sands Region is within a sub-humid region of the boreal forest that experiences a high degree of seasonality with daily temperatures varying by up to 60 °C between winter lows and summer highs. Annual average precipitation is approximately 450 mm, with one third occurring as snow (Huang et al., 2015). The average annual potential evapotranspiration is approximately 500 mm per year (Huang et al., 2015). Monthly means of air temperature within the region range from -19 °C in January to 17 °C for July, with a mean annual temperature near 1°C. Daily relative humidity follows a seasonal pattern ranging from 77% in winter months to 65% during the evaporative months of May to October (RAMP, 2015).

Mildred Lake mine site has been active since operations began in 1978. Operations began at the Aurora North Mine, 35 km northeast of the Mildred Lake site, in 2000. Both sites use a common extraction and upgrading facility located on the Mildred Lake mine site. The current total daily production capacity is 350, 000 barrels per day with a cumulative production exceeding 2.4 billion barrels since operations began. The mine sites cover approximately 200 km^2 of which a variety of landforms are present including active mining pits, tailings sand structures, overburden dumps, above ground and in-pit tailings facilities and freshwater reservoirs.

Historically, water demands required in the extraction and upgrading of bitumen were met through the import of Athabasca River water — a primary water source within the Northern Alberta Oil Sands Region. Currently, these water demands are met primarily through the recycling of OSPW stored within tailings ponds on-site in an effort to limit the import of river water. However, processes involved in the upgrading of bitumen still require fresh or “raw” water to avoid scaling and corrosion of necessary equipment. Imported water that is not consumed during the upgrading of bitumen is added to the RCW circuit via a blowdown stream from operational cooling towers. The cooling towers

are the final stage of use for imported “raw” water before it is added to the inventory of OSPW on site to be reused in extraction and hydrotransport of bitumen.

The Mildred Lake and Aurora North mines each have their own mining and extraction facilities; however, the two mines are hydraulically connected. OSPW from the RCW circuit at Mildred Lake mine is sent to Aurora North via an intersite water line and water is returned from Aurora North to Mildred Lake through the hydrotransport of bitumen froth. Water export from Mildred Lake Mine to Aurora North has decreased from 21.3 Mm^3 in 2012 to 8.4 Mm^3 in 2016 with the majority of water demand at the Aurora North site now currently being provided by basal aquifer pumping (W. Zubot, personal communication; D. Heisler, personal communication. Syncrude, 2019). Bitumen froth is pipelined to Mildred Lake mine from Aurora North for further processing using a froth treatment that removes the water and solids from the bitumen froth, resulting in an average return of 3.7 Mm^3 of process water to the Mildred Lake recycle water circuit.

Mildred Lake and Aurora North mines each have their own tailings management facilities (*i.e.* tailings ponds) for the storage of tailings produced at each respective mine site. There are five tailings ponds at Mildred Lake Mine and four at Aurora North Mine that are connected to the RCW circuit in various degrees depending on operational requirements. Water and solids produced during the bitumen frothing process, which separates bitumen from the bitumen-rich ore, are transported and deposited into tailings ponds as in slurry form referred to as fluid tailings. As the fluid tailings settle, pore water is released and becomes available as clarified OSPW for reuse in the extraction and hydrotransport of bitumen. This clarified water is directed to a centralized location at Mildred Lake mine site referred to as the recycle pond. The management of tailings discharge, and collection and return of OSPW from the various tailings ponds is a primary activity in managing tailings and improving water use efficiency — thus limiting the demand for water import.

The tailings ponds that are involved in the recycle water circuit at Mildred Lake mine site are East in pit (EIP), Southwest in pit (SWIP), Southwest sand storage (SWSS), North mine south pit west, and Mildred Lake settling basin (MLSB) (*Fig. 3.1)*. The tailings ponds at Aurora North Mine are the Aurora settling basin (ASB), Aurora east pit

north west (AEPN-W), Aurora east pit north east (AEPN-E), and Aurora east pit south (AEPS).

Figure 3.1 Aerial view of site wide surface waters of Mildred Lake Mine and Aurora North Mine (original map reproduced from Google Earth, DigitalGlobe 2018).

3.3 Methods

3.3.1 Field sampling

Water samples were collected in 30mL HDPE Nalgene bottles, filled to the top to minimize the headspace (and potential for evaporative fractionation), with the caps tightly sealed. The sampling was done primarily by SCL's Environmental Group or operational personnel. Sampling locations were selected in consultation with SCL to accurately represent the RCW circuit as well as contributing source waters. Samples obtained from 2012-2014 were collected as part of the initial characterization study performed by Baer et al., (2016). Primary sampling of the recycle water circuit resumed in 2016 with key components sampled bi-weekly to capture temporal evolution of the recycle water circuit with respect to seasonal changes.

This study presents analyses from 220 samples collected at Mildred Lake mine from the recycle water circuit including: an above ground sand tailings storage facility, Southwest Sand Storage (SWSS; n=47); a fluid fine tailings (FFT) and process water containment structure, Mildred Lake Settling Basin (MLSB; n=61); an in-pit tailings basin containing composite tailings, Southwest in-pit (SWIP; n=57), as well as the reservoir that supplies recycled water directly to the mine circuit, recycle pond (n=55). Each tailings pond is sampled from the pump line supplying clarified water from the respective pond to the recycle pond. The tailings slurry line from the extraction plant was also sampled (n=41).

Sampling at Aurora North Mine began in 2016 on a biweekly basis. These samples include 129 samples collected from three Aurora North mine tailings ponds: an in pit tailings basin containing FFT and coarse tailings, Aurora east pit north west (AEPN-W; n=41); an in pit basin containing FFT, coarse tailings and composite tailings, Aurora east pit north east (AEPN-E; n= 43); and an out of pit FFT and process water containment structure, Aurora settling basin (ASB; n= 45).

Rain samples (n=263) were collected over a 9-year period (2009-2018). Samples were collected from rain collectors constructed by Dr. Sean Carey of McMaster

University designed to minimize the atmospheric interactions and evaporative effects (further details outlined in Baer, 2014). The rainfall collectors are located at 7 different locations between the Mildred Lake site (5 collectors) and Aurora Mine site (2 collectors). Rainfall depths associated with each isotope-sampling event were based on a meteorological station operated by O'Kane Consultants on site.

Snow samples (n=147) were collected during annual snow depth surveys over the same period. Snow sampling for this study was performed along several transects and primarily collected from the top and bottom of the snowpack. Snow samples were sealed in Ziploc® freezer bags and allowed to melt at room temperature then transferred to water sample bottles.

A total of 46 samples were collected from the cooling towers. Initial cooling tower blowdown samples were collected in the spring of 2016 from all cooling towers on site with a more extensive sampling campaign (bi-weekly) initiated in the fall of 2016. There are four different operational cooling towers on site; however, only samples from the upgrading cooling tower could be obtained past the initial spring sampling of 2016.

Freshwater samples were also collected from the freshwater storage reservoir at the Mildred Lake mine site, Mildred Lake Reservoir (n=22), as provided by the Baer at al., (2016) study and Athabasca River samples (n=122) provided by Gibson et al., (2016).

3.3.2 Laboratory analysis

All isotope samples were shipped to the Saskatchewan Isotope Laboratory at the University of Saskatchewan, Saskatoon, SK, for analysis. The methods of isotope analysis for this study have been outlined in Lis et al. (2008). An OA-ICOS water isotope analyzer (Picarro L-2130) is coupled to a CTC LC-PAL liquid autosampler for simultaneous $^{2}H/^{1}H$ and $^{18}O/^{16}O$ ratios measurements of H_2O. The autosampler injected 1.80 µL of H_2O into a vapourizer using a 5µL SGE analytical syringe (SGE 001982). Water samples were heated to 110°C with a Picarro Vapourization Module A0211 and the vapour was then analyzed by the water isotope analyzer. Data output was imported using LIMS for Light Stable Isotopes (U.S. Geological Survey, http://isotopes.usgs.gov).

All measured water samples were calibrated and normalized to internal laboratory standards (USGS 46, 47, and 48) relative to VSMOW (0‰) and VSLAP (δ^2H-428‰ and δ^{18}O -55.5‰) using conventional IRMS (isotope-ratio mass spectrometers) systems. All measured values reported are relative to VSMOW. Error values associated with this method are ±0.8‰ VSMOW for δ^2H and ±0.3‰ VSMOW for δ^{18}O.

3.3.3 Cooling tower blowdown fractionation model

Process units involved in the upgrading facility and other mining processes that require cooling are treated by open circulating evaporative cooling towers, where water is continuously circulated through heated process units and returned back to the cooling towers. Details outlining how such cooling towers operate can be found in Zubot (2010). The efficiency of the cooling towers is evaluated by the ratio of concentration of a dissolved species in the blowdown water (C_b) to the make-up water (C_{mu}) referred to as the cycles of concentration (COC; $COC = C_b/C_{mu}$). If the COC is 10 or greater, performance is rated as very high, a COC of 7 is high, and if 2 or less it is rated as very poor (Zubot, 2010). The amount of water released as blowdown and thus how many cycles make-up water encounters in the circuit is related to the COC. Based on cooling tower operational data supplied by SCL the measured net blowdown or fraction of water remaining after evaporation (ie. make up water minus evaporative loss) can be calculated by the inverse of COC ($f=1/COC$).

The following outlines the estimation of cooling tower blowdown signatures by linking the relationship of COC with observed blowdown signatures. Ideally, these estimates can replace the need for long-term sampling by utilizing the regularly monitored COC values for operational purposes. As outlined above COC levels will play a large role in the amount of evaporation occurring, but the resulting fractionation is governed by temperature (T), relative humidity (RH), and the ^{18}O and ^{2}H concentrations within the water vapour of the air (δ_A) inside the cooling towers. Modelling the blowdown signatures resulting from evaporative loss requires knowledge of these parameters, which are not currently monitored for operational purposes — this results in four unknown parameters to adjust (T, RH, δ_{A18}, δ_{A2}) when predicting the isotopic signatures of blowdown in relation to COC values.

I found that when the ^{18}O and ^{2}H values of blowdown were plotted against the fraction of water remaining (*f*; where *f=1/COC*) the enrichment proceeded in a linear relationship similar to that of closed-system Rayleigh distillation. Therefore, I attempted to constrain T and RH by using a closed-system fractionation model:

$$\delta_f = \frac{[\alpha_{tot} \cdot \delta_i + 1000 \cdot f(\alpha_{tot} - 1)]}{[\alpha_{tot}(1 - f) + f]} \qquad (Eq. 3.1)$$

Where δ_i and δ_f are the initial and final isotopic composition of the reservoir over the model period, *f* is the residual water fraction (V_f/V_0), and α_{tot} is the total fractionation factor between liquid and vapour calculated by:

$$\alpha_{tot} = \frac{(\varepsilon^* + \varepsilon_K)}{1000} + 1 \qquad (Eq. 3.2)$$

Where ε^* and ε_K are the equilibrium and kinetic enrichment in permille (‰) calculated based on relationships with temperature and humidity as outlined in Horita et al. (2008).

The enrichment of the cooling tower blowdown was modelled using a fraction-dependent model that requires δ_A values and incorporates the Craig and Gordon linear resistance model (Craig and Gordon, 1965) for estimating the isotopic composition of the evaporate. The enrichment of the cooling tower blowdown was modelled based on the adaptation of the Craig and Gordon model outlined by Gonfiantini (1986):

$$\delta_f = \left(\delta_i - \frac{A}{B}\right) f^B + \frac{A}{B} \qquad (Eq. 3.3)$$

Where

$$A = \frac{h\delta_A + \varepsilon_K + \frac{\varepsilon^*}{\alpha}}{1 - h + \varepsilon_K} \qquad (Eq. 3.4)$$

and

$$B = \frac{h - \varepsilon_K - \frac{\varepsilon^*}{\alpha}}{1 - h + \varepsilon_K} \qquad (Eq. 3.5)$$

All variables are as previously defined with the exception of h (humidity) represented by RH for our purposes and α is the equilibrium enrichment factor determined by empirical relationships with temperature as outlined in Horita et al. (2008).

3.4 Results

Here I present the isotopic data collected from source waters to the RCW circuit (Sec. 3.4.1) and waters comprising the RCW circuit itself (Sec. 3.4.2) to identify temporal patterns within the isotopic compositions of said waters.

3.4.1 Documenting the temporal trends of ^{2}H and ^{18}O within source waters to the recycle water circuit

The isotopic composition of rain and snow samples collected across the site are shown in *Fig. 3.2a*. In total there were 263 rain samples over 9 years (2009-2018, with the exception of 2010). The most depleted sample (October 17, 2009) had a $\delta^{18}O$ of -26.23 ‰ and a $\delta^{2}H$ of -201.62 ‰) with the most enriched sample (June 23, 2014) having a $\delta^{18}O$ of -7.03 ‰ and a $\delta^{2}H$ of -71.3 ‰.

The non-weighted means of the rain sample set for $\delta^{18}O$ and $\delta^{2}H$ were -15.10 ‰ and -123.40 ‰ respectively. Volume weighted means of rain for $\delta^{18}O$ and $\delta^{2}H$ were -14.77 ‰ and $\delta^{2}H$ -120.06 ‰ respectively. The annual rainfall recorded from the years 2009-2017 from an on-site meteorological station operated by O'Kane Consultants ranged from 151 mm in 2011 to 387 mm in 2016 with an annual mean of 310 mm.

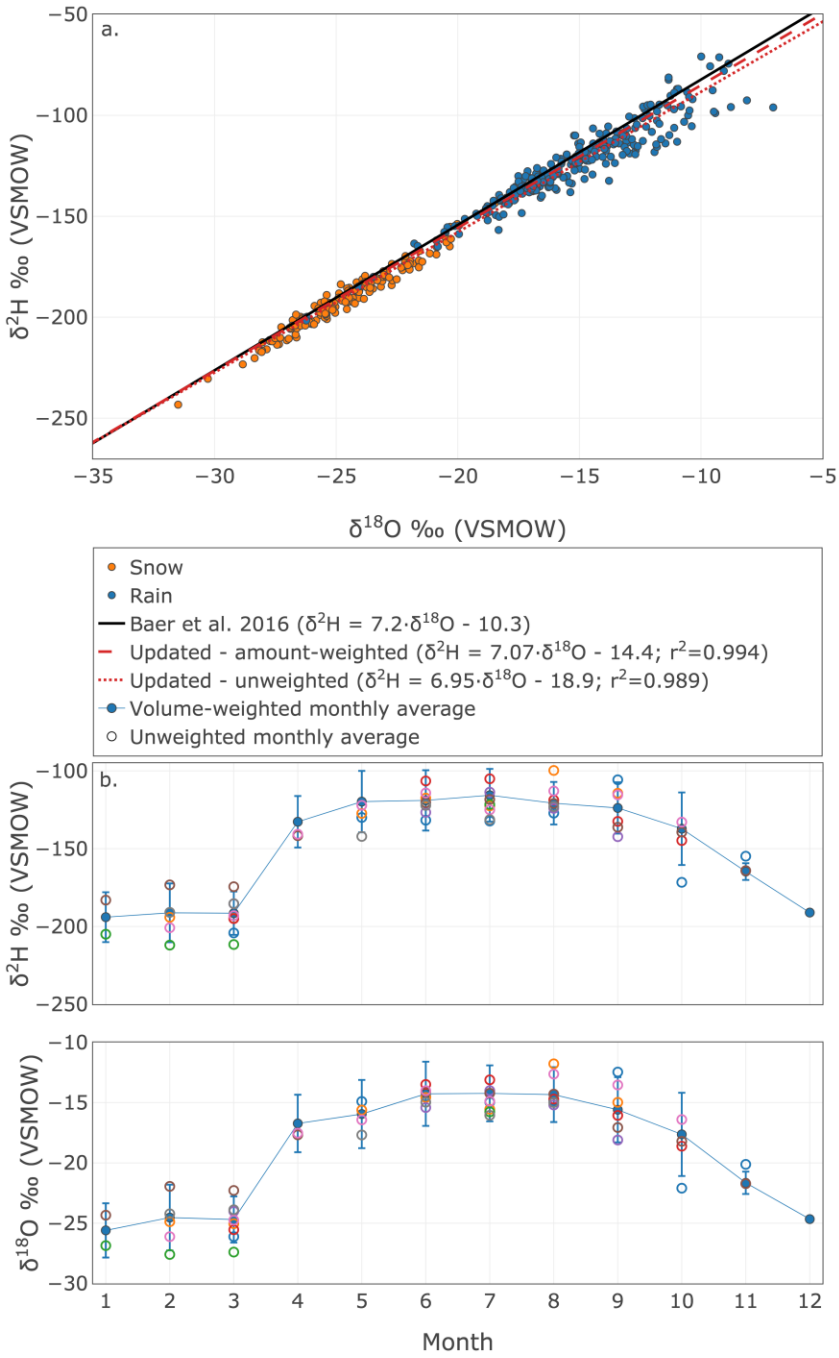

Figure 3.2 a.) Stable isotopic signatures of site wide meteoric water samples with published LMWL (Baer et al., 2016) and updated LMWL (amount weighted and unweighted). b.) Monthly volume-weighted isotopic signatures of ^{18}O and ^{2}H in precipitation samples collected from 2009-2018. Numbers 1-12 represent the calendar month, error bars indicate the monthly standard deviations, and coloured open circles are the unweighted monthly means from each year of collection.

Snow samples (n=147) were provided from annual snow surveys completed by O'Kane Consultants, completed primarily in February or March from 2009 to 2018. The SWE during these surveys ranged from 22 mm (2009) to 80 mm (2017). Only a bulk representation of the isotopic composition was possible given the collection methodology. The non-weighted mean isotopic composition of all snow samples was used to represent the input of snow water equivalent (SWE) during spring melt each season. These values were found to be $\delta^{18}O$ of -24.67‰ and $\delta^{2}H$ of -191.04‰ (Figure 3.2b).

The precipitation dataset was analyzed on a monthly scale in an effort to characterize the seasonality in the isotopic composition of precipitation (*Fig.* 3*.2b; Table. A3.1)*. The total (or annual) amount-weighted mean value for precipitation (rain and snow) was calculated using the rainfall amounts and corresponding isotopic composition of rain events and the total average of snow composition along with the corresponding annual SWE amounts over the sampling period. The annual amount-weighted mean values for precipitation were -18.04‰ for $\delta^{18}O$ and -143.54‰ for $\delta^{2}H$.

Baer et al., (2016) developed an initial LMWL ($\delta^2H = 7.20 \cdot \delta^{18}O - 10.3$ [‰]) for the Mildred Lake mine site based on precipitation data collected in 2009 and 2012. Similar techniques were used within this work to update the LMWL $\delta^2H = 7.07 \cdot \delta^{18}O - 14.4$ [‰] (volume-weighted; r-squared=0.994) and $6.95 \cdot \delta^{18}O - 18.9$ [‰] (unweighted; r-squared=0.989) by adding precipitation data collected following the initial study (2014-2018) as shown in *Figure 3.2a.* This led to a relative percent difference (RPD) of 1.82% between the initial LMWL and the updated volume-weighted LMWL and 3.53% for the unweighted LMWL.

Athabasca river samples (n=122) collected by Gibson et al. (2016a) both upstream and downstream of Fort McMurray, AB (35 km south of Mildred Lake Mine site) are included within this study. *Figure 3.3* shows the temporal isotopic trends of both ^{18}O and ^{2}H within the Athabasca River over a 12-year period (2002-2014). The 12-year average isotopic compositions of $\delta^{18}O$ and $\delta^{2}H$ were found to be -17.93‰ and -142.81‰ over the 12-year period.

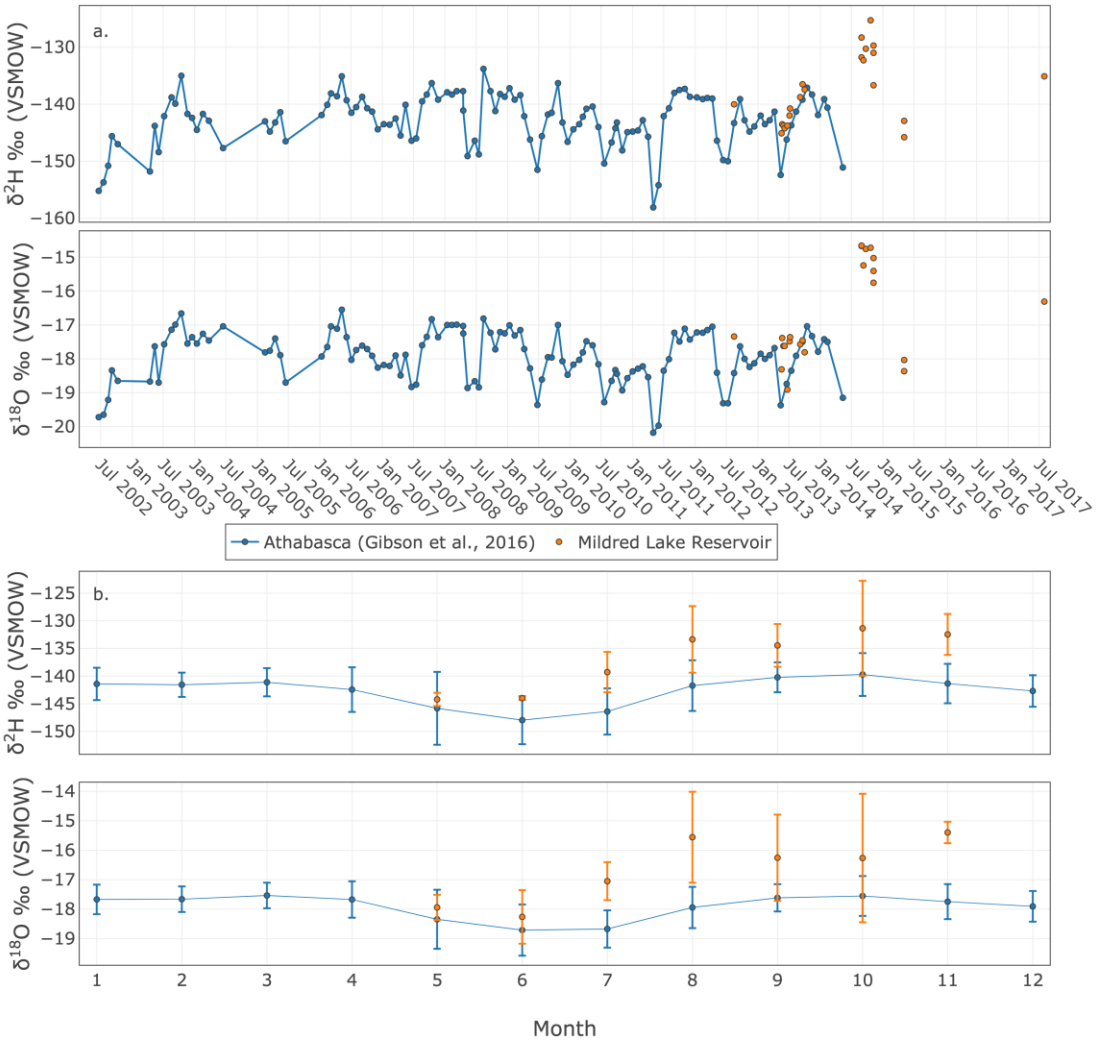

Figure 3.3 a.) Time-series summary of $\delta^{18}O$ and $\delta^{2}H$ from 122 water samples collected from the Athabasca River upstream and downstream of Fort McMurray, AB over the years 2002-2014 provided by Gibson et al. (2016) and 22 water samples collected from the Mildred Lake Reservoir during the ice-free period over years 2012-2017. b.) Monthly means of ^{18}O and ^{2}H from Athabasca River and Mildred Lake Reservoir water, error bars represent the standard deviation for each month.

The Athabasca River dataset was grouped by month to highlight seasonal patterns that could influence the isotopic composition of the imported waters for extraction, with the monthly mean and standard deviations shown *Fig. 3.3b* (monthly statistics are presented in *Table. A3.2*). There was little variability in the isotopic signature of the Athabasca River samples on a monthly basis with the monthly mean of $\delta^{18}O$ shifting by only ~1.00 ‰ and $\delta^{2}H$ by ~8.00 ‰ between the most enriched months (Mar/Sept/Oct) and most depleted months (June/July). The coefficient of variation (CV) for all river samples assessed was -4.18% and -3.19% for ^{18}O and ^{2}H respectively.

Mildred Lake Reservoir (MLR) is used to hold the raw water imported on site from the Athabasca River. Surface water samples (n=22) were collected from MLR over the period of 2012-2017 with the majority of samples occurring in 2013 and 2014. *Fig. 3.3a* shows the temporal distribution of $\delta^{18}O$ and $\delta^{2}H$ from the sampling period. The mean of all samples spanning the five years was -16.72 ‰ and -137.49 ‰ for ^{18}O and ^{2}H respectively, which was more enriched than the average isotopic composition the Athabasca River (^{18}O = -17.93‰ and $\delta^{2}H$ = -142.81‰). The samples collected during spring from 2013 and 2015 are very similar (*Fig. 3.3a*) and appear to be largely influenced by the spring freshet as a result of snowmelt on site and from the Athabasca River composition based on their depleted isotopic signatures. Samples collected in 2013 and 2014 during the late summer and early fall differ isotopically with 2014 displaying much more enriched values for both $\delta^{18}O$ and $\delta^{2}H$. The monthly mean and standard deviations of all years are shown in *Fig. 3.3b* with monthly statistics in *Table. A3.3*. Standard deviations were low for the spring and early summer months (May-July), but became much higher in late summer and fall (Aug-Oct) with isotopic ranges greater than 4‰ and 15‰ for ^{18}O and ^{2}H respectively. The CVs of all MLR samples were found to be -8.44% and -4.52% respectively.

A total of 46 blowdown samples were collected from the cooling tower blowdown streams (CAP: n=2; UE-1: n=2; Utility: n=2; Upgrading: n=40) over the period of 2016-2018. Of the 46 samples collected the lightest isotopic signatures were -16.18‰ and -132.5‰ for ^{18}O and ^{2}H respectively. These signatures occurred on 8 Nov 2017 and were

collected from the upgrading tower. The most enriched values were -10.03‰ and -95.5‰ for ^{18}O and ^{2}H respectively and collected from the CAP tower on 7 March 2016. The mean of all samples spanning the 2 years was -13.37 ‰ and -116.25 ‰ for ^{18}O and ^{2}H respectively. Raw water discharge was also measured in April of 2016 to estimate the input water before fractionation effects. It had an isotopic signature of -18.32‰ and -144.4‰ for ^{18}O and ^{2}H respectively, very close to the stable Athabasca River signature.

Both ^{18}O and ^{2}H of cooling tower blowdown appear to become enriched as COC increases—where water circulating will have had more time to experience evaporative enrichment (Fig. 3.4). All the samples fell along a similar enrichment trendline (referred to as evaporation line or EL) governed by the internal conditions of the cooling towers (*i.e.* temperature and humidity). The further along the EL the samples plot the more evaporation they experienced as a result of higher COC values. The samples presented a cluster around the COC range of 1.5-2.0, which could represent a deviation in internal conditions of the cooling tower during collection affecting the slope of evaporative enrichment. When sorted by month of collection, the samples collected in the cooler months (Oct-May) plotted between the EL and the LMWL whereas the warmer months (June-Sept) plotted below the EL. This is likely due to seasonal shifts within the internal ambient temperature and humidity.

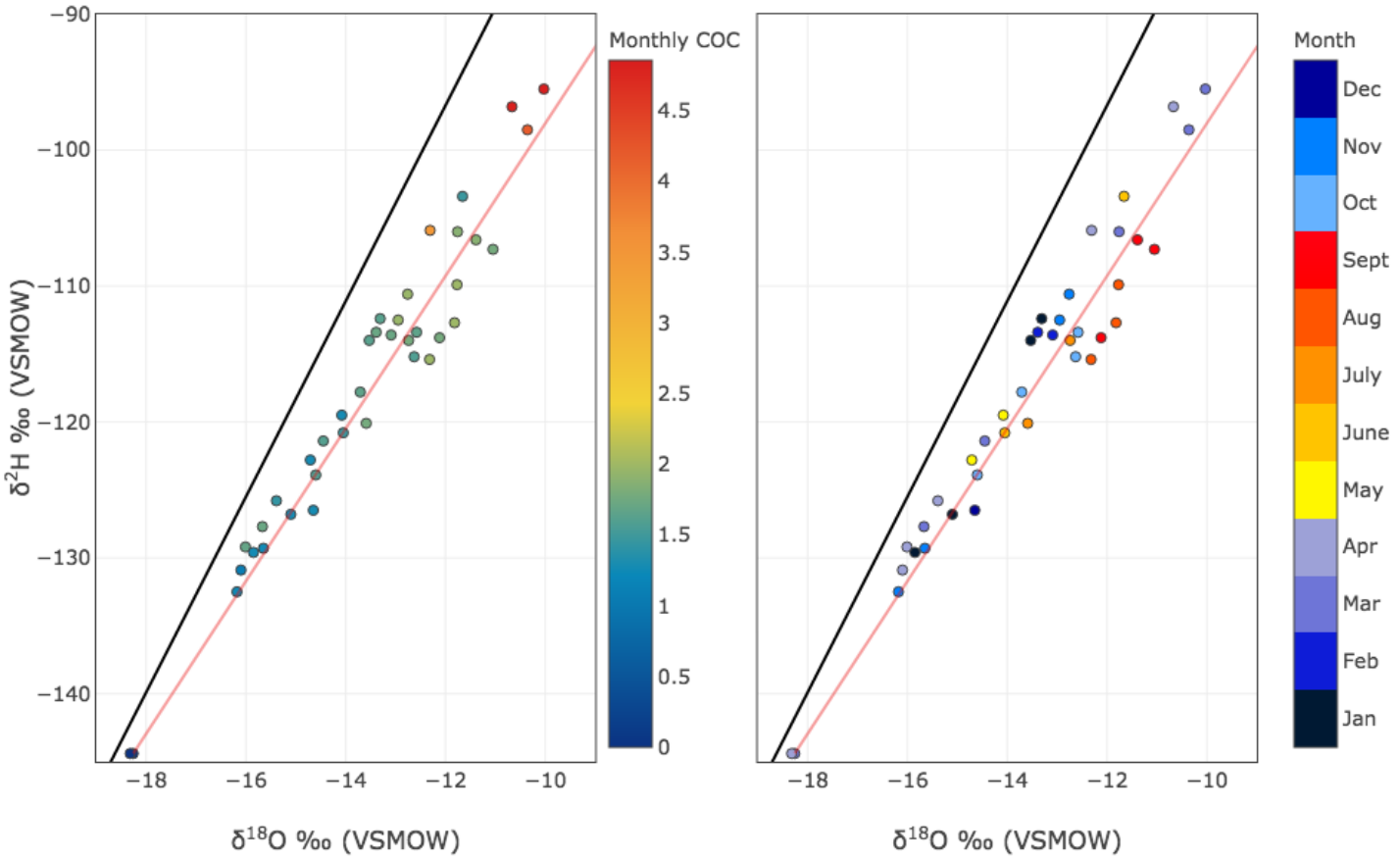

Figure 3.4 Cooling tower samples are plotted in dual isotope space in relation to the LMWL and categorized by reported monthly COC (cycles of concentration; left plot) and by month of collection (right plot). The LMWL is indicated by the black line and the evaporation trendline is indicated by the red line.

3.4.2 Estimating cooling tower fractionation

One of the goals of this study was to quantify the isotopic signatures of input waters to the recycle water circuit for future isotope tracer studies. Here I utilized a closed-system fractionation model to estimate the isotopic signature of cooling tower blowdown using operational data provided by SCL. The primary controls affecting the fractionation of raw water circulating through cooling towers is the amount of cycles the water experiences, measured as cycles of concentration (COC) by SCL, and the internal temperature and humidity within the cooling tower units. COCs at each cooling tower were provided by SCL, but internal temperature and humidity are not measured.

A sensitivity analysis of the effects of shifting temperature was conducted by humidity constant at an estimated RH of 85% (Fig 3.5). The blowdown signatures were contained between the temperatures of 5 and 65°C with 35°C appearing to be a best fit for the average linear enrichment.

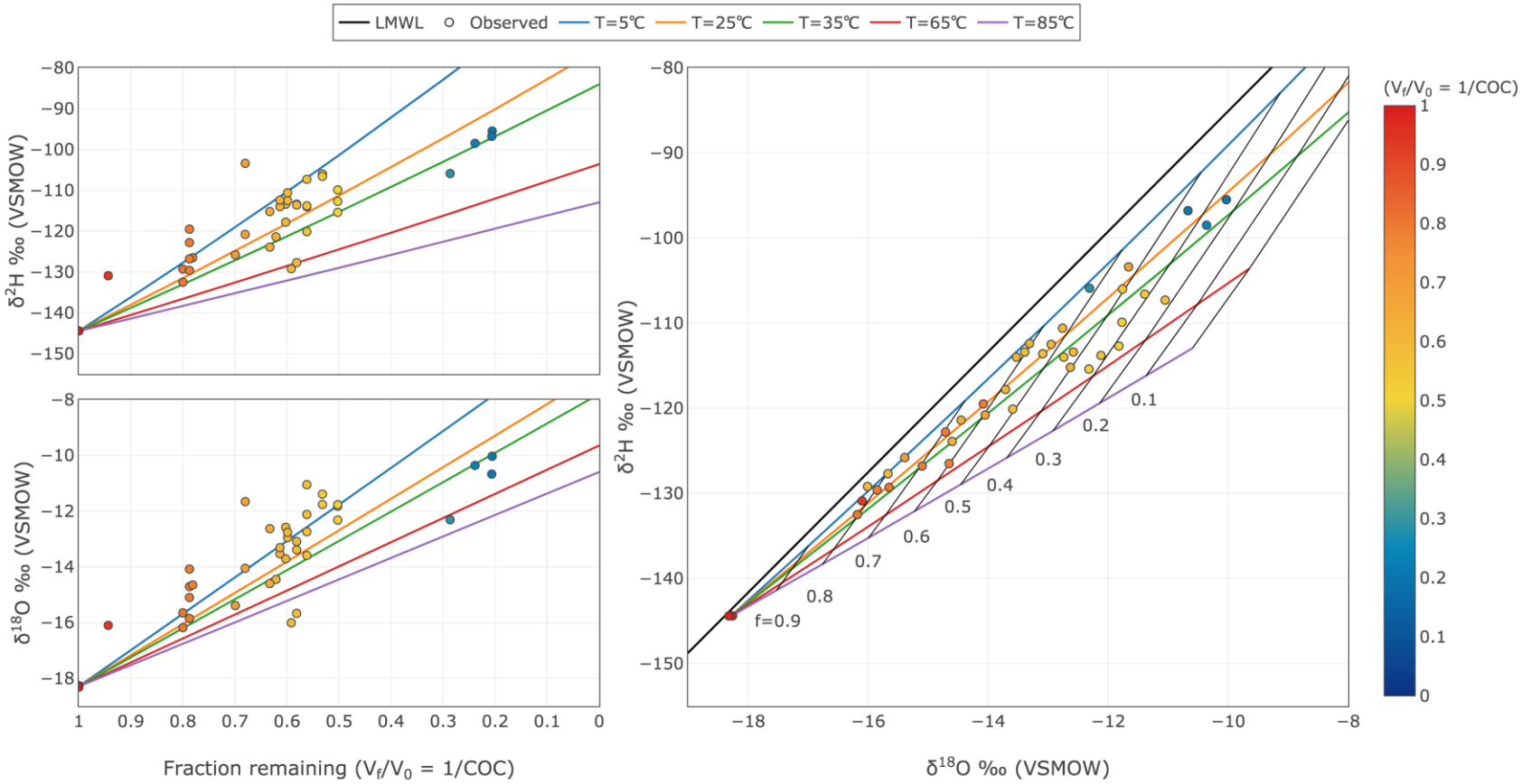

Figure 3.5 Results of the closed-system Rayleigh model to estimate enrichment of cooling tower blowdown as a function of temperature and fraction of water remaining (*f*). RH is set to remain constant at 85%.

The annual mean air temperature on-site was 3°C, with a minimum of -35°C and maximum of 25°C. Based on this range the internal conditions could potentially be operating at 30 to 40 degrees higher than the ambient air conditions outside the cooling towers throughout the year, with 35°C representing the mean internal conditions that are roughly 30°C higher than the mean annual temperature.

The effects of shifting humidity were then tested while holding T constant at 35°C based on the previous sensitivity analysis (Fig. 3.6). Here the blowdown signatures are largely in the RH range of 75 to 95% with 85% appearing to be a best fit for the average linear enrichment, with few samples plotting beyond this range.

A range of δ_A values were tested using *Eq. 3.3* to assess how cooling tower blowdown would be affected while maintaining constant RH and T as determined by the previous sensitivity tests (Fig. 3.7).

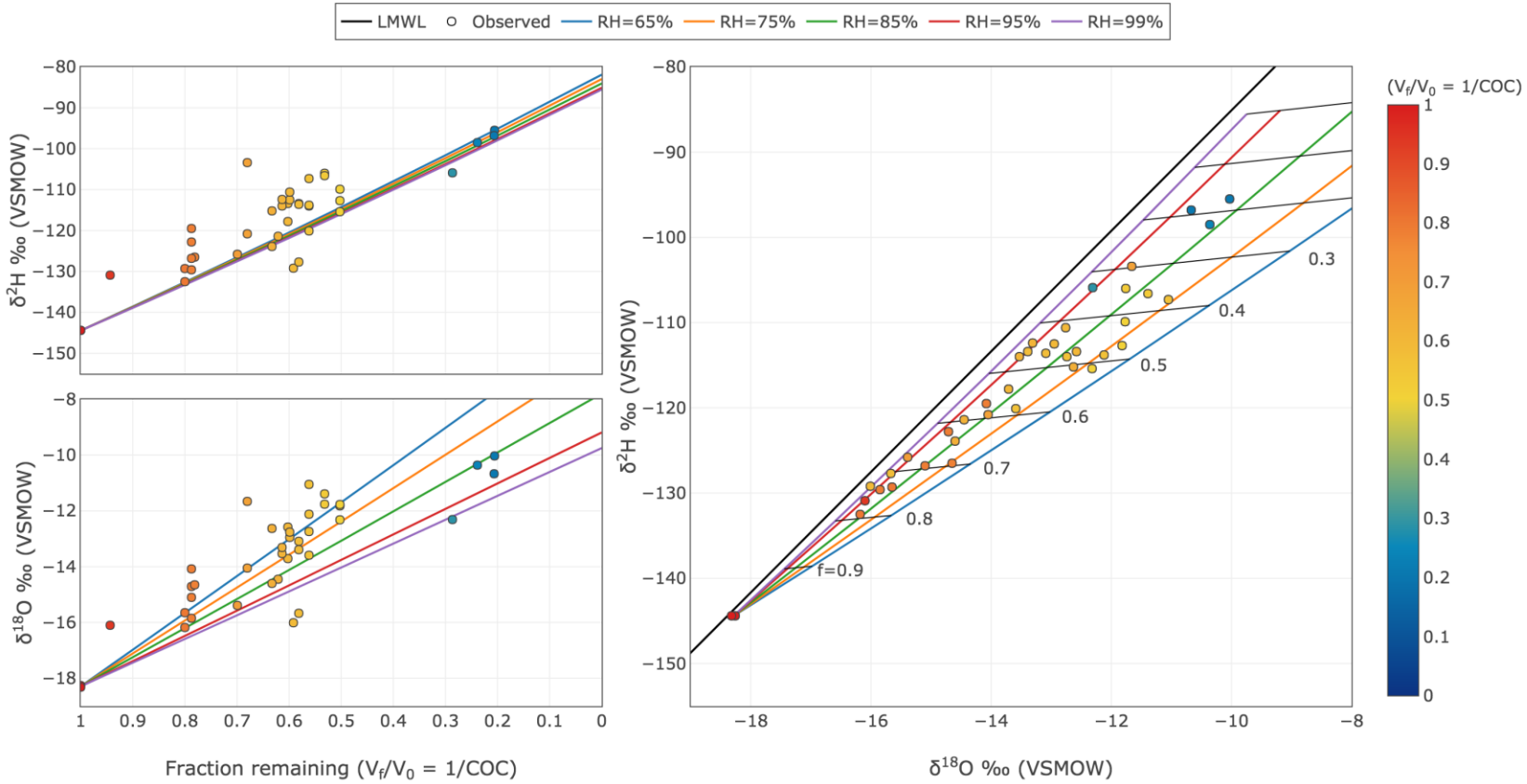

Figure 3.6 Results of the closed-system Rayleigh model to estimate enrichment of cooling tower blowdown as a function of humidity and fraction of water remaining. Temperature is set to remain constant at 35°C.

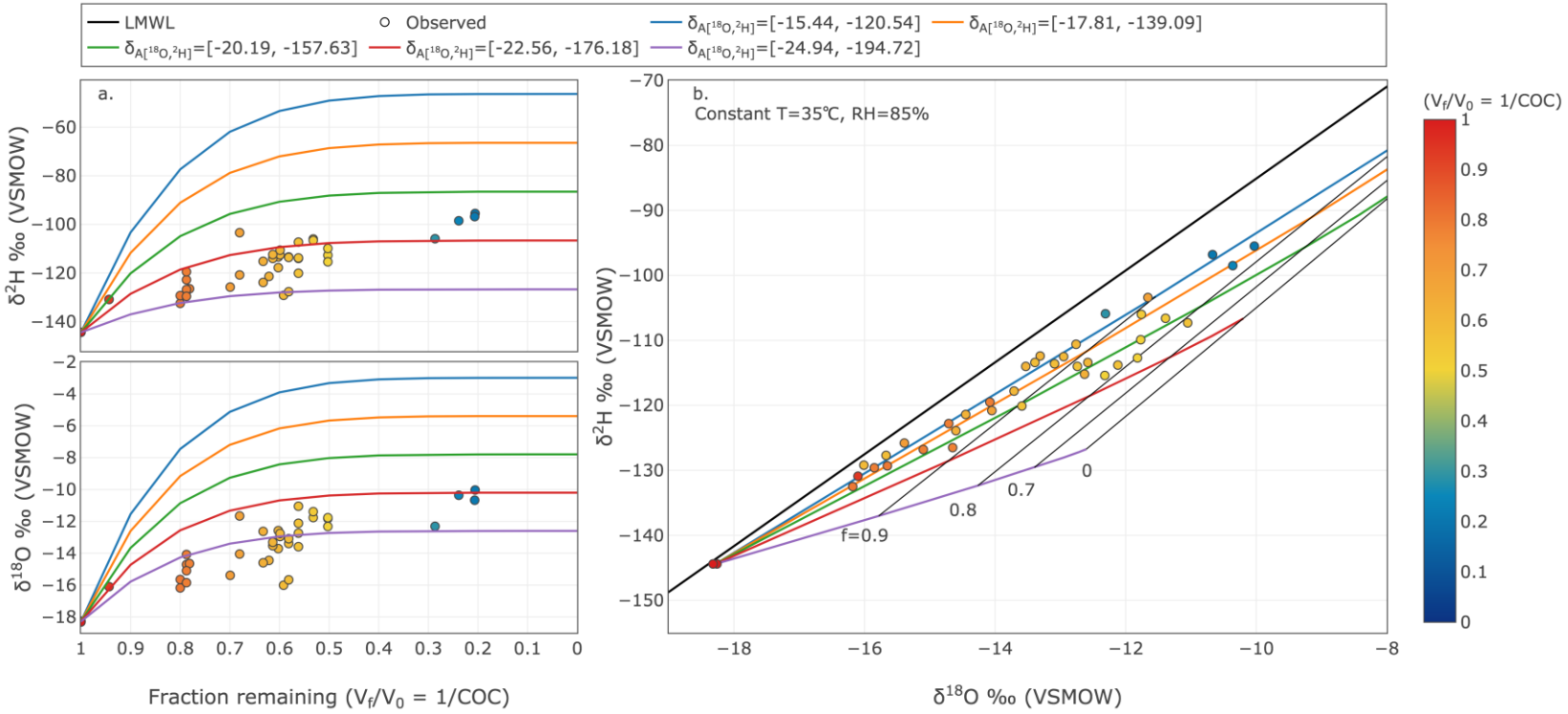

Figure 3.7 a.) Sensitivity analysis of δ_A for predicting ^{18}O and ^{2}H of cooling tower blowdown based on fraction of water remaining following evaporative loss. Temperature and humidity are held constant at 35°C and 85%, as best determined from the previous sensitivity analysis of temperature and humidity. b.) Linear enrichment of the isotopic signature of cooling tower blowdown in dual isotope space. Observed isotopic signatures of cooling tower blowdown in all subplots are referenced by colour to the reported COC values provided by Syncrude.

The lower boundary for the δ_A values ($\delta^{18}O$ = -24.94‰, $\delta^{2}H$ = -194.72‰) was calculated using the weighted mean value of precipitation during the period of May-Oct and the assumption that atmospheric moisture is in equilibrium with precipitation (Gibson et al., 2016b). The three most enriched sets of δ_A fit the observed slopes the best; however, enrichment was largely overpredicted with decreasing volume using these values. The range of δ_A values that fit ^{18}O and ^{2}H when plotted against the fraction remaining did not capture any of the observed samples in dual isotope space. The inability to predict reasonable δ_A values further verifies our initial hypothesis that the cooling towers are operating most similar to a closed-system and are controlled primarily by temperature and humidity shifts rather than δ_A.

Using the closed-system model, average Athabasca River signature as the input signature, and best-fit temperature and humidity results from the sensitivity analysis, the estimated blowdown signatures were calculated for each tower that would be associated with observed COC values and the resulting fraction of water remaining. Following this, volume-weighted monthly and annual integrated blowdown signatures were calculated using historical operational records from the years 2002-2017 consisting of COC values and blowdown volumes (*Fig. 3.8a; Fig. 3.8b)* provided by SCL (*Table. A3.5; Table. A3.6*).

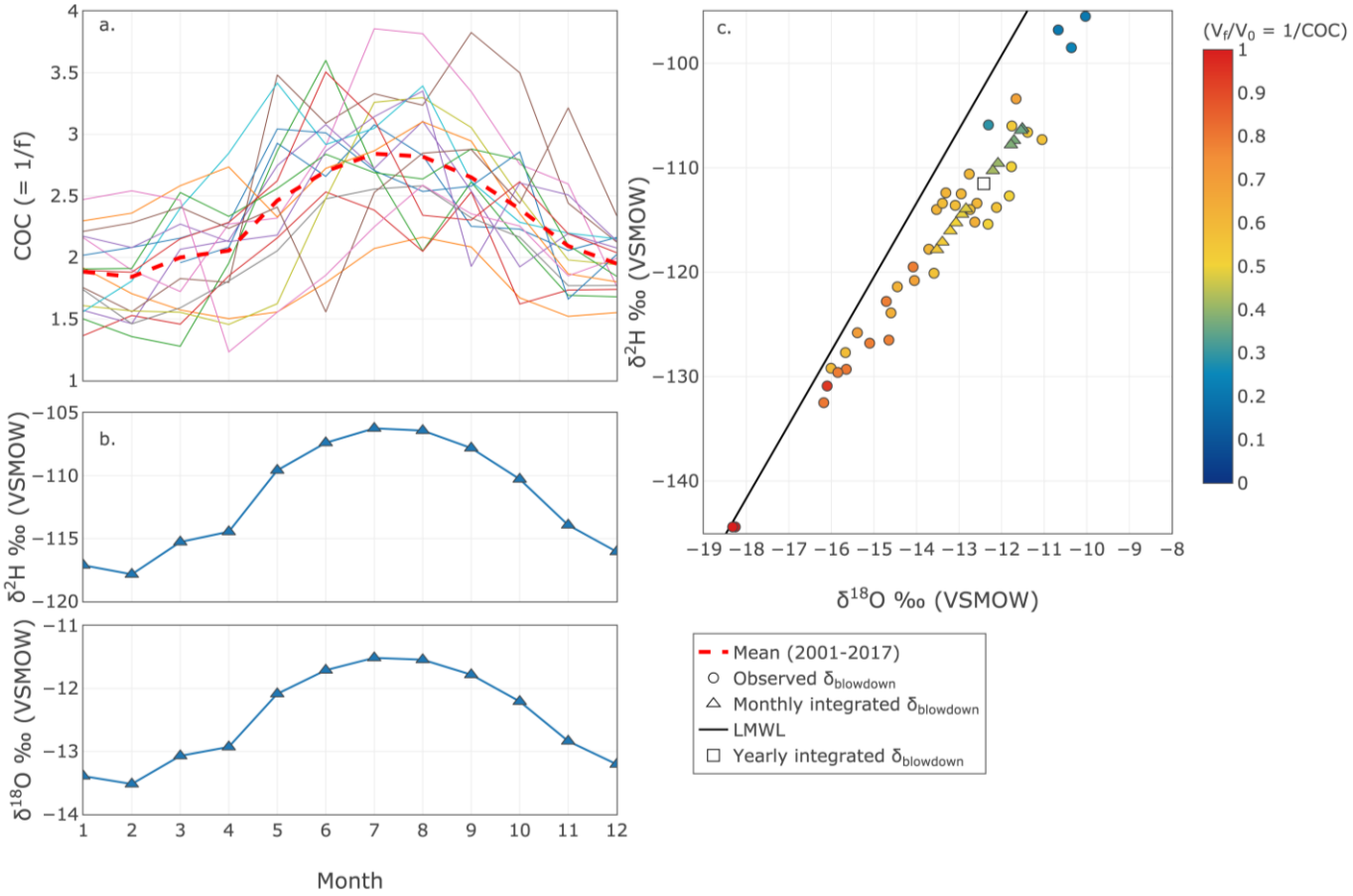

Figure 3.8 a.) Mean monthly COC values plotted alongside the historical monthly blowdown values from 2002-2017 (coloured lines); b.) Volume-weighted monthly-integrated blowdown signatures based on the closed-system model in conjunction with historical operations data of cooling towers. Model parameters are T=35°C, RH=85%, and initial isotopic composition equal to the average annual Athabasca River signature; c.) Dual isotope plot of both monthly and annual blowdown signatures alongside observed blowdown signatures for reference. It should be noted that the observed signatures are primarily collected from only one tower, whereas the integrated signatures are representative of a collective signature from all towers.

The monthly range for $\delta^{18}O$ was -13.52‰ to -11.51‰ ($\delta^{2}H$ = -117.84‰ to -106.24‰) with a monthly mean volume for blowdown of 490,000 m^3. The integrated annual signature was calculated as -12.53‰ and -112.16‰ for ^{18}O and ^{2}H respectively, with a blowdown volume of 5.9 Mm^3.

3.4.3 Seasonal and interannual evolution of ^{2}H and ^{18}O within oil sands process-affected waters making up the recycle water circuit

The interannual and seasonal fluctuations of ^{18}O and ^{2}H from the Mildred Lake mine (n=220) over a 6-year period (2012-2018) and Aurora North mine (n=129) over a 2-year period (2016-2018) were identified by plotting the temporal trends of each tracer (Fig 3.9a).

Up until 2015 all three tailings ponds tracked closely to each other indicating similar hydrometric conditions. However, samples collected at Southwest Sand Storage (SWSS) from the end of 2016 onward were significantly more enriched than Mildred Lake Settling Basin (MLSB) and Southwest In-Pit (SWIP). This is an indication that SWSS involvement within the recycle water circuit may have changed – an important observation for assessing which tailings ponds are contributing to the overall RCW circuit signature. The total mean values of SWIP and MLSB are almost identical with similar maximum and minimum isotopic compositions, whereas the mean SWSS composition is higher as a result of the enrichment past 2016.

All samples from the four ponds were grouped by the month of collection to assess the long-term seasonality trends and similarities between ponds (*Fig. 3.9b; Table. A3.7*). The monthly means calculated from all years for MLSB and the recycle pond were very close, with SWIP following similar levels of enrichment, but less depletion during the spring and winter. The SWSS monthly means were consistently higher than the other ponds with the exception of December. The enrichment of SWSS was also observed when the samples were plotted in dual-isotope space (*Fig. 3.9c*) as samples plotted well beyond the rest of the OSPW samples.

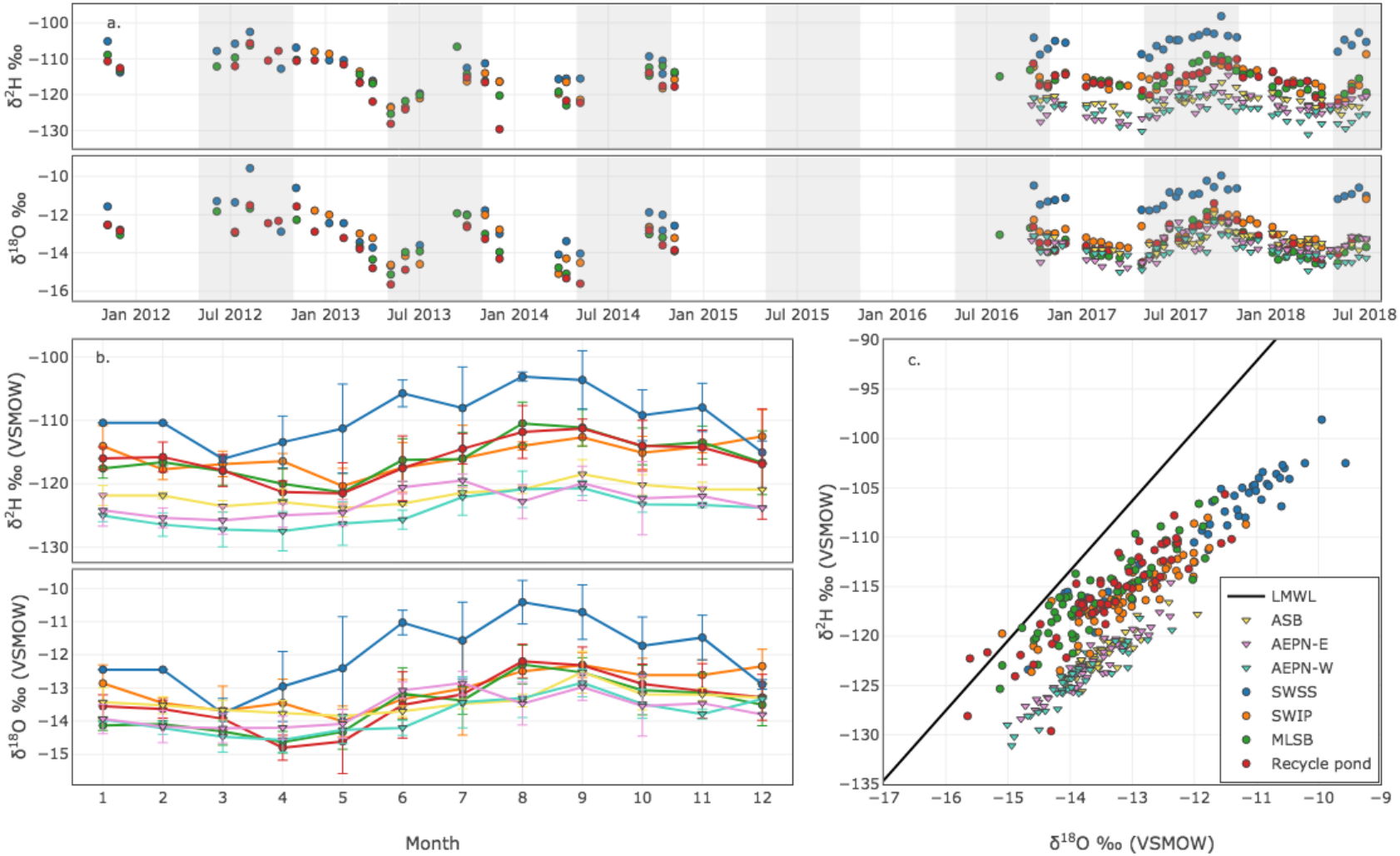

Figure 3.9 a.) Time series summary of ^{18}O and ^{2}H values of OSPW samples collected from tailings ponds at Mildred Lake Mine (n=220) from a 6-year period (2012-2018) and Aurora North Mine (n=129) from a 2-year period (2016-2018), b.) Monthly means of each tailings pond with standard deviations, and c.) OSPW samples plotted in dual isotope space along the LMWL.

The MLSB samples plotted closer to the LMWL than the other ponds, while the recycle pond samples generally clustered in the middle of all the total OSPW samples representing a mixture of the three tailings ponds. Based on the observable similarities of the recycle pond to the tailings ponds (*Fig. 3.9c*) it is assumed that the recycle pond is a fair representation of the recycle water circuit as a whole.

Table 3.2 shows the annual mean, maximum and minimum $\delta^{18}O$ and $\delta^{2}H$ values from MLSB, SWIP, and the recycle pond. SWSS was excluded due to the suspected limited connectivity to the RCW circuit based on observed isotopic trends (further discussion provided in Section 3.5.4). The recycle water circuit appears to enrich annually on average by 2.74‰ and 12.24‰ for ^{18}O and ^{2}H respectively, although not all years have been sampled during the primary periods of peak depletion (spring freshet) or evaporation (late summer/early fall). At an annual time scale the RCW circuit seems to be operating under isotopically steady state conditions. Maximum enrichment year over year was in the ranges of -11‰ to -12‰ and -105‰ to -110‰ for ^{18}O and ^{2}H respectively. The highest degree of enrichment observed was in 2013 when $\delta^{18}O$ and $\delta^{2}H$ values enriched by 24% (3.87‰) and 18% (23.01‰) respectively. This was also the year that presented the most depleted $\delta^{18}O$ and $\delta^{2}H$ values (that occurred in early spring); most likely attributed to the highest SWE volumes (73 mm) from our observation period.

Table 3.1 Annual statistical analysis of MLSB, SWIP, and recycle pond grouped together to represent the recycle water circuit.

	$\delta^{18}O$ [‰]						$\delta^{2}H$ [‰]					
Year	n	Mean	STD	CV	Min	Max	n	Mean	STD	CV	Min	Max
2011	4	-12.74	0.26	-2.04	-13.06	-12.53	4	-111.32	1.92	-1.72	-113.13	-108.90
2012	11	-12.19	0.55	-4.51	-12.95	-11.51	11	-109.39	2.18	-1.99	-112.13	-105.65
2013	26	-13.59	1.05	-7.73	-15.65	-11.93	26	-118.19	5.59	-4.73	-129.62	-106.61
2014	18	-13.88	0.99	-7.13	-15.61	-12.64	18	-117.10	3.51	-3.00	-122.97	-112.00
2016	16	-13.22	0.51	-3.86	-13.96	-12.27	16	-115.08	1.95	-1.69	-118.00	-111.30
2017	64	-13.07	0.76	-5.81	-14.58	-11.40	64	-114.78	2.82	-2.46	-121.00	-108.90
2018	34	-13.68	0.66	-4.82	-14.59	-11.17	34	-117.94	2.87	-2.43	-122.90	-108.70

Figure 3.9a shows the samples collected from Aurora North Mine presented alongside the Mildred Lake Mine tailings samples to assess the influence of their hydraulic connectivity. Aurora North Mine initially relied on clarified water supplied by Mildred Lake Mine for bitumen extraction; with water demand decreasing from 21.3 Mm^3 in 2012 to 8.4 Mm^3 in 2016 as basal aquifer pumping has become the primary source to meet water demands. Aurora North returns an average of 3.7 Mm^3 of water in the form of bitumen froth to Mildred Lake Mine annually. ^{18}O values are similar to those at Mildred Lake Mine site and follow the same magnitude of seasonal enrichment (*Fig 3.9b*). However, ^{2}H values are consistently lower than those at Mildred Lake mine by approximately 10-15 ‰. This leads to the Aurora samples plotting as an isolated cluster from the Mildred Lake samples in dual isotope space (*Fig. 3.9c*). The enrichment slopes from each mine site, calculated by regression analysis of ^{18}O and ^{2}H in dual isotope space, are somewhat similar with the Mildred Lake Mine and Aurora North Mine equal to 4.20 and 4.54 respectively. This represents similar evaporative conditions at each mine site.

Tailings slurry samples (n=41) were collected between the years 2013-2018 ranging from -14.82 ‰ to -11.75 ‰ and-124.10 ‰ to -106.90 ‰, with a mean of -13.58 ‰ and -117.89 ‰ for ^{18}O and ^{2}H respectively (*Table. A3.7*). When plotted temporally, the ^{18}O and ^{2}H values of the tailings slurry track closely with the recycle pond values over time (Fig 3.10a). The recycle pond values are even slightly more enriched than the tailings slurry, potentially due to evaporative enrichment.

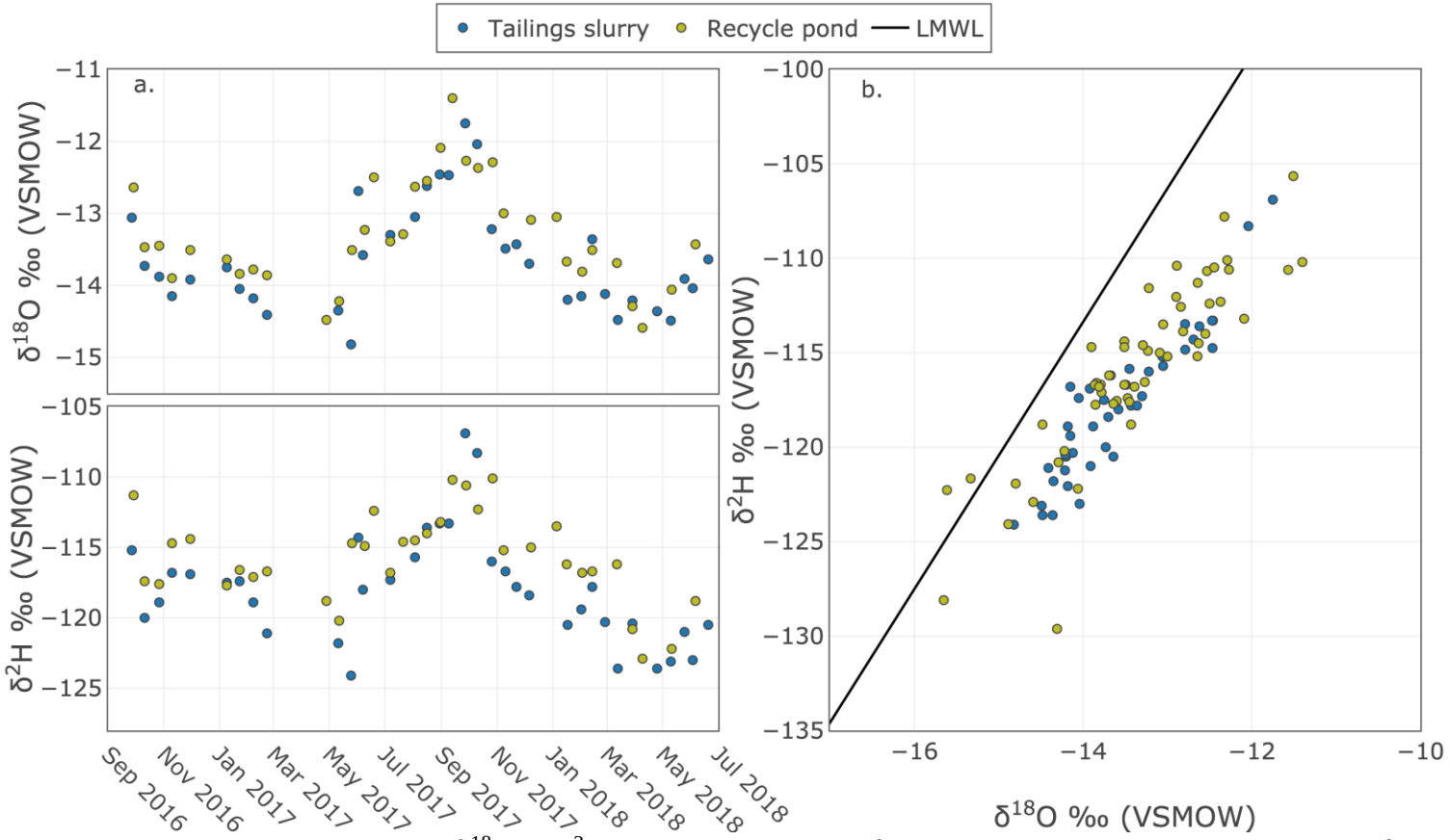

Figure 3.10 a.) Temporal evolution of ^{18}O and ^{2}H in samples collected from the recycle pond and tailings slurry feed line at Mildred Lake mine. b.) Isotopic signatures of the recycle pond and tailings slurry samples plotted in dual-isotope space.

This enrichment of the recycle pond in relation to the tailings slurry is more prominent when plotted in dual isotope space (*Fig. 3.10b*) with most of the recycle pond samples plotting further away from the LMWL.

3.5 Discussion

3.5.1 Tracing meteoric waters through the RCW circuit

Isotopic signatures of meteoric waters were observed to display consistent seasonal patterns. Highly enriched precipitation values were observed during mid-summer convective events, while precipitation in late season rain and snowfalls occurring during cooler temperatures had negative signatures in comparison to warmer months. The isotopic composition of snow was the most depleted of all sampled precipitation since these signatures are set at the times of coldest air temperatures. The most enriched monthly means occurred in June-August and showed progressively more negative values over the months of September-November as temperatures cooled (*Table. A3.1*). These seasonal trends can be seen in the distribution of individual precipitation samples plotted in dual isotope space and categorized by month of collection (*Fig. 3.2b*). Meteoric waters enter and mix with the current stores of OSPW through direct contact with the open water tailings ponds and as direct surface runoff during spring melt events. Our observations of the RCW circuit indicate that the influence of individual precipitation events on the RCW circuit cannot be observed in the signatures of individual tailings ponds, but the influence of larger seasonal events such as the spring freshet can be observed.

Cumulative evaporation and sublimation (evapo-sublimation) and melt can contribute to enrichment of the snowpack over the winter and spring seasonal cycles as melting progresses (Moser and Stichler 1975; Clark and Fritz 1997; Taylor et al., 2002). Nevertheless, minimal evidence was found for evapo-sublimation of our snowpack samples based on the range of observed isotopic compositions within the snowpack. As a result, the assumption that the average value of the snow samples collected are a representative bulk estimate of snowmelt input to surficial waters on site was applied. This is consistent with Lee et al., (2010) who found the mean isotopic values of new

snow, snowpack, and meltwater were not significantly different based on observations of temporal variation of the isotopic composition of the evolving snowpack and melt.

The intersection of the LEL with the LMWL has been commonly used to estimate the representative isotopic signature of source waters to surface ponds (Gat 1996; Gibson et al., 2005). Employing this approach for the case of the Mildred Lake reclaimed areas, these source waters are primarily associated with snow melt runoff. The LEL was developed for three shallow ponds on reclaimed sites at the Mildred Lake mine using samples collected throughout 2003 to 2018 between May and November. The point of intersection of the LEL with the LMWL was -23.2‰ and -178.5‰ for ^{18}O and ^{2}H respectively. This was interpreted as the upper boundary of the potential snowmelt signature and is more enriched than the average observed snow pack signature ($\delta^{18}O$ = -24.67‰ and $\delta^{2}H$ = -191.04‰). However, in reality this intersection point is representative of both the contribution of rain and snowmelt (*i.e.* volume-weighted annual precipitation signature) and will be enriched beyond the snowmelt signature due to the contribution of rainfall. Therefore, our estimates of the snowmelt signature based on the average values observed through the snowpack are assumed to be reasonable.

Our comprehensive isotope dataset of meteoric waters shows the large variability of isotopic composition of individual precipitation events. Consequently, when using isotope mass balance modelling to assess water balance parameters of the RCW circuit, individual precipitation events may be nearly impossible to distinguish. Therefore, seasonal or annual volume-weighted averages of the isotopic signature of meteoric waters are required. The data presented here suggests predictable seasonal patterns of the precipitation isotopic signatures based on the collection of 9 years of isotopic data. As such, $\delta^{18}O$ and $\delta^{2}H$ values of rain and snow were developed that can be used monthly (non weighted and amount weighted means) as well as an annual weighted precipitation isotopic signature to be used for conceptual and numerical model development within the Alberta Oil Sands Region.

3.5.2 Tracing river import to the RCW circuit

Low isotopic variability was observed within the samples collected from the Athabasca River, which may suggest the influence of "old" (*i.e.* Devonian and/or

Cretaceous) groundwater sources on isotopic composition of the Athabasca River, as discussed in Ellis and Jasechko (2018). There was a lag in the spring freshet signal of the Athabasca River samples when compared to the surface water bodies sampled on-site. Such evaporated surface waters generally exhibited this depletion trend earlier in the spring (May/June) rather than late spring-early summer (June/July) as observed in the Athabasca River. This lag is likely due to the influence of glacial melt headwaters that feed the Athabasca River.

Mildred Lake Reservoir (MLR) is used to hold the raw water imported on site from the Athabasca River. The volume of stored raw water in MLR is dependent on site water demands, with annual volumes ranging from 4.0 - 5.5 Mm^3, representing an average depth of 5 m (D. Heisler, personal communication. 2018). The reservoir is exposed to meteoric water inputs both as direct precipitation and surface runoff and melt events. MLR does freeze over during the winter, with ice on occurring generally in November and ice off in April/May; however, MLR does still receive water from the Athabasca and supply water to the mine site throughout the ice-on period.

When the samples collected in 2013 and 2014 are plotted in dual isotope space alongside the Athabasca River data there is a clear separation between the two years (*Fig. 3.11*). The 2013 data are constrained primarily by the Athabasca samples whereas all of the 2014 are more enriched than the 2013 samples and plot outside of the Athabasca River samples.

In 2013 (n=8) the mean of the samples is -17.75‰ and -141.58‰ for ^{18}O and ^{2}H respectively, which is almost identical to the Athabasca River mean ($\delta^{18}O$ = -17.93; $\delta^{2}H$ = -142.81), and had an $\delta^{18}O$ maximum and minimum of -17.36 ‰ and -18.91 ‰ respectively ($\delta^{2}H$ = -136.50 ‰ and -145.01 ‰). In 2014 (n=8) the mean of the $\delta^{18}O$ and $\delta^{2}H$ samples was -15.03‰ and -130.6‰ respectively, with a maximum and minimum of -14.66 ‰ and -15.75 ‰ for $\delta^{18}O$, and -125.28 ‰ and -136.67 ‰ for $\delta^{2}H$. The 2014 observed isotopic signatures displayed no overlap with the Athabasca samples when plotted in dual isotope space.

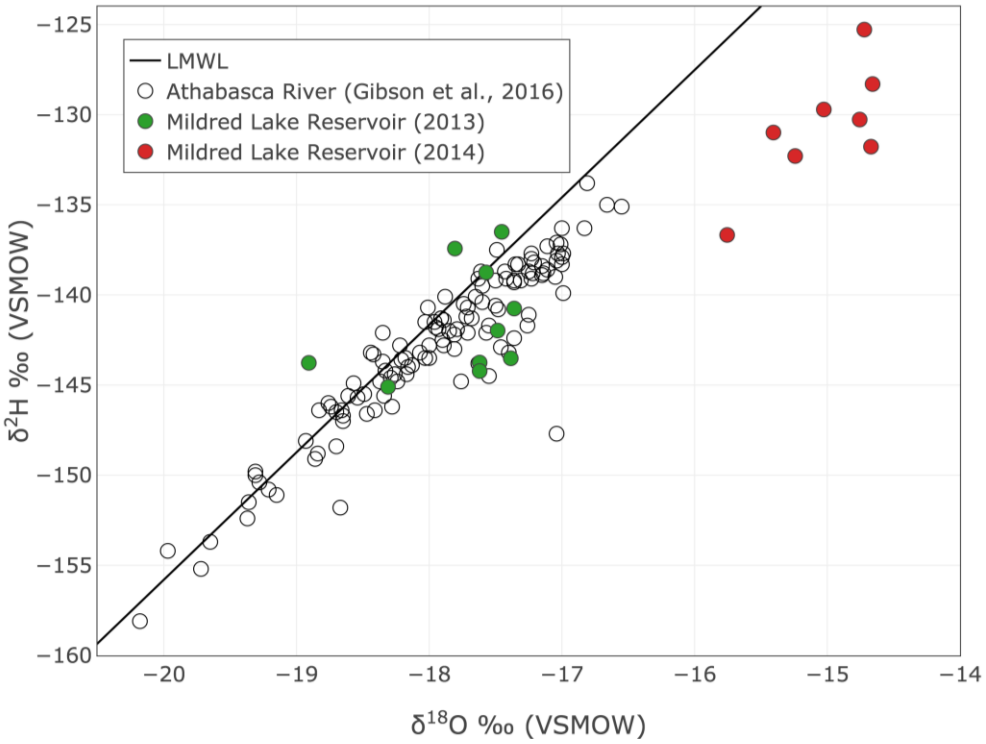

Figure 3.11 Dual isotope plot of Mildred Lake Reservoir samples from 2013 and 2014 with Athabasca River samples.

The pumping rates from MLR to site were higher in 2013 between April and October than 2014 (*i.e.*, 4.52 Mm^3 compared to 3.51 Mm^3 in September; *Table. 3.2*), which encompass the open water period when evaporative enrichment would be occurring. The variation in water volume of MLR in relation to the monthly pumping rates will affect the residence time of the MLR. Based on the range of volume and pumping rates provided by SCL, it is possible that a full turnover of MLR may occur at a monthly timescale, limiting the build-up of enriched isotopic values within the reservoir from evaporative fractionation. In 2014, less water was pumped to the mine from MLR monthly when compared to 2013. These differing pumping rates likely contributed to the difference in observed isotopic signatures of MLR between years due to longer residence times facilitating evaporative enrichment. However, based on estimates from a fraction-dependent enrichment model encompassing volume reduction resulting from evaporation (details outlined in Gonfiantini, 1986), a reduction in volume by 10%, or 500 mm of evaporation, is required to shift the isotopic composition of the average Athabasca River signature to the 2014 average MLR signature. A maximum residence time of two months

is estimated using the maximum volume (5.5 Mm^3) and lowest monthly pumping rate from 2014 (2.64 $Mm^3\,month^{-1}$).

Based on average potential evapotranspiration rates of ~500 mm yr^{-1} for the region it is not plausible that this degree of evaporation would occur over this short period. Therefore, these samples are believed to be an anomaly potentially resulting from a change in sampling protocol (*i.e.*, artifact of edge water sampling). Unfortunately, these samples were collected as part of the initial study performed by Baer et al. (2016) and protocol cannot be verified. As a result, the MLR isotopic signature is believed to be primarily controlled by the Athabasca River composition due to high pumping rates and low residence time. This needs to be confirmed with further sampling of MLR.

Table 3.2 Raw water imported to site for each month during 2013 and 2014. All volumes are in Mm^3. Coefficient of variation is calculated between years.

Year	Jan	Feb	Mar	Apr	May	June	July	Aug	Sept	Oct	Nov	Dec
2013	3.20	2.78	2.97	3.18	3.75	4.31	3.96	4.28	4.52	3.96	3.14	3.31
2014	3.24	2.86	3.21	3.02	2.64	2.89	3.44	3.55	3.51	3.66	3.47	3.45
CV (%)	0.62	1.42	3.88	2.58	17.37	19.72	7.03	9.32	12.58	3.94	4.99	2.07

3.5.3 Cooling tower blowdown

The raw water drawn from MLR is primarily used to support upgrading of bitumen. The upgrader requires imported fresh or ‘raw’ water rather than recycled tailings water because the chemical composition of OSPW can lead to scaling and corrosion of equipment negatively affecting the efficiency of the upgrading process. The raw water requirement is met by diverting freshwater from the Athabasca River and represents one of the largest uses for imported raw water on site (Matte, 2005; Zubot, 2010). This imported raw water is also circulated through evaporative cooling towers to cool heated process units and vessels within the upgrader and extraction plant.

The recirculating system works by using water stored in a basin and passing it through a process unit or vessel that requires cooling. The heated water is then returned to a cooling tower where the water is dispersed onto fill media providing maximum surface area for the water to collect. As the hot water interacts with circulating warm air within

the cooling tower a percentage will evaporate removing heat from the water. The cooled water is collected in a basin at the base of the cooling tower and recirculates throughout the circuit.

The make-up water or imported freshwater within the cooling tower circuit contains dissolved impurities that are not removed during evaporation. As the water goes through cycles of circulation the dissolved solids will become increasingly concentrated. A blowdown stream exists from the cooling towers to remove a portion of the water from the basin to be replaced with freshwater. Blowdown and freshwater additions maintain low levels of dissolved impurities and also balances the losses from evaporation. The blowdown stream is the point where water used in the upgrading process joins the recycle water circuit supplementing water supply for extraction purposes.

There are four different operational cooling towers on site (Utility, CAP, UE-1, Upgrading), with varying operating conditions resulting in a range of COCs and blowdown volumes (*Table. A3.5).* Initially each of the four cooling towers were sampled once each in April and May of 2016. In the fall of 2016, a higher frequency sampling campaign (bi-weekly) was initiated, although it was limited to the upgrading cooling tower due to limitations of sampling access on site.

The isotopic composition of cooling tower blowdown is largely controlled by the amount of cycles (and resulting evaporative enrichment) water has experienced. However, if the isotopic composition of the input water varies seasonally (*ie.* storage reservoir experiences enrichment from open water evaporation) this signal may persist in the blowdown composition — although largely overshadowed by the evaporation enrichment during cooling tower processes.

Our modelling efforts have demonstrated that the cooling tower blowdown signatures may actually be more sensitive to internal and external climate conditions (*i.e.*, humidity and temperature) affecting evaporative fractionation of ^{18}O and ^{2}H. The annual mean relative humidity on-site was 71%, with a minimum of 22% and maximum of 99%. Initially, the humidity levels were speculated to be high (*i.e.*, near ~100%) within the cooling towers due to high evaporation rates; however, it appears that humidity levels may decrease as the ambient air temperature increases within the cooling towers, influenced potentially by the air circulating through the towers from outside. Air needs to

be circulated constantly from outside the cooling towers through the interior to prevent saturation of atmospheric moisture within the chamber limiting evaporation. Therefore, the internal conditions will be affected by the climatic seasonality on site. Variations in climatic conditions will affect the slope of enrichment as evaporation is occurring. Humidity will be higher when cooler air is circulating through the cooling towers since it can hold less moisture than warm air. Humidity and temperature appear to influence the slope of the EL, but do not play a consistent role in the extent of enrichment. This is demonstrated by inconsistent extent along the EL when sorted by month in dual isotope space (*i.e.,* samples collected in the spring are some of the most depleted as well as enriched values in *Fig. 3.4*).

The design of cooling towers leads to the release of water vapour as steam at the top of the tower. Based on this the cooling towers may be operating somewhere between an open and closed system. The closed system behaviour may be due to the high humidity near the evaporative media causing constant interaction between the water vapour and liquid reservoir. However, the ambient air conditions may change as the distance from this evaporative interface is increased towards the cooling tower opening. Circulation of air from outside the towers also provides unsaturated air with varying δ_A values that will affect the evaporative fractionation.

Within this work I have developed integrated blowdown signatures from all four towers, both monthly and annually, using parameters found to best fit the limited cooling tower isotope data. The monthly-integrated isotopic cooling tower compositions appear to reflect the expected influence that seasonal shifts in climatic parameters would have on evaporative fractionation within the cooling towers.

3.5.4 OSPW isotope signatures and hydraulic connectivity of site wide waters

This study aims to not only characterize the contributing source waters to the recycle water circuit as well the isotopic evolution of the system itself, but also provide an initial assessment on the feasibility of the isotope tracer methods to estimate hydrological processes, such as evaporative pond losses, based on the limited hydrometric data available from water management operations at SCL. The most

common approach for isotope mass balance studies of natural systems to assess water balance parameters like evaporation or groundwater flux is to assume the system is in isotopic and hydrologic steady state annually (Gibson et al., 2014; Gibson et al., 2016a). Here I show that although the same water is recycled year over year, with the exception of water lost to evaporation, there are consistent levels of depletion in spring and enrichment in fall for both ^{18}O and ^{2}H each year based on our six years of sampling—thus verifying the steady state assumption for isotope mass balance considerations.

At Mildred Lake Mine site, water samples were collected from the three largest and most active tailings ponds (SWSS, MLSB, and SWIP), as well as the recycle pond. Clarified OSPW is drawn from all tailings ponds concurrently and stored in a centralized location, the recycle pond, to provide "recycled" water to meet operational demands — primarily extraction of bitumen and hydrotransport of tailings. Therefore, samples collected from the recycle pond should represent the overall isotopic signature of the RCW circuit.

Samples collected from SWSS between 2016 and 2018 were observed to have enriched beyond the rest of the sampling points within the RCW circuit, whereas in previous years isotopic signatures from all sampling points within the RCW circuit were quite similar. This shift in the SWSS signature was believed to be indicative of operational changes to SWSS altering the degree of hydraulic connectivity to the RCW circuit. SCL was able to confirm that in 2017, the placement of fresh tailings from extraction to SWSS stopped and only mature fine tailings (tailings that have undergone some form of dewatering) are transferred to the pond while clarified water is still removed for recycling (D. Heisler, personal communication, 2019). These changes allow for a higher degree of enrichment resulting from evaporative fractionation, as there could be noticeable volumetric loss within the pond. Ending the deposition of fresh tailings to SWSS also halts the mixing of tailings porewater to the overall clarified water within the tailings pond.

Samples were collected from three tailings ponds (AEPN-E, AEPN-W, and ASB) at Aurora North mine. These samples were analyzed alongside the Mildred Lake mine samples to investigate the influence of the hydraulic connectivity between the two mine sites on the overall isotopic composition of the RCW circuit.

The temporal signatures between the two mine sites indicate that although the mine sites are hydraulically connected, the source waters to each influence the evolution of the isotopic signatures within the tailings ponds. Source waters to the Mildred Lake Mine site have been extensively reviewed in the previous sections. However, Aurora North Mine currently relies on a regional aquifer composed of water-saturated sands in the Lower McMurray Formation. Based on 58 samples collected from a groundwater-monitoring network surrounding the Aurora Settling Basin that access the basal aquifer, mean $\delta^{18}O$ and $\delta^{2}H$ values are -19.92 ‰ and -158.76 ‰ respectively with standard deviations of 0.76 and 4.20. These values are quite different from the mean Athabasca River signature of $\delta^{18}O$ = -17.93 ‰ ($\delta^{2}H$ = -142.81 ‰) that is representative of the primary source water to Mildred Lake mine prior to the influence of mining processes. As a result, the RCW circuit cannot be assessed as a whole between the two sites. This also highlights the importance of understanding the isotopic signatures of source waters and their volumetric contributions to an engineered system for isotope tracer studies.

The tailings ponds at Mildred Lake Mine and Aurora North experience clear seasonal trends that are similar to a natural lake system. The periods of open water evaporation (May-Oct) indicated by the shaded areas in *Fig. 3.10a*, all display enrichment with the exception of 2012 where data is sparse. A downward spike in $\delta^{18}O$ and $\delta^{2}H$ during springmelt is representative of the influence of snow and ice melt and associated runoff to the ponds observed in cold region lakes.

The samples also progress in a linear pattern away from the LMWL indicative of evaporative fractionation. The further away the samples are from the LMWL the more fractionation they have experienced as a result of phase change — in this case evaporation leading to enrichment (Gibson et al., 2016b).

200 Mm^3 of OSPW circulates through the recycle water circuit annually to meet on site water demands for operations. This represents high pumping rates both removing water from the ponds but also returning it in the form of fluid tailings, also referred to here as tailings slurry. As the fluid tailings settle, pore water that was bound by extraction and transport processes is released to be reused in operations. Therefore, the three main inputs to the recycle water circuit are meteoric water, cooling tower blowdown, and pore water released from the settlement of fluid tailings.

The tailings slurry composition should be similar to that of the recycle pond and by association the tailings ponds since the water bound within it is composed of the clarified OSPW removed from the tailings ponds. If evaporation occurred during the extraction or hydrotransport processes, which reuses the OSPW, the tailings slurry would be more enriched than the tailings ponds upon deposition signifying the occurrence of fractionation.

3.5.5 A conceptual model of mine source waters and the RCW circuit from an isotope perspective

Here I present a conceptual model of how water is imported and circulated through an oil sands mine from an isotope perspective as perceived by our isotopic assessment (Fig. 3.12). Raw water is sourced from the Athabasca River, which has been shown to have a relatively stable isotopic composition with little seasonal variation when compared to other mine site waters. This water is stored in a reservoir (MLR) and is pumped at varying rates to meet operational water demands. Our samples indicate that when water demands are high (*i.e* high pumping rates from MLR), the isotopic signature of the reservoir is reflective of the imported river water due to low residence time. However, if pumping rates are low in high evaporative months (*i.e.*, late summer) the residence time may be high enough for the observable enrichment resulting from evaporative fractionation.

This raw water is primarily used for bitumen upgrading processes and is circulated through process units and cooling towers. The cooling towers are postulated as the dominant mechanism responsible for enriching the isotopic signature of raw water originating from the Athabasca River before it enters the RCW circuit. As heat is lost from the evaporation of water with each recirculation, isotopic enrichment occurs within the water as evaporation progresses. The isotopic signature of the cooling tower blowdown varies depending on the number of cycles, and the internal and external climatic conditions (*i.e.*, temperature and humidity). This reliance on climatic conditions affects both kinetic and equilibrium fractionation. Once dissolved impurities within the recirculated water have become too high, the water is released as blowdown to current stores of OSPW held within tailings ponds making up the RCW circuit. Mixing

calculations to assess the influence of cooling tower blowdown on the RCW circuit are provided in Appendix B.

This blowdown stream will then mix with the current stores of clarified OSPW or "recycle" water contained within the tailings ponds of the RCW circuit. Analysis of isotopic signatures of the clarified OSPW collected within this study demonstrated that the isotopic signature within the various storage facilities of the RCW circuit fluctuates seasonally but appears to be in an isotopically steady-state at an annual time scale. The isotopic composition of the RCW circuit appears to replicate typical seasonal patterns associated with natural systems in cold lake regions. Depleted OSPW signatures were observed following the spring melt of depleted snow accumulated on both the ponds, and across the site. A systematic enrichment of OSPW was observed over the duration of the open water period attributed to evaporative fractionation resulting in isotopic enrichment within the RCW circuit. The RCW circuit remains active throughout the winter despite freeze-up of the tailings pond surfaces. OSPW samples collected throughout the ice-on period demonstrated progressive isotopic depletion. This pattern is believed to be in part due to fractionation during the formation of ice as heavy water molecules preferentially freeze, and to the release of OSPW from tailings pore water during fluid tailings settlement. Further commentary on isotope fractionation during ice formation is provided in Appendix B.

The tailings ponds act as both storage facilities for OSPW and settling basins for fluid tailings created during the extraction of bitumen from ore. OSPW originally used for extraction is returned to the tailings ponds as a tailings slurry, where settling and consolidation of the fluid tailings releases the pore water comprised of OSPW. The continuous mixing of liberated tailings pore water during the ice-on period is likely to be contributing to the progressive isotopic depletion of the RCW circuit throughout the winter.

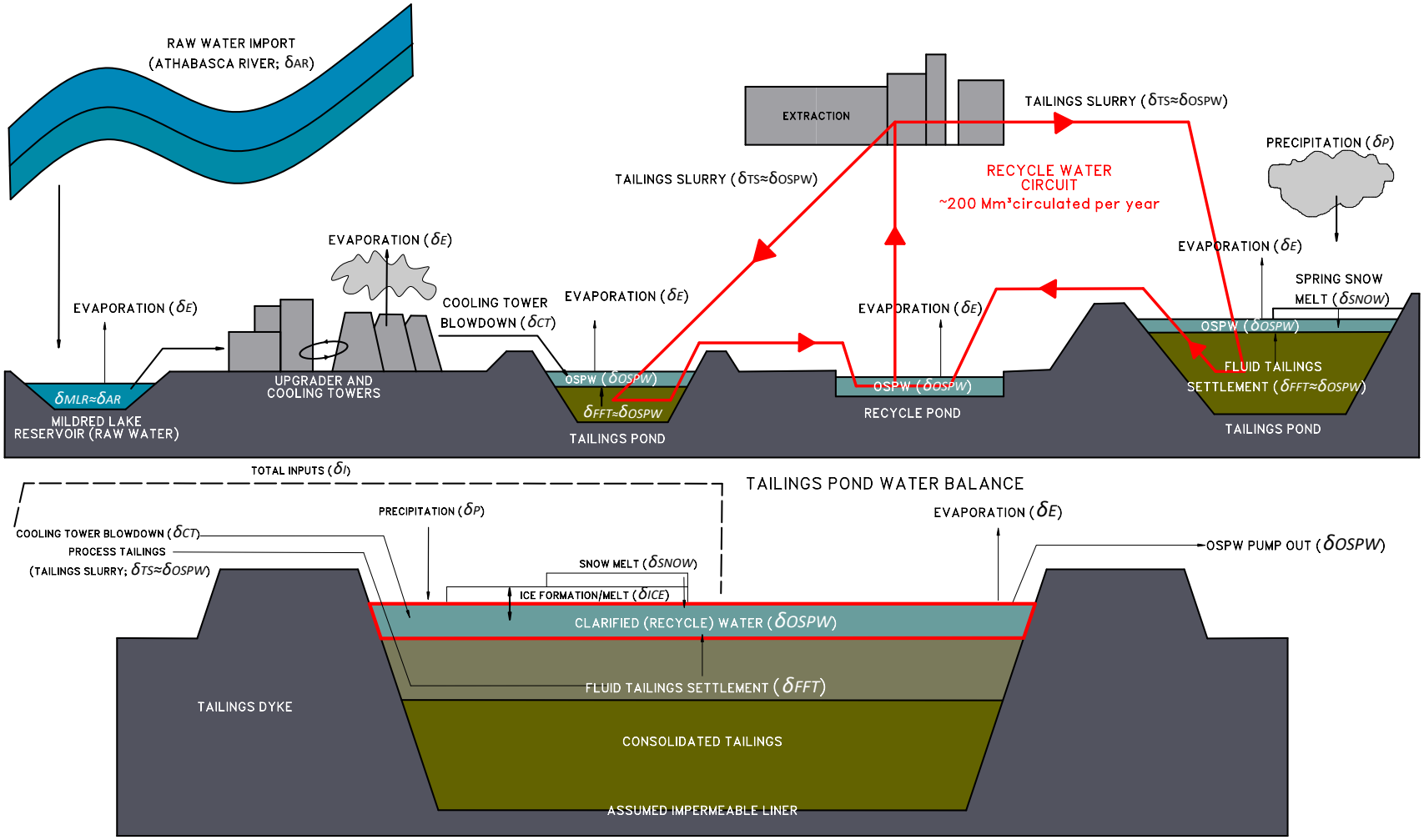

Figure 3.12 Diagram illustrating raw water import to an oil sands mine, recycling of process water, and a standard water balance of a tailings pond.

In order to assess the fractionation associated with evaporative losses from the recycle water circuit, the contributing waters making up the input signature must be fully understood. The further away the system plots away from the input signature the more evaporation it has experienced. Past studies implementing isotope mass balance techniques to assess water balance parameters of natural systems have primarily used the annual weighted precipitation signature to represent input to the system often estimated as the intersection between the LEL of the water body and the LMWL (Edwards et al., 2004; Gibson et al., 2014; Kang et al., 2017). However, as outlined above, engineered systems such as this mining water circuit involve complex mixing and fractionating processes contributing to the overall reservoir signature when compared to natural systems. Therefore, such simplifications as estimating the total input signature to the system by means of intersecting the LEL and LMWL are not applicable. Fractionation of naturally occurring source waters (*i.e.*, river import or groundwater) is affected by mining operations before it can be added to the RCW circuit.

The clarified water within the recycle water circuit is mixed with input waters involved in mining processes such as cooling tower blowdown and pore water expressed during tailings settlement. The deposition and settlement of the fluid tailings as tailings slurry is in essence just redistribution of water within the system. However, when removed for extraction or bound within tailings it is unavailable to experience evaporative enrichment. The $\delta^{18}O$ and $\delta^{2}H$ values of tailings slurry samples are similar to those of the Mildred Lake tailings ponds. Therefore, from an isotope mass balance perspective the tailings settlement may act as a buffer to evaporative enrichment and the annual mean tailings slurry signature should be an appropriate value to represent the contribution of fluid tailings settlement at any given time within the system. Settlement rates and volumes of fluid tailings are difficult to monitor and require complex models due to the scale of operations and dynamic nature of oil sands operations on site. Therefore, there is still much work to be done in assessing the overall isotopic evolution of tailings stores and their contribution to the RCW.

3.6 Concluding remarks

The RCW circuit is crucial to minimizing the demand for freshwater in oil sands mining operations. Isotope tracers provide the opportunity to quantify site wide water balance parameters, such as meteoric water inputs and evaporative losses, which are difficult for industry to directly measure. Better understanding of these parameters would aid in improving efficiency of site wide water use and management.

Within this work I characterized both the temporal evolution of the isotopic signatures of source waters to an oil sands mine and the process-affected waters that make up the RCW circuit based on a bi-weekly water isotope-monitoring program at SCL's oil sands mine in the Alberta Oil Sands Region, which builds upon previous isotope monitoring programs at this site (Baer et al., 2016). Following this characterization, I developed a conceptual model outlining the isotopic evolution of raw water as it transitions from a freshwater signature, to one reflective of oil sands mining processes. This model highlighted primary mixing and phase change mechanisms during water cycling contributing to the unique isotopic signature of OSPW observed relative to naturally occurring waters within the Alberta Oil Sands Region.

This study has shown that the RCW circuit exhibits seasonal isotopic patterns characteristic of cold region reservoirs, specifically a rapid depletion following the spring freshet, which is then followed by systematic enrichment during the open water period. Interannually, the RCW circuit appears to be in an isotopically steady state, with isotopic signatures collected from the late summer and fall (*i.e.,* following prime evaporative months) consistently falling between -11 ‰ to -12 ‰ and -105 ‰ to -110 ‰ for ^{18}O and ^{2}H respectively. Expressed pore water released from the settlement of fluid tailings appears to be contributing to a systematic depletion of the clarified OSPW stores within the RCW circuit during the ice-on period.

Isotopic signatures and temporal trends were found to be similar within the three tailings ponds sampled throughout the RCW circuit, as well as the recycle pond, which acts as a storage reservoir for clarified OSPW to the extraction plant. I postulate that interconnectivity between each reservoir in the RCW circuit, and high pumping rates resulting in low residence times of clarified OSPW in each pond have contributed to an

isotopically well-mixed system. This finding allows for the isotopic signatures collected from the recycle pond - the collection point for all clarified OSPW pumped from ponds - to act as a proxy for the entire RCW circuit. This finding will aid in future isotope mass balance work for quantifying water balance parameters.

This study not only provides a detailed presentation of mine site waters from the Alberta Oil Sands Region but provides the initial characterization of how source waters will impact the evolution of an operating recycle water circuit both resulting from seasonality and mining operations leading to mixing and fractionation. The observed seasonal enrichment within the recycle water circuit associated with the open water period provides evidence for the implementation of isotope mass balance studies to estimate evaporative losses from tailings ponds. Future work is currently underway to apply isotope mass balance techniques to the recycle water circuit, as well the first demonstration end pit lake located within the oil sands region.

3.7 References

Allen, D. M., & Voormeij, D. A. (2002). Oxygen-18 and deuterium fingerprinting of tailings seepage at the Sullivan Mine. *Mine Water and the Environment*, *21*(4), 168-182.

Arnason, B. (1969). The exchange of hydrogen isotopes between ice and water in temperate glaciers. *Earth Planet Sci Lett*, *6*, 423-430.

Baer, T., & University of Saskatchewan, College of Graduate Studies Research. (2014). *An Evaluation of the Use of Natural Stable Isotopes of Water to Track Water Movement through Oil Sands Mine Closure Landforms*.

Baer, T., Barbour, S. L., & Gibson, J. J. (2016). The stable isotopes of site wide waters at an oil sands mine in northern Alberta, Canada. *Journal of Hydrology*, *541*, 1155-1164.

Barbour, S. L., Hendry, M. J., & Carey, S. K. (2016). High-resolution profiling of the stable isotopes of water in unsaturated coal waste rock. *Journal of Hydrology*, *534*, 616-629.

Buttle, J. M. (1994). Isotope hydrograph separations and rapid delivery of pre-event water from drainage basins. *Progress in Physical Geography*, *18*(1), 16-41.

Clark, I., & Fritz, P. (1997). *Environmental isotopes in hydrogeology*. Boca Raton, FL: CRC Press/Lewis.

COSIA Water EPA (2019). 2018 Water Research Report. Canada's Oil Sands Innovation Alliance. https://www.cosia.ca/sites/default/files/attachments/COSIA%20Annual%20Report%202018_WATER_FINAL%20Nov%2021_0.pdf

Craig, H. (1961). Isotopic variations in meteoric waters. *Science*, *133*(3465), 1702-1703.

Craig, H., & Gordon, L.I. (1965). Deuterium and oxygen 18 variations in the ocean and marine atmosphere. In *Stable Isotopes in Oceanographic Studies and Paleotemperatures,* E. Tongiorgi (Ed.) pp. 9-130, Laboratorio di Geologia Nucleare, Pisa.

Dansgaard, W. (1964). Stable isotopes in precipitation. *Tellus*, *16*(4), 436-468.

Dincer, T. (1968). The use of oxygen 18 and deuterium concentrations in the water balance of lakes. *Water Resources Research*, *4*(6), 1289-1306.

Dompierre, K. A., & Barbour, S. L. (2016). Characterization of physical mass transport through oil sands fluid fine tailings in an end pit lake: a multi-tracer study. *Journal of contaminant hydrology*, *189*, 12-26.

Edwards, T. W., Wolfe, B. B., Gibson, J. J., & Hammarlund, D. (2004). Use of water isotope tracers in high latitude hydrology and paleohydrology. In *Long-term environmental change in Arctic and Antarctic lakes* (pp. 187-207). Springer, Dordrecht.

Ellis, J., & Jasechko, S. (2018). Formation waters discharge to rivers near oil sands projects. Hydrological Processes, 32(4), 533-549.

Evaristo, J., Jasechko, S., & McDonnell, J. J. (2015). Global separation of plant transpiration from groundwater and streamflow. *Nature*, *525*(7567), 91.

Feng, X., Faiia, A. M., & Posmentier, E. S. (2009). Seasonality of isotopes in precipitation: A global perspective. *Journal of Geophysical Research: Atmospheres*, *114*(D8).

Gammons, C. H., Duaime, T. E., Parker, S. R., Poulson, S. R., & Kennelly, P. (2010). Geochemistry and stable isotope investigation of acid mine drainage associated with abandoned coal mines in central Montana, USA. *Chemical Geology*, *269*(1-2), 100-112.

Gat, J. R. (1996). Oxygen and hydrogen isotopes in the hydrologic cycle. *Annual Review of Earth and Planetary Sciences*, *24*(1), 225-262.

Gibson, J. (2002). Short-term evaporation and water budget comparisons in shallow Arctic lakes using non-steady isotope mass balance. *Journal of Hydrology*, *264*(1), 242-261.

Gibson, J. J., Edwards, T. W. D., Birks, S. J., St Amour, N. A., Buhay, W. M., McEachern, P., ... & Peters, D. L. (2005). Progress in isotope tracer hydrology in Canada. *Hydrological Processes*, *19*(1), 303-327.

Gibson, J. J., Fennell, J., Birks, S. J., Yi, Y., Moncur, M. C., Hansen, B., & Jasechko, S. (2013). Evidence of discharging saline formation water to the Athabasca River in the oil sands mining region, northern Alberta. *Canadian Journal of Earth Sciences*, *50*(12), 1244-1257.

Gibson, J. J., & Reid, R. (2014). Water balance along a chain of tundra lakes: A 20-year isotopic perspective. *Journal of Hydrology*, *519*, 2148-2164.

Gibson, J. J., Birks, S. J., Yi, Y., Moncur, M. C., & McEachern, P. M. (2016a). Stable isotope mass balance of fifty lakes in central Alberta: Assessing the role of water balance parameters in determining trophic status and lake level. *Journal of Hydrology: Regional Studies*, *6*, 13-25.

Gibson, J. J., Birks, S. J., & Yi, Y. (2016b). Stable isotope mass balance of lakes: a contemporary perspective. *Quaternary Science Reviews*, *131*, 316-328.

Gibson, J. J., Yi, Y., & Birks, S. J. (2016c). Isotope-based partitioning of streamflow in the oil sands region, northern Alberta: Towards a monitoring strategy for assessing flow sources and water quality controls. *Journal of Hydrology: Regional Studies*, *5*, 131-148.

Gonfiantini, R. (1986). Environmental isotopes in lake studies. *Handbook of environmental isotope geochemistry*, *2*, 113-168.

Gosselin, P., Hrudey, S. E., Naeth, M. A., Plourde, A., Therrien, R., Van Der Kraak, G., & Xu, Z. (2010). *Environmental and health impacts of Canada's oil sands industry*. Royal Society of Canada, 2010: p. 22.

Harman, C. J., & Kim, M. (2014). An efficient tracer test for time-variable transit time distributions in periodic hydrodynamic systems. *Geophysical Research Letters*, *41*(5), 1567-1575.

Horita, J., Rozanski, K., & Cohen, S. (2008). Isotope effects in the evaporation of water: a status report of the Craig–Gordon model. *Isotopes in environmental and health studies*, *44*(1), 23-49.

Huang, M., Hilderman, J. N., & Barbour, L. (2015). Transport of stable isotopes of water and sulphate within reclaimed oil sands saline–sodic mine overburden. *Journal of Hydrology*, *529*, 1550-1561.

Jasechko, S. (2016). Partitioning young and old groundwater with geochemical tracers. *Chemical Geology*, *427*, 35-42.

Jasechko, S., Wassenaar, L. I., & Mayer, B. (2017). Isotopic evidence for widespread cold-season-biased groundwater recharge and young streamflow across central Canada. *Hydrological processes*, *31*(12), 2196-2209.

Kang, S., Yi, Y., Xu, Y., Xu, B., & Zhang, Y. (2017). Water isotope framework for lake water balance monitoring and modelling in the nam co basin, Tibetan plateau. *Journal of Hydrology: Regional Studies*, *12*, 289-302.

Klaus, J., & McDonnell, J. J. (2013). Hydrograph separation using stable isotopes: Review and evaluation. *Journal of Hydrology*, *505*, 47-64.

Kuhn, W., & Thurkauf, M. (1958). Isotopic separation during the freezing of water and diffusion constants of deuterium and oxygen-18 in ice. *Helv. Chim. Acta*, *41*, 938-971.

Lee, J., Feng, X., Faiia, A., Posmentier, E., Osterhuber, R., & Kirchner, J. (2010). Isotopic evolution of snowmelt: A new model incorporating mobile and immobile water. *Water Resources Research*, *46*(11).

Matte, C. (2005). Water Conservation, Recycling and Reuse. Houston: NACE Int.

Moser, H. & Stichler, W. (1975) Deuterium and oxygen-18 contents as index of the properties of snow blankets. In: Snow Mechanics (Proc. Grindelwald Symp., April 1974), 122-135. IAHS Publ. No. 114.

O'Neill, J.R. (1968) Hydrogen and oxygen fractionation between ice and water. *Journal of Physical Chemistry, 72, 3683-3684.*

Peng, H., Mayer, B., Harris, S., & Roy Krouse, H. (2004). A 10-yr record of stable isotope ratios of hydrogen and oxygen in precipitation at Calgary, Alberta, Canada. *Tellus B*, *56*(2), 147-159.

RAMP (Regional Aquatic Monitoring Program), 2015. Steepbank Climate Station (C#-RAMP), 3 November 2010- 31 October 2014 <http://www.ramp-alberta.org/data/ClimateHydrology/climate/DailyClimate.aspx>.

Suzuoki, T., & Kimura, T. (1973). D/H and 18O/16O fractionation in ice-water system. *Journal of the Mass Spectrometry Society of Japan*, *21*(3), 229-233.

Taylor, S., Feng, X., Williams, M., & McNamara, J. (2002). How isotopic fractionation of snowmelt affects hydrograph separation. *Hydrological Processes*, *16*(18), 3683-3690.

Tetzlaff, D., Piovano, T., Ala-Aho, P., Smith, A., Carey, S., Marsh, P., . . . Soulsby, C. (2018). Using stable isotopes to estimate travel times in a data-sparse Arctic catchment: Challenges and possible solutions. *Hydrological Processes*, *32*(12), 1936-1952.

Tondu, J. M. E., Turner, K. W., Wolfe, B. B., Hall, R. I., Edwards, T. W. D., & McDonald, I. (2013). Using water isotope tracers to develop the hydrological component of a long-term aquatic ecosystem monitoring program for a northern lake-rich landscape. *Arctic, antarctic, and alpine research*, *45*(4), 594-614.

Tost, M., Hitch, Chandurkar, Moser, & Feiel. (2018). The state of environmental sustainability considerations in mining. Journal of Cleaner Production, 182, 969-977.

Turner, K. W., Wolfe, B. B., & Edwards, T. W. (2010). Characterizing the role of hydrological processes on lake water balances in the Old Crow Flats, Yukon Territory, Canada, using water isotope tracers. *Journal of Hydrology*, *386*(1-4), 103-117.

Turner, K. W., Wolfe, B. B., Edwards, T. W., Lantz, T. C., Hall, R. I., & Larocque, G. (2014). Controls on water balance of shallow thermokarst lakes and their relations with catchment characteristics: a multi-year, landscape-scale assessment based on water isotope tracers and remote sensing in Old Crow Flats, Yukon (Canada). *Global change biology*, *20*(5), 1585-1603.

Wassenaar, L. I., Athanasopoulos, P., & Hendry, M. J. (2011). Isotope hydrology of precipitation, surface and ground waters in the Okanagan Valley, British Columbia, Canada. *Journal of Hydrology*, *411*(1), 37-48.

Zimmermann, U., & Ehhalt, D. H. (1970). Stable isotopes in study of water balance of Lake Neusiedl, Austria. *Isotope hydrology*, 129-138.

Zuber, A. (1983). On the environmental isotope method for determining the water balance components of some lakes. *Journal of Hydrology*, *61*(4), 409-427.

Zubot, W. (2010). Removal of Naphthenic Acids from Oil Sands Process Water Using Petroleum Coke (Master's thesis, University of Alberta, Calgary, AB).

3.8 Appendix A

Table A 1 Summary of 9-year (2009-2018) dataset of $\delta^{18}O$ and $\delta^{2}H$ values for site wide precipitation at Mildred Lake mine site sorted by month of collection. Monthly mean, maximum, minimum, standard deviation, and coefficient of variation are calculated based on the entire sample set. Not all samples collected had measurements of the amount of precipitation from each event. As a result, the monthly amount weighted means were calculated using only samples that could be matched with corresponding amounts of precipitation occurring during each event.

	Observed												Amount weighted mean		
	$\delta^{18}O$ [‰]						$\delta^{2}H$ [‰]						$\delta^{18}O$ [‰]	$\delta^{2}H$ [‰]	
Month	Mean	Max	Min	STD	CV	n	Mean	Max	Min	STD	CV	n			n
Jan	-25.60	-20.49	-27.74	2.25	-8.79	8	-194.00	-160.80	-211.32	16.03	-8.26	8	-	-	-
Feb	-24.53	-18.47	-30.28	2.73	-11.13	30	-191.20	-143.50	-230.49	18.91	-9.89	30	-	-	-
Mar	-24.69	-20.02	-31.50	1.93	-7.82	123	-191.44	-153.80	-243.31	14.00	-7.31	123	-	-	-
Apr	-16.71	15.06	-18.84	1.94	-11.61	3	-134.50	-122.10	-146.10	12.02	-8.94	3	-16.73	-132.68	2
May	-15.82	-11.30	-20.88	2.83	-17.89	12	-127.69	-106.50	-162.00	19.75	-15.47	12	-15.94	-119.73	6
June	-14.42	-7.03	-19.20	2.66	-18.45	62	-118.92	-70.89	-156.79	19.41	-16.32	62	-14.26	-118.94	20
July	-14.52	-9.06	-18.30	2.32	-15.98	77	-118.85	-78.01	-150.26	16.93	-14.24	77	-14.23	-115.64	29
Aug	-13.86	-9.41	-20.55	2.27	-16.38	44	-116.90	-90.93	-157.78	13.66	-11.69	44	-14.33	-120.75	21
Sept	-15.69	-8.77	-19.95	2.70	-17.21	38	-127.18	-87.60	-154.60	16.49	-12.97	38	-15.59	-123.79	14
Oct	-18.35	-9.47	-26.23	3.45	-18.80	22	-144.09	-98.20	-201.62	23.32	-16.18	22	-17.63	-137.14	8
Nov	-21.19	-20.12	-21.79	0.93	-4.39	3	-161.00	-154.81	-164.70	5.40	-3.35	3	-21.65	-164.70	1
Dec*	-24.66	-	-	-	-	-	-191.04	-	-	-	-	-	-	-	-

*No samples were collected during December and therefore the mean of all snow samples collected is used to represent the stable isotope composition of December precipitation.

Table A 2 Summary of 12-year (2002-2014) dataset of $\delta^{18}O$ and $\delta^{2}H$ values from Athabasca River water provided by Gibson et al. (2016) sorted by month of collection. Monthly mean, maximum, minimum, standard deviation, and coefficient of variation are presented.

	$\delta^{18}O$ [‰]						$\delta^{2}H$ [‰]					
Month	Mean	Max	Min	STD	CV	n	Mean	Max	Min	STD	CV	n
Jan	-17.67	-17.00	-18.37	0.50	-2.83	10	-141.41	-137.20	-144.80	2.93	-2.07	10
Feb	-17.66	-17.00	-18.29	0.43	-2.43	11	-141.56	-138.30	-144.60	2.20	-1.55	11
Mar	-17.54	-16.99	-18.22	0.43	-2.45	10	-141.11	-137.70	-144.80	2.55	-1.81	10
Apr	-17.67	-17.03	-18.67	0.62	-3.51	11	-142.44	-137.70	-151.80	4.04	-2.84	11
May	-18.35	-16.55	-20.18	1.00	-5.45	11	-145.83	-135.10	-158.10	6.59	-4.52	11
June	-18.71	-17.04	-19.97	0.87	-4.65	12	-147.97	-139.30	-155.20	4.35	-2.94	12
July	-18.68	-17.57	-19.65	0.63	-3.37	10	-146.39	-141.50	-153.70	4.18	-2.85	10
Aug	-17.94	-16.81	-19.21	0.70	-3.90	10	-141.72	-133.80	-150.80	4.58	-3.23	10
Sept	-17.62	-16.99	-18.34	0.46	-2.61	10	-140.22	-137.70	-145.60	2.71	-1.93	10
Oct	-17.55	-16.66	-18.65	0.68	-3.87	10	-139.71	-135.00	-147.00	3.88	-2.77	10
Nov	-17.75	-17.11	-18.93	0.59	-3.32	9	-141.24	-137.30	-148.10	3.56	-2.52	9
Dec	-17.91	-17.25	-18.57	0.52	-2.90	8	-142.69	-138.70	-146.60	2.86	-2.00	8
All	-17.93	-16.55	-20.18	0.75	-4.18	122	-142.81	-133.80	-158.10	4.55	-3.19	122

Table A 3 Summary of $\delta^{18}O$ and $\delta^{2}H$ values from Mildred Lake surface water sorted by month of collection. Monthly mean, maximum, minimum, standard deviation, and coefficient of variation are presented.

	$\delta^{18}O$ [‰]						$\delta^{2}H$ [‰]					
Month	Mean	Max	Min	STD	CV	n	Mean	Max	Min	STD	CV	n
May	-17.94	-17.39	-18.36	0.43	-2.39	5	-17.94	-17.39	-18.36	0.43	-0.82	5
June	-18.26	-17.62	-18.91	0.91	-4.98	2	-18.26	-17.62	-18.91	0.91	-0.22	2
July	-17.05	-16.31	-17.48	0.65	-3.78	3	-17.05	-16.31	-17.48	0.65	-2.63	3
Aug	-15.56	-14.66	-17.34	1.54	-9.93	3	-15.56	-14.66	-17.34	1.54	-4.51	3
Sept	-16.26	-14.76	-17.57	1.47	-9.01	4	-16.26	-14.76	-17.57	1.47	-2.87	4
Oct	-16.26	-14.72	-17.81	2.18	-13.41	2	-16.26	-14.72	-17.81	2.18	-6.54	2
Nov	-15.40	-15.03	-15.75	0.36	-2.37	3	-15.40	-15.03	-15.75	0.36	-2.80	3
All	-16.72	-14.66	-18.91	1.41	-8.44	22	-137.49	-125.28	-145.78	6.21	-4.52	22

Table A 4 Summary of $\delta^{18}O$ and $\delta^{2}H$ values from the upgrading-cooling tower blowdown water sorted by month of collection. Monthly mean, maximum, minimum, standard deviation, and coefficient of variation are presented.

	$\delta^{18}O$ [‰]						$\delta^{2}H$ [‰]					
Month	Mean	Max	Min	STD	CV	n	Mean	Max	Min	STD	CV	n
Jan	-14.45	-13.31	-15.85	1.23	-8.50	4	-120.70	-112.40	-129.60	8.76	-7.26	4
Feb	-14.25	-13.09	-15.36	1.17	-8.23	4	-119.88	-113.40	-126.70	7.37	-6.15	4

Mar	-14.43	-13.59	-15.67	0.90	-6.21	4	-121.68	-117.50	-127.70	4.33	-3.56	4
Apr	-14.79	-12.89	-16.10	1.69	-11.40	3	-123.10	-112.60	-130.90	9.44	-7.67	3
May	-13.41	-11.50	-14.71	1.39	-10.36	4	-116.45	-107.50	-122.80	6.58	-5.65	4
June	-12.70	-11.57	-14.05	1.27	-10.02	4	-112.55	-103.40	-120.80	8.38	-7.44	4
July	-13.17	-12.74	-13.59	0.60	-4.57	2	-117.05	-114.00	-120.10	4.31	-3.69	2
Aug	-11.97	-11.77	-12.32	0.30	-2.54	3	-112.67	-109.90	-115.40	2.75	-2.44	3
Sept	-11.52	-11.05	-12.12	0.55	-4.75	3	-109.23	-106.60	-113.80	3.97	-3.63	3
Oct	-13.38	-12.58	-14.60	0.97	-7.22	4	-117.58	-113.40	-123.90	4.59	-3.90	4
Nov	-14.39	-12.76	-16.18	1.78	-12.38	4	-121.23	-110.60	-132.50	11.27	-9.30	4
Dec	-14.65	-14.65	-14.65	-	-	1	-126.50	-126.50	-126.50	-	-	1
All	-13.60	-11.05	-16.18	1.44	-10.59	40	-117.90	-103.40	-132.50	7.53	-6.39	40

Table A 5 Blowdown to the RCW circuit and COC values reported over a 15-year period (2002-2017) from operational data supplied by SCL and summarized by month and cooling tower.

		Blowdown (m^3)						Monthly COC					
Source	Month	n	Mean	STD	CV	Min	Max	n	Mean	STD	CV	Min	Max
CAP	Jan	16	38150	15551	41	19654	69472	16	4.50	1.14	25.41	2.88	6.74
	Feb	15	32663	8097	25	18441	44642	15	4.56	0.94	20.64	2.79	6.41
	Mar	16	39309	15249	39	15210	75303	16	4.50	1.02	22.56	2.61	6.20
	Apr	16	35190	14894	42	10588	73817	16	4.40	1.20	27.33	2.09	5.74
	May	16	32078	17592	55	5820	75026	16	5.00	1.62	32.32	1.76	7.35
	Jun	16	29230	12254	42	8026	51084	16	5.56	1.51	27.11	2.27	7.63
	Jul	16	36293	22636	62	4431	87246	16	5.89	1.53	25.91	3.15	7.90
	Aug	17	28346	15895	56	12832	75259	17	6.22	1.70	27.32	2.81	8.25
	Sep	17	28832	14196	49	12839	63391	17	5.93	1.84	31.04	1.75	7.98
	Oct	16	29513	13534	46	11671	59174	16	5.64	1.59	28.13	2.36	7.84
	Nov	16	33131	14107	43	14000	64834	16	5.20	1.40	26.90	2.79	7.41
	Dec	16	35022	9921	28	19599	54503	16	4.83	1.35	28.02	3.07	7.35
UE-1	Jan	14	121041	52333	43	20678	240825	14	3.45	0.60	17.32	2.11	4.17
	Feb	13	127117	71646	56	4262	249982	13	3.15	0.68	21.60	1.94	4.03
	Mar	13	128836	113480	88	33915	485256	13	3.68	0.86	23.26	1.76	4.78
	Apr	13	101204	40245	40	38520	195710	13	3.83	1.19	30.91	1.28	5.62
	May	13	100882	79883	79	19091	348786	13	4.47	1.48	33.10	1.56	6.57
	Jun	13	109835	49593	45	58643	235828	13	4.30	1.33	30.84	1.94	6.83
	Jul	13	113863	32334	28	75108	192471	13	4.37	1.08	24.71	3.28	6.49
	Aug	13	96240	27155	28	51541	139746	13	4.94	0.84	16.93	3.53	6.25
	Sep	13	104620	25749	25	79926	150328	13	4.45	1.19	26.76	2.99	6.41
	Oct	13	117617	32795	28	64581	191009	13	4.22	1.27	30.01	2.00	6.46
	Nov	14	116257	69598	60	43561	329258	14	3.91	1.10	28.14	1.82	6.57
	Dec	14	115009	68616	60	9233	310904	14	3.78	0.98	26.03	1.84	5.39

Upgrading	Jan	17	371522	143004	38	214564	726957	17	1.24	0.16	12.72	1.06	1.63
	Feb	16	349524	158489	45	179226	634578	16	1.25	0.17	13.34	1.09	1.72
	Mar	17	360079	207718	58	133366	750862	17	1.35	0.24	17.53	1.08	1.90
	Apr	17	318601	153304	48	145896	680333	17	1.35	0.17	12.97	1.06	1.62
	May	17	278959	139222	50	66930	619434	17	1.68	0.36	21.36	1.25	2.30
	Jun	17	264127	107117	41	131797	579962	17	1.91	0.41	21.51	1.24	2.93
	Jul	17	287790	100072	35	167231	563905	17	2.00	0.27	13.61	1.61	2.61
	Aug	17	317354	129638	41	145787	575002	17	1.96	0.29	14.79	1.51	2.41
	Sep	17	282022	81535	29	146591	468167	17	1.84	0.26	14.33	1.50	2.37
	Oct	17	290746	118088	41	136254	529184	17	1.57	0.17	10.61	1.23	1.84
	Nov	17	336525	141883	42	185165	639174	17	1.35	0.24	17.55	1.02	1.97
	Dec	17	359515	146638	41	201305	668138	17	1.26	0.16	12.71	1.01	1.63
Utility	Jan	17	55433	46831	84	18161	182999	17	2.49	0.85	34.29	1.26	3.64
	Feb	16	44622	34906	78	20388	161342	16	2.49	0.79	31.70	1.23	4.00
	Mar	17	51535	29287	57	20489	105015	17	2.60	0.74	28.38	1.65	4.15
	Apr	17	46859	31674	68	22928	118514	17	2.94	1.02	34.79	1.18	4.55
	May	17	55307	42239	76	20227	148586	17	3.24	1.48	45.88	1.43	6.57
	Jun	17	64464	35761	55	21058	148661	17	3.41	1.83	53.58	1.38	7.64
	Jul	17	55296	28532	52	20568	111263	17	4.06	1.82	44.76	1.87	7.46
	Aug	17	55918	31646	57	18966	122424	17	4.07	1.72	42.37	2.17	7.36
	Sep	17	50124	31387	63	17796	124722	17	3.64	1.70	46.81	1.78	7.12
	Oct	17	51957	31483	61	15677	112483	17	3.18	1.40	44.03	1.77	6.54
	Nov	17	46831	28102	60	20172	116429	17	2.96	1.05	35.52	1.74	5.26
	Dec	17	51175	34532	67	20141	132588	17	2.78	1.13	40.69	1.30	4.51

Table A 6 Integrated monthly weighted input signal for cooling tower blowdown based on COC and blowdown data from all four towers modelled based on the closed-system fractionation model

Month	$\delta^{18}O$ [‰]	$\delta^{2}H$ [‰]	Blowdown (m^3)
Jan	-13.39	-117.12	546671
Feb	-13.52	-117.84	528049
Mar	-13.07	-115.27	547132
Apr	-12.93	-114.46	475972
May	-12.09	-109.58	441602
Jun	-11.71	-107.39	440093
Jul	-11.51	-106.24	464315
Aug	-11.54	-106.42	475213
Sep	-11.78	-107.81	440981
Oct	-12.21	-110.28	460422
Nov	-12.84	-113.93	510279

Dec	-13.20	-116.04	538365
Total	-12.53	-112.16	5869095

Table A 7 Summary of 9-year (2012-2018) ^{18}O and ^{2}H values from the recycle water circuit at Mildred Lake Mine consisting of three tailings ponds (Southwest Sand Storage: SWSS; Mildred Lake Settling Basin: MLSB; Southwest In-Pit: SWIP), the recycle water storage pond (Recycle pond), and the tailings slurry deposition line (Tailings slurry) grouped by month of collection, as well as a 2-year (2016-2018) dataset collected from three tailings ponds at Aurora North Mine (Aurora Settling Basin: ASB, Aurora End Pit North-East: AEPN-E, and Aurora End Pit North-West: AEPN-W). Monthly mean, maximum, minimum, standard deviation, and coefficient of variation are presented.

		$\delta^{18}O$ [‰]						$\delta^{2}H$ [‰]					
Source	Month	Mean	Max	Min	STD	CV	n	Mean	Max	Min	STD	CV	n
MLSB	Jan	-14.13	-13.98	-14.35	0.15	-1.08	5	-117.56	-116.00	-119.70	1.55	-1.32	5
	Feb	-14.09	-13.93	-14.17	0.11	-0.78	4	-116.58	-116.10	-117.30	0.59	-0.51	4
	Mar	-14.31	-13.68	-14.77	0.41	-2.88	5	-117.99	-114.36	-120.20	2.23	-1.89	5
	Apr	-14.63	-14.34	-15.09	0.32	-2.21	4	-119.99	-116.90	-122.97	2.50	-2.08	4
	May	-14.32	-13.82	-15.13	0.52	-3.64	5	-121.33	-117.60	-125.34	2.95	-2.43	5
	June	-13.17	-11.83	-13.96	0.78	-5.92	6	-116.26	-112.13	-121.75	3.37	-2.90	6
	July	-13.38	-12.95	-13.91	0.41	-3.10	5	-116.09	-109.65	-120.07	4.18	-3.60	5
	Aug	-12.29	-11.67	-13.16	0.58	-4.75	5	-110.49	-106.24	-115.40	3.36	-3.04	5
	Sept	-12.53	-11.93	-13.01	0.44	-3.55	6	-111.14	-106.61	-114.73	2.92	-2.63	6
	Oct	-13.06	-12.03	-13.96	0.75	-5.73	6	-114.12	-110.30	-118.00	2.90	-2.54	6
	Nov	-13.14	-12.27	-13.91	0.58	-4.38	8	-113.49	-108.90	-116.20	2.58	-2.27	8
	Dec	-13.51	-13.06	-13.95	0.63	-4.68	2	-116.68	-113.13	-120.24	5.03	-4.31	2
	All	-13.47	-11.67	-15.13	0.86	-6.41	61	-115.64	-106.24	-125.34	4.10	-3.55	61
Recycle pond	Jan	-13.55	-13.05	-13.84	0.34	-2.54	4	-116.00	-113.50	-117.70	1.78	-1.53	4
	Feb	-13.64	-13.22	-13.86	0.27	-1.98	5	-115.78	-111.58	-117.10	2.35	-2.03	5
	Mar	-13.92	-13.69	-14.29	0.32	-2.31	3	-117.90	-116.20	-120.80	2.53	-2.15	3
	Apr	-14.80	-14.48	-15.33	0.38	-2.55	4	-121.32	-118.80	-122.90	1.76	-1.45	4
	May	-14.61	-13.51	-15.65	0.97	-6.63	5	-121.49	-114.70	-128.10	4.81	-3.96	5
	June	-13.51	-12.50	-14.89	1.00	-7.40	4	-117.54	-112.40	-124.07	5.09	-4.33	4
	July	-13.19	-12.90	-13.39	0.26	-1.98	3	-114.48	-112.04	-116.80	2.38	-2.08	3
	Aug	-12.19	-11.51	-12.63	0.52	-4.23	4	-111.84	-105.65	-114.50	4.16	-3.72	4
	Sept	-12.31	-11.40	-12.81	0.55	-4.47	5	-111.29	-110.20	-113.87	1.50	-1.35	5
	Oct	-12.88	-12.29	-13.60	0.60	-4.66	7	-113.99	-107.80	-117.60	3.98	-3.49	7
	Nov	-13.09	-11.57	-13.90	0.83	-6.30	7	-114.27	-110.61	-117.75	2.73	-2.39	7
	Dec	-13.28	-12.84	-14.31	0.69	-5.21	4	-116.89	-110.39	-129.62	8.69	-7.43	4
	All	-13.37	-11.40	-15.65	0.95	-7.10	55	-115.86	-105.65	-129.62	4.69	-4.05	55
SWIP	Jan	-12.86	-12.00	-13.41	0.55	-4.32	5	-114.06	-108.61	-116.80	3.25	-2.85	5
	Feb	-13.46	-13.24	-13.61	0.16	-1.20	4	-117.75	-116.10	-119.60	1.59	-1.35	4

	Mar	-13.68	-12.99	-15.09	0.74	-5.42	6	-116.87	-113.55	-119.75	2.01	-1.72	6
	Apr	-13.45	-12.60	-14.30	0.72	-5.35	4	-116.44	-114.90	-117.90	1.23	-1.06	4
	May	-14.00	-13.48	-14.62	0.46	-3.29	6	-120.35	-115.70	-123.62	2.79	-2.32	6
	June	-13.34	-12.54	-14.16	0.59	-4.41	5	-117.42	-112.50	-123.49	3.93	-3.35	5
	July	-13.01	-11.17	-14.59	1.40	-10.79	4	-116.00	-108.70	-121.01	5.22	-4.50	4
	Aug	-12.49	-12.29	-12.68	0.20	-1.57	3	-114.03	-113.40	-114.70	0.65	-0.57	3
	Sept	-12.31	-11.76	-12.68	0.38	-3.05	5	-112.66	-111.10	-114.40	1.39	-1.23	5
	Oct	-12.61	-12.01	-13.20	0.51	-4.05	6	-115.12	-111.60	-118.24	2.60	-2.26	6
	Nov	-12.61	-12.01	-13.22	0.46	-3.62	6	-114.17	-112.90	-115.75	0.95	-0.83	6
	Dec	-12.34	-11.78	-12.78	0.51	-4.13	3	-112.53	-108.02	-116.37	4.21	-3.74	3
	All	-13.06	-11.17	-15.09	0.79	-6.04	57	-115.79	-108.02	-123.62	3.34	-2.88	57
SWSS	Jan	-12.45	-12.45	-12.45	-	-	1	-110.39	-110.39	-110.39	-	-	1
	Feb	-12.45	-12.45	-12.45	-	-	1	-110.39	-110.39	-110.39	-	-	1
	Mar	-13.77	-13.45	-14.09	0.45	-3.29	2	-116.07	-115.64	-116.50	0.60	-0.52	2
	Apr	-12.95	-11.75	-13.72	1.06	-8.15	3	-113.44	-108.70	-116.11	4.12	-3.63	3
	May	-12.40	-11.03	-14.68	1.55	-12.54	6	-111.29	-104.70	-123.40	7.00	-6.29	6
	June	-11.03	-10.58	-11.51	0.37	-3.37	5	-105.75	-102.70	-107.83	2.11	-2.00	5
	July	-11.57	-10.80	-13.60	1.15	-9.98	5	-108.07	-104.80	-119.63	6.48	-6.00	5
	Aug	-10.41	-9.57	-10.96	0.66	-6.30	4	-103.10	-102.50	-104.00	0.73	-0.71	4
	Sept	-10.71	-9.95	-11.88	0.82	-7.67	4	-103.63	-98.10	-109.32	4.60	-4.44	4
	Oct	-11.72	-10.62	-12.89	0.87	-7.40	8	-109.20	-103.60	-114.19	4.02	-3.68	8
	Nov	-11.48	-10.60	-12.58	0.67	-5.87	6	-107.98	-105.00	-114.09	3.81	-3.53	6
	Dec	-12.89	-12.79	-13.00	0.15	-1.13	2	-115.07	-113.79	-116.34	1.80	-1.56	2
	All	-11.74	-9.57	-14.68	1.19	-10.10	47	-108.69	-98.10	-123.40	4.10	-3.77	47
Tailings Slurry	Jan	-13.70	-12.79	-14.20	0.63	-4.63	4	-117.56	-114.84	-120.50	2.32	-1.97	4
	Feb	-14.04	-13.36	-14.41	0.40	-2.84	5	-119.50	-117.80	-121.10	1.27	-1.06	5
	Mar	-14.35	-14.21	-14.48	0.19	-1.33	2	-122.00	-120.40	-123.60	2.26	-1.85	2
	Apr	-14.36	-14.36	-14.36	-	-	1	-123.60	-123.60	-123.60	-	-	1
	May	-14.39	-13.91	-14.82	0.38	-2.62	4	-122.50	-121.00	-124.10	1.37	-1.12	4
	June	-13.49	-12.69	-14.04	0.57	-4.22	4	-118.95	-114.30	-123.00	3.71	-3.12	4
	July	-13.74	-13.30	-14.18	0.62	-4.53	2	-119.68	-117.30	-122.06	3.37	-2.82	2
	Aug	-12.71	-12.46	-13.05	0.31	-2.40	3	-114.20	-113.30	-115.70	1.31	-1.15	3
	Sept	-12.52	-11.75	-13.06	0.57	-4.52	4	-112.22	-106.90	-115.20	3.65	-3.25	4
	Oct	-13.07	-12.04	-13.88	0.80	-6.10	5	-115.59	-108.30	-120.00	4.59	-3.97	5
	Nov	-13.69	-13.43	-14.15	0.33	-2.39	5	-116.81	-115.86	-117.80	0.69	-0.59	5
	Dec	-13.96	-13.70	-14.21	0.36	-2.60	2	-119.81	-118.40	-121.23	2.00	-1.67	2
	All	-13.58	-11.75	-14.82	0.74	-5.46	41	-117.89	-106.90	-124.10	3.89	-3.30	41
AEPN-E	Jan	-13.93	-13.41	-14.42	0.44	-3.16	5	-124.18	-120.90	-127.10	2.50	-2.01	5
	Feb	-14.16	-13.84	-14.72	0.48	-3.39	3	-125.37	-124.10	-127.10	1.55	-1.24	3
	Mar	-14.22	-13.73	-14.79	0.44	-3.09	5	-125.76	-123.20	-128.40	2.18	-1.73	5

	Apr	-14.20	-13.82	-14.51	0.35	-2.46	3	-124.97	-123.00	-126.70	1.86	-1.49	3
	May	-14.08	-13.63	-14.54	0.43	-3.05	4	-124.58	-122.50	-126.40	2.06	-1.65	4
	Jun	-13.07	-12.70	-13.24	0.25	-1.91	4	-120.58	-119.10	-121.20	1.00	-0.83	4
	Jul	-12.85	-12.39	-13.26	0.36	-2.80	4	-119.48	-118.00	-120.30	1.04	-0.87	4
	Aug	-13.47	-12.73	-13.90	0.64	-4.75	3	-122.80	-119.90	-125.20	2.69	-2.19	3
	Sep	-12.97	-12.56	-13.36	0.40	-3.08	3	-119.93	-117.60	-122.90	2.71	-2.26	3
	Oct	-13.54	-12.38	-14.50	0.91	-6.72	4	-122.28	-114.60	-127.60	5.78	-4.73	4
	Nov	-13.46	-13.45	-13.47	0.01	-0.07	4	-121.93	-120.20	-123.80	1.49	-1.22	4
	Dec	-13.80	-13.80	-13.80	-	-	1	-123.80	-123.80	-123.80	-	-	1
	All	-13.65	-12.38	-14.79	0.64	-4.69	43	-122.98	-114.60	-128.40	3.10	-2.52	43
ASB	Jan	-13.43	-12.96	-13.84	0.43	-3.20	5	-121.84	-119.40	-123.30	1.57	-1.29	5
	Feb	-13.52	-13.37	-13.82	0.26	-1.92	3	-121.83	-121.40	-122.40	0.51	-0.42	3
	Mar	-13.67	-13.24	-14.03	0.30	-2.19	5	-123.54	-122.80	-125.10	0.91	-0.74	5
	Apr	-13.77	-13.49	-14.04	0.39	-2.83	2	-122.90	-121.40	-124.40	2.12	-1.72	2
	May	-13.85	-13.56	-14.13	0.22	-1.59	6	-123.83	-121.40	-125.60	1.39	-1.12	6
	Jun	-13.70	-13.55	-13.86	0.16	-1.17	3	-123.13	-122.80	-123.40	0.31	-0.25	3
	Jul	-13.48	-13.27	-13.62	0.15	-1.11	5	-121.40	-120.60	-122.30	0.74	-0.61	5
	Aug	-13.37	-13.15	-13.51	0.20	-1.50	3	-120.90	-120.40	-121.60	0.62	-0.51	3
	Sep	-12.52	-11.95	-13.20	0.63	-5.03	3	-118.47	-116.60	-121.00	2.27	-1.92	3
	Oct	-13.19	-12.86	-13.88	0.47	-3.56	4	-120.18	-117.90	-121.60	1.60	-1.33	4
	Nov	-13.19	-13.07	-13.53	0.19	-1.44	5	-120.84	-119.60	-122.60	1.10	-0.91	5
	Dec	-13.29	-13.29	-13.29	-	-	1	-120.90	-120.90	-120.90	-	-	1
	All	-13.44	-11.95	-14.13	0.43	-3.20	45	-121.81	-116.60	-125.60	1.87	-1.54	45
AEPN-W	Jan	-13.95	-13.86	-14.04	0.08	-0.57	4	-125.00	-123.60	-125.80	0.97	-0.78	4
	Feb	-14.21	-14.02	-14.40	0.19	-1.34	3	-126.43	-124.30	-127.60	1.85	-1.46	3
	Mar	-14.47	-14.12	-15.01	0.46	-3.18	5	-127.20	-124.70	-131.10	2.73	-2.15	5
	Apr	-14.56	-14.15	-14.90	0.38	-2.61	3	-127.47	-124.10	-130.20	3.10	-2.43	3
	May	-14.26	-13.74	-14.68	0.42	-2.95	4	-126.28	-121.70	-129.50	3.41	-2.70	4
	June	-14.20	-13.98	-14.51	0.23	-1.62	4	-125.65	-124.30	-127.70	1.50	-1.19	4
	July	-13.43	-12.75	-14.27	0.77	-5.73	3	-122.10	-120.40	-125.40	2.86	-2.34	3
	Aug	-13.31	-12.88	-13.97	0.58	-4.36	3	-120.87	-118.20	-123.90	2.87	-2.37	3
	Sept	-12.84	-12.36	-13.11	0.42	-3.27	3	-120.67	-119.40	-121.70	1.17	-0.97	3
	Oct	-13.48	-13.07	-13.95	0.44	-3.26	4	-123.23	-121.50	-124.50	1.27	-1.03	4
	Nov	-13.79	-13.64	-13.96	0.15	-1.09	4	-123.33	-122.80	-123.80	0.41	-0.33	4
	Dec	-13.33	-13.33	-13.33	-	-	1	-123.80	-123.80	-123.80	-	-	1
	All	-13.89	-12.36	-15.01	0.61	-4.39	41	-124.54	-118.20	-131.10	2.95	-2.37	41

3.9 Appendix B

Quantifying the influence of cooling tower blowdown inputs and ice formation on the isotopic evolution of the RCW circuit

The cooling tower blowdown signatures exhibit the largest variability in regard to the other contributing sources based on our observations. The slope of the evaporation trendline of cooling towers is 5.44 in comparison to the slope of the combined tailings ponds at Mildred Lake Mine of 4.20. Since the cooling tower blowdown is a key contributor to the recycle water circuit annually, the difference in slopes will represent the contributions of mixing from other inputs such as meteoric waters as well as the fractionation associated with open water evaporation. The difference in evaporative conditions that affect fractionation of ^{18}O and ^{2}H (*i.e.*, temperature and humidity) within the cooling towers versus the open water evaporation occurring from the surface of tailings ponds affects the steepness of the slope, with slope increasing as humidity increases (Gonfiantini, 1986).

Here I developed an integrated blowdown signature to represent the total cooling tower contribution to the RCW using historical COC data. In *Fig 3.13a* the extent of the monthly-integrated signature tracks relatively close to the recycle pond signatures.

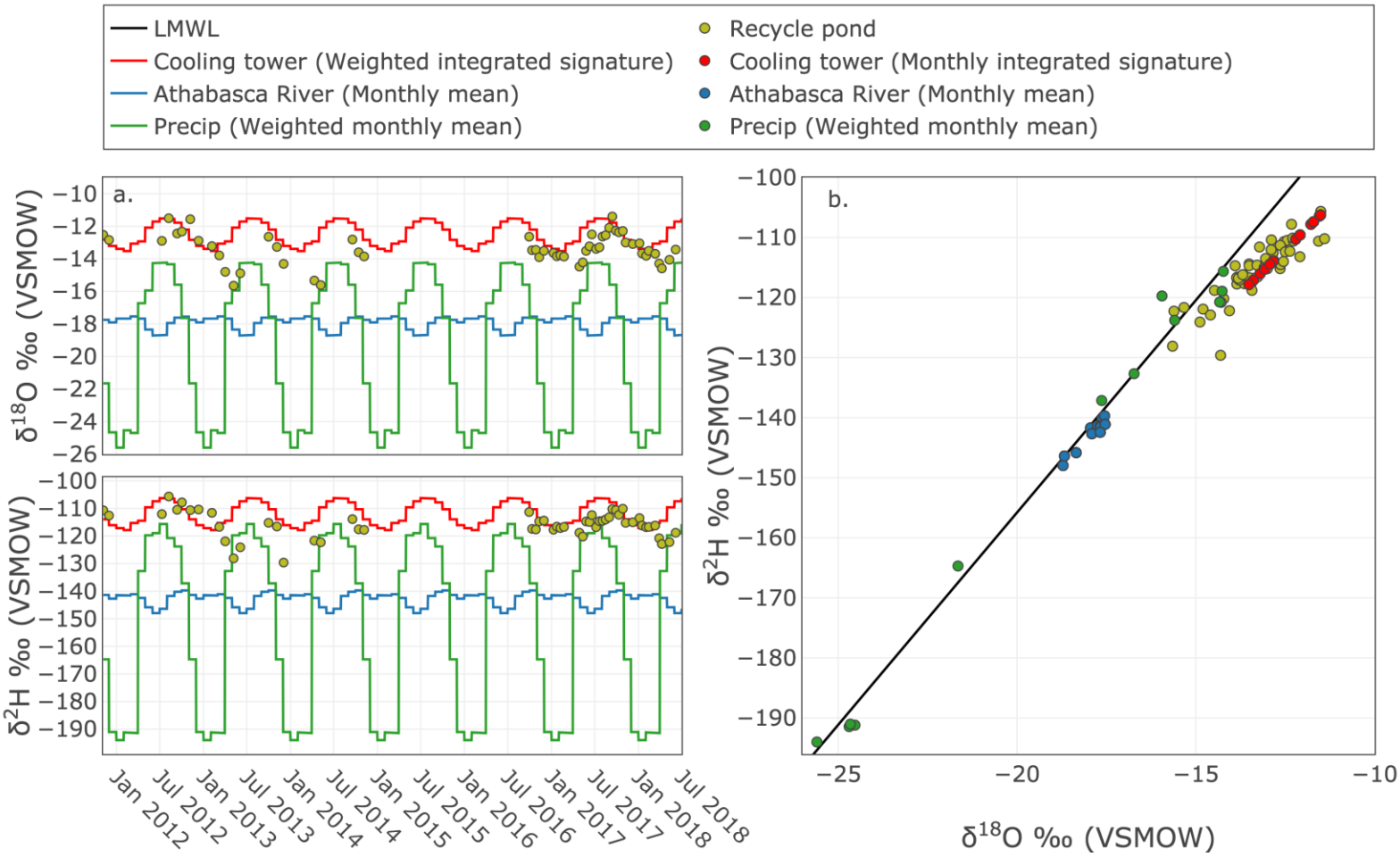

Figure 3.13 a.) Temporal variability of ^{18}O and ^{2}H from recycle pond samples plotted with the integrated monthly cooling tower signature, monthly weighted average of precipitation, and monthly average of Athabasca River water; b.) Dual isotope plot displaying the variations of each component relative to the LMWL.

In order to verify the contribution of the cooling tower blowdown observed ($V_{input;}$ δ_{input}) I used a simple mixing model to calculate the resulting RCW circuit signature (δ_f):

$$\delta_f = \frac{\left(V_{input} \cdot \delta_{input} + V_{initial} \cdot \delta_{initial}\right)}{\left(V_{input} + V_{initial}\right)} \qquad (Eq. B1)$$

The initial volume ($V_{initial}$) of free water within the recycle water circuit is estimated to be 29.7 Mm^3 (based on 2016 tailings management reports supplied by Syncrude and excluding SWSS) and $\delta_{initial}$ was estimated from the monthly recycle pond values (Table. A3.7). The effects of cooling tower blowdown are minimal based on the mixing equation — leading to an overall enrichment of only 0.16 ‰ for ^{18}O (RCW = -13.38‰) and 0.70‰ for ^{2}H (RCW = -115.36‰) over the total addition of 5.86 Mm^3 of blowdown in a 12-month period. Therefore, the rest of the enrichment that is observed within the RCW circuit near the end of summer must be attributed primarily to evaporation.

Similarly, using the mixing equation to calculate the potential contributions of cooling tower blowdown during the ice on period lead to an under prediction of the depleted values typically observed. Using Eq. 3.5 and mixing 50 mm of SWE over the area of 12.6 km^2 (tailings pond areas provided by W. Zubot, personal communication. 2017) in conjunction with the cooling tower blowdown results in an average $\delta^{18}O$ RCW value of -13.72‰ for May, which is typically around -14.61‰ based on *Table. A3.7.* Cooling tower blowdown and snowmelt together are therefore unable to replicate the depletion observed following springmelt.

Mixing calculations of current input volumes of cooling tower blowdown with present day stores of OSPW appear to have no significant effect on the overall isotopic signature of the RCW circuit. This is likely due to the engineered system having reached near isotopic steady-state conditions based on the natural and engineered mechanisms contributing to the evolution of the present-day isotopic signature since the beginning of operations. Without the forced fractionation from cooling tower operations, OSPW signatures may have evolved to resemble isotopic signatures of natural reservoirs within the region.

Another mechanism that could be contributing to the systematic depletion observed throughout the ice on period is the fractionation of heavy isotopes to the formation of ice layers at the surface thus depleting the RCW circuit. Here I use the average shift in isotopic composition of the RCW circuit from October (prior to freeze up) to March (prior to influence of springmelt) to predict the isotopic composition of ice based on an assumed ice thickness of 61 cm. Based on the observed shift from -12.88‰ to -13.92‰ and -113.99‰ to -117.90‰ of ^{18}O and ^{2}H respectively, the isotopic composition of ice would have to be $\delta^{18}O$ = -9.9 ($\delta^{2}H$ = -102.8). This works out to an isotopic separation factor ($\varepsilon_{ice-liquid} = 1000(\alpha - 1) \approx \delta_{ice} - \delta_{liquid}$) of 2.99‰ for ^{18}O and 11.18 ‰ for ^{2}H. Studies have experimentally determined that $\varepsilon_{ice-liquid}$ in freshwater systems is 2.8 to 3.1‰ for ^{18}O and 17.0 to 20.6‰ for ^{2}H near 0°C during natural freezing rates (<2mm hr^{-1}) (Suzuoki and Kimura, 1973, O'Neill, 1968; Kuhn and Thurkauf, 1958, Arnason, 1969). The isotopic separation factor calculated for ^{18}O falls within the experimentally determined range; however, is lower than the experimentally determined range for ^{2}H. Ice profile samples (n=5) were collected from Base Mine Lake, an end pit test lake on Mildred Lake mine site, in early March 2017 and ranged from -11.65‰ to -9.78‰ and -108.40‰ to -96.50‰ for ^{18}O and ^{2}H respectively, which agrees with our calculated ice values. Base Mine Lake has a similar isotopic signature and chemical composition to OSPW due to expressed pore water from fluid fine tailings and therefore is expected to exhibit similar fractionation during freezing as the tailings ponds.

iii. Transition statement

Chapter 4 expands on the previous work identifying seasonal and interannual isotopic patterns of the RCW circuit in *Chapter 3*. The observations of seasonal enrichment during the open water season provide the opportunity to apply isotope mass balance techniques to estimate the evaporative fluxes contributing to the degree of observed enrichment. Within this chapter I implement various forms of the isotope mass balance equation to quantify evaporative losses from the RCW circuit and Base Mine Lake, the first demonstration end pit lake within the oil sands region.

Chapter 4: Applications of stable isotopes (^{18}O and ^{2}H) to quantify evaporative losses from water management systems at an oil sands mine

iv. Abstract

An ongoing challenge at Oil sands operations in Northern Alberta is to minimize freshwater import, improve operational water management, and track water release during operations and following mine closure. This study took place at an oil sands mine site currently storing over 1.7 Gm^3 of oil sands process affected waters (OSPW), most of this contained within tailings management facilities and the concomitant recyle water (RCW) circuit. A key component of managing the RCW circuit is tracking the site wide water balance. Here I focus on the use of stable isotopes found within water (^{18}O and ^{2}H) to track evaporative losses from open water within tailings ponds and RCW circuit, as well as a demonstration end pit lake for future mine closure.

Oxygen-18 (^{18}O) and deuterium (^{2}H) were measured in site wide waters over a six-year period. Isotope mass balance methods were used to make an initial estimate of evaporation/inflow (E/I) ratios based on the observable annual isotopic enrichment of the RCW circuit from a volume-weighted source water signature integrated over the open water period. The E/I ratios were found to range from 0.11 to 0.22, These ratios correspond to evaporative losses of 67 to 133 mm yr^{-1} from the RCW circuit.

The isotope mass balance model was then adapted to identify controls on seasonal evaportation cycles assuming all isotopic enrichment was associated with evaporation. This simplifying assumption resulted in an over-estimate of evaporation rates as compared to those predicted by the Penman combination method and eddy covariance (EC) tower measurements. The isotope mass balance predicted annual rates in the range of 418 to 931 mm yr^{-1}, much higher than 373 to 513 mm yr^{-1} by the Penman combination method and 351 to 466 mm yr^{-1} by EC.

Applications of the isotope mass balance model to the end pit lake, which incorporated highly monitored water balance data not available for RCW circuit, resulted in good agreement between the evaporation rates estimated from the isotope mass balance model and those from Penman and EC. It is important to note that the model was

better able to capture the seasonal variation in the isotopic composition of the lake water when ^{18}O was the tracer rather than ^{2}H. This may be due to the chemical composition of OSPW affecting rates of ^{2}H evaporative fractionation.

This work demonstrates the first application of stable isotope tracers for isotope mass balance methods to quantify evaporation from tailings management facilities at an oil sands mine site. This work is useful as an additional tool for monitoring site wide water balance, as well as tracking the hydrological evolution of tailings closure landscapes.

4.1 Introduction

Water management during operations and water release following closure are of primary environmental concerns associated with oil sands development in Northern Alberta, Canada. The volumes of water that are imported for extraction and ultimately stored on site are large. For example, one of the largest oil sands producers, Syncrude Canada Ltd, requires approximately 40 Mm^3 of freshwater import annually to support extraction—a total of 1.2 Gm^3 of water since operations began in 1983 (based on personal communications with W. Zubot, Syncrude).

The imported water that is not chemically consumed or evaporated during extraction becomes oil sands process affected water (OSPW) stored within tailings management facilities—commonly referred to as tailings ponds. This water is sequestered as pore water within deposited tailings or as clarified water within the tailings ponds. The clarified water is moved between tailings ponds and the extraction plant as part of a recycle water (RCW) circuit. As of 2017, approximately 1.7 Gm^3 of OSPW is stored on site with 200 Mm^3 present as clarified water making up the RCW circuit.

Oil sands mines such as the Mildred Lake mine are operated as ‘zero release’ facilities during operations and consequently the accumulated imported water volumes must be stored on site. The mines are able to track the volumes of freshwater import and do have climate monitoring to track seasonal and annual precipitation. However, generally speaking, they all experience difficulty in closing a site wide water balance for

the RCW circuit due to difficulties quantifying evaporation (COSIA, 2019). This challenge will continue following mine closure due to the inclusion of end pit lakes in the final closure design.

The use of stable isotopes as tracers in water balance studies has generally been limited to ungauged basins when hydrometric data is difficult to obtain (see Gibson et al, 2016a, Gibson et al., 2016b for a comprehensive review of methods; Gibson and Reid, 2014; Tondu et al., 2013; Turner et al., 2014; Turner et al., 2010). While much progress has been made in basic research and applications to natural systems, the implementation of isotope mass balance modelling for water balance purposes in mining has been minimal.

I am aware of no studies to date that have used isotope mass balance techniques to quantify the water balance, and more specifically evaporative losses from water management systems within the Alberta Oil Sands Region. A limited amount of work has been done in monitoring and interpreting ^{18}O and ^{2}H signatures within mining environments; however, most of this work has focused on characterizing rates of recharge or water movement through mine waste and identifying the presence of mining process waters in adjacent off site water (Barbour et al., 2016; Dompierre and Barbour, 2016a; Dompierre et al., 2017; Huang et al., 2015, Gammons et al., 2010, Ghomshei and Allen, 2000, Ingraham et al., 1994).

Some initial work has been done to investigate the roles of evaporation within tailings ponds as well as the isotopic evolution of process water signatures at other mines within Canada. For example, Gibson et al. (1998) compared evaporation rates calculated by ^{18}O mass balance modelling to more traditional methods (*i.e.*, evaporations pans and Penman combination equation) at a small lake located near two gold mines in the Canadian subarctic region to provide evaporation estimates from tailings ponds at the mines. The study found that evaporation rates estimated from an isotope mass balance were within 20% of those estimated by both a standard water balance and the Penman combination method. Interannual variability of evaporation rates calculated from the isotopic approach was found to be up to 30-50% greater than predicted by evaporation pans.

Characterization of ^{18}O and ^{2}H signatures within the oil sands first began as part of a geochemical characterization pilot study performed by Gibson et al., (2011). This was the first oil sands study to hypothesis that OSPW signatures were not necessarily controlled by pond water balance alone, as is the case at natural lakes. OSPW signatures were found to plot to the right of the LMWL, thus exhibiting evaporative enrichment. However, the degree of offset was not as great as natural lakes within the area indicating low ratios of evaporation to inflow and high throughflow rates. Baer et al., (2016) undertook a characterization of site-wide waters at Syncrude's Mildred Lake Mine. They found that the unique OSPW signatures were most likely due to enrichment of the imported Athabasca River water by cooling towers where fractionation occurs near-equilibrium, as well as open water kinetic enrichment from surface water evaporative losses of the recycle water circuit.

Isotope tracers could provide a new tool for industry to improve the efficiency of on-site water management and usage, including limiting current demands of raw water import. Gibson et al., (2011) and Baer et al., (2016) both postulated that evaporative enrichment was a dominant mechanism contributing to the unique isotopic signature of OSPW, but no work has yet been done to quantify the actual evaporative losses. Here, I take this a step further by implementing various forms of the isotope mass balance equation to quantify open water evaporative losses associated with this enrichment using additional isotope data collected from mine source waters and the RCW circuit.

The purpose of this study is to evaluate the potential application of isotope mass balance concepts to track seasonal and interannual changes in the evaporation from operational oil sands mine tailings ponds and RCW circuit, as well as a demonstration end pit lake. This study highlights the operational value of isotope mass balance techniques at an oil sands mine while identifying key limitations in implementation. The estimates of evaporation from this study are compared to more common hydrological methods of estimating evaporation from surface water bodies to provide further evidence to hypotheses presented by Baer et al., (2016) as to whether operational conditions (e.g., the presence of residual bitumen) influence the evaporation rates from tailings ponds compared to natural lakes of the region.

Traditional isotope mass balance modelling practices applied to natural systems are likely not directly transferable to oil sands water management system. Within this study we demonstrate a "proof of concept" approach to how isotope tracers may be used to answer key water balance questions associated with an operational mining circuit, in addition to developing an isotope framework for mass balance modelling. This work highlights the shortfalls of the isotope mass balance techniques implemented and provides insight to further develop the technique for industry uses where applicable. This study builds upon the characterization of the isotopic signatures pertaining specifically to the RCW circuit and its source waters presented in *Chapter 3*.

The specific objectives of this chapter are to:

1. Estimate the annual evaporation from tailings ponds and RCW circuit for an operational oil sands mine using ^{18}O and ^{2}H tracers.
2. Simulate the seasonal variation in the isotopic signature of the free water within an oil sands demonstration end pit lake, utilizing this model to estimate periodic and annual evaporative losses.
3. Compare the estimates of evaporation obtained using the two methods to more conventional hydrological methods for estimating evaporation.

4.2 Study site

Mildred Lake Mine, operated by Syncrude Canada Ltd., is an open pit bitumen mine located 35 km north of Fort McMurray, Alberta. The mine site is located within the Alberta Oil Sands Region, a sub humid region of the boreal forest characterized by high seasonality. Meteorological stations located around Mildred Lake Mine have recorded daily temperatures varying by up to 60°C from winter lows to summer highs, with an annual mean temperature of approximately 3°C (2002-2018) and a mean temperature of 13°C during the open water season (May-Oct). The observed mean relative humidity (RH) during the open water period was 66% with RH ranging from 20% to near 100% throughout the year.

The mine site covers approximately 200 km^2 and includes a variety of landforms including active mining pits, tailings sand structures, overburden dumps, above ground and in-pit tailings management facilities and freshwater reservoirs. This study is focused

on the active and historic tailings management facilities at Mildred Lake Mine site including those comprising the RCW circuit and an end pit lake referred to as Base Mine Lake. An aerial image of Mildred Lake Mine is shown in *Fig. 4.1* highlighting sampled surficial water bodies. A more detailed description of sampling locations related to the RCW circuit and its source waters can be found in *Chapter 3*.

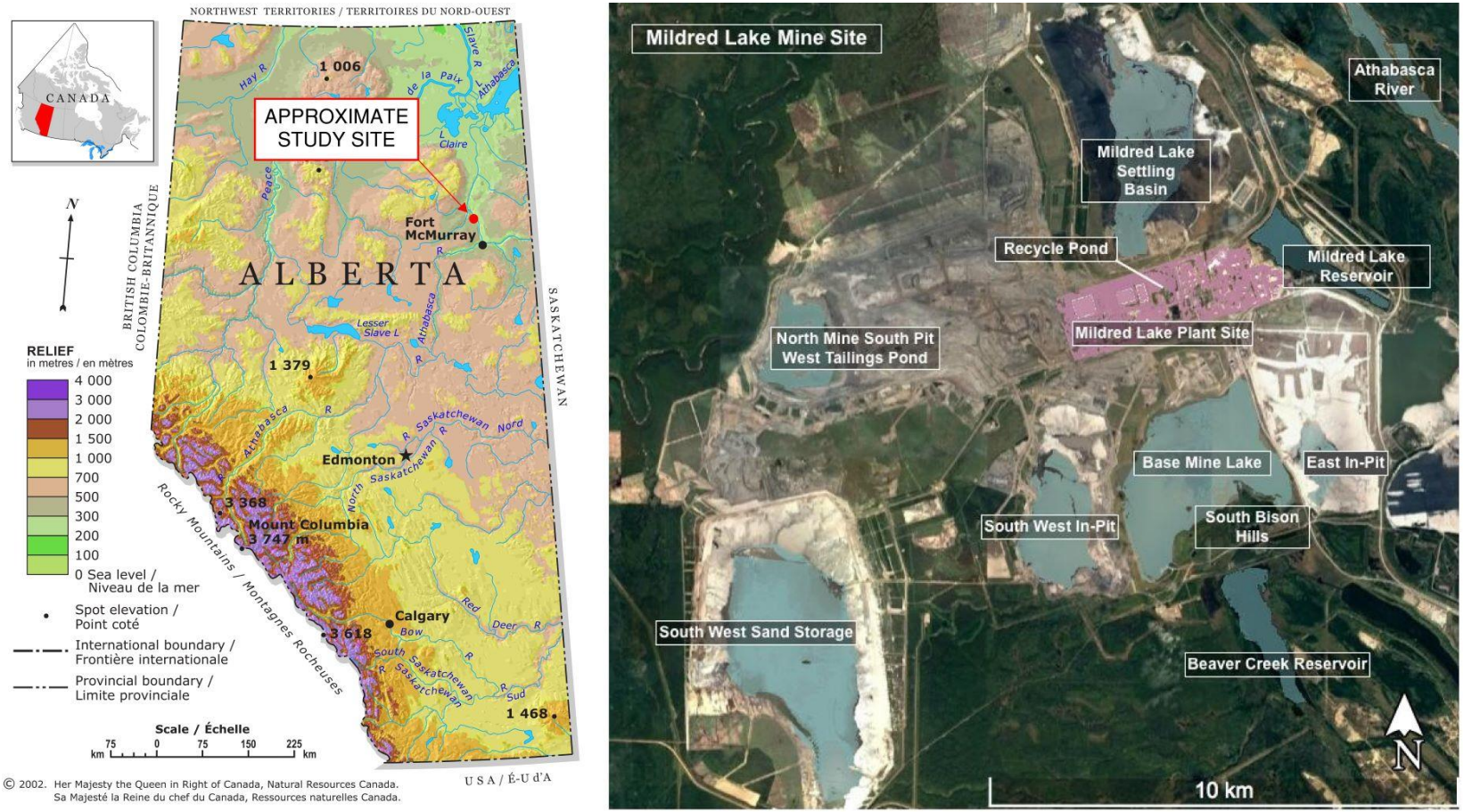

Figure 4.1 Aerial view of Syncrude's Mildred Lake Mine site with isotope sampling locations of site wide surface water bodies identified (original map reproduced from Google Earth, DigitalGlobe 2018).

Base Mine Lake (BML) is the first demonstration end pit lake in the oil sands region. It was an in-pit tailings management facility used to store mature fine tailings dredged from other tailings ponds located at Mildred Lake mine. In 2012 the in-pit facility was capped with freshwater as part of an ongoing reclamation strategy. It no longer receives process water from mining operations and any water pumped from BML to maintain controlled water levels is returned to the RCW circuit. Ongoing research studies investigating all aspects of BML (*i.e.*, geochemical/biological processes, settlement rates and redistribution of fluid fine tailings, physical water balance, etc.) have included a high frequency isotope-sampling program. Further details surrounding the development of Base Mine Lake can be found in Dompierre et al. (2017).

4.3 Methods

4.3.1 Isotope collection and analysis

This work follows the initial site water characterization study of Mildred Lake Mine site performed by Baer et al., (2016) where samples were collected from 2012-2014. Here I added to the previous inventory by initiating a higher frequency (biweekly) sampling of the RCW circuit from 2016 to 2018. Methods for isotope collection and laboratory analysis implemented within this study have been outlined in *Chapter 3*.

BML water samples have been collected as part of an ongoing monitoring program and were collected biweekly at depth intervals from the surface to the mudline at three platforms within the reservoir. Samples collected during the same sampling event were averaged to represent one single value for isotope mass balance calculations.

All stable isotope signatures are reported in δ-notation in per mille [‰] and relative to Vienna Standard Mean Ocean Water (VSMOW) (Coplen, 1996).

4.3.2 Water volumes, evaporation rates, and climate parameters

This study is an initial evaluation of the potential to implement isotope mass balance methods into operational water balance monitoring at an oil sands mine site. Therefore, the water volumes and surface areas have been taken from published licensing reports, provided by Syncrude as part of operations monitoring, communicated

anecdotally by site personnel, or are approximations made to be consistent with available information. Climate parameters such as relative humidity, air temperature, net solar radiation, and wind speed have all been collected from meteorological stations operated by O'Kane Consultants across Mildred Lake Mine site.

Evaporation estimates for the RCW circuit were calculated using the Penman combination method for estimating open water evaporation as outlined in McMahon et al., (2013 and 2016). Eddy covariance (EC) towers operated by Dr. Sean Carey of McMaster University at BML were also used as direct measurements of evaporation and are used as a reference in both the analysis of the RCW circuit and BML.

The daily evaporation and precipitation rates ($mm\ day^{-1}$) over meteorological years 2014-2017 are presented in *Fig. 4.2a* & *b*. Evaporation rates were calculated using the Penman combination method and from EC tower observations, while daily precipitation rates were taken from the met station database operated by O'Kane Consultants. Annual cumulative evaporation and precipitation rates ($mm\ yr^{-1}$) for the same period are presented in Fig *4.2c.*

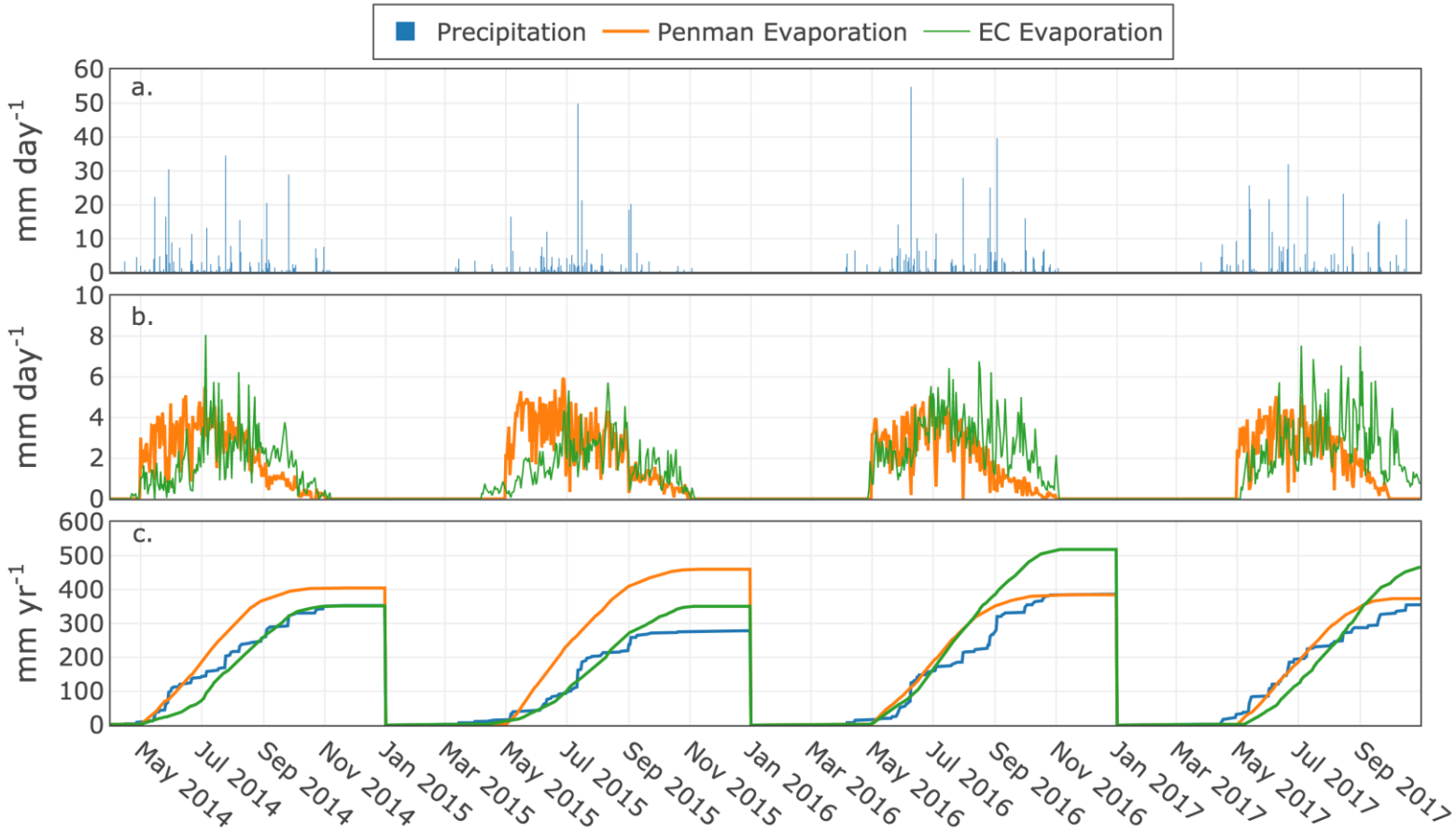

Figure 4.2 a.) Daily precipitation rates measured at Mildred Lake Mine site. b.) Daily evaporation rates calculated by the Penman combination method for open water and Eddy Covariance towers. c.) Annual cumulative precipitation and evaporation rates for 2014-2017.

4.3.3 Analyses methods — Isotope mass balance

4.3.3.1 Theoretical development

The basic equations for the water balance and isotope mass balance of any reservoir can be written as follows:

$$\frac{dV}{dt} = I - Q - E \qquad (Eq. 4.1)$$

and

$$\delta_L \frac{dV}{dt} + V \frac{d\delta_L}{dt} = I\delta_I - Q\delta_Q - E\delta_E \qquad (Eq. 4.2)$$

where *V* is volume of the reservoir, *I*, *Q*, and *E* define the input, output, and evaporation rates expressed as either a depth *mm* or volume m^3 per unit time (over a given time period). Delta notations (δ) denote the isotopic composition of each parameter. It is assumed that for a well-mixed reservoir the isotopic signature of the output is equal to that of the overall reservoir signature $\delta_Q = \delta_L$.

Another useful and often necessary simplification is the assumption of steady state conditions for the duration of the time interval (*dt*) — that is $dV/dt = 0$ and $d\delta_L/dt = 0$, where inflows are balanced by outflow and evaporation. The steady state assumption is generally implemented at either a very short time scale where minute changes in storage are considered negligible (*e.g.*, one day) or an annual time scale where seasonal evaporation and hydrologic events generally result in minimal net change in storage. This assumption is implemented within our study to deal with limited hydrometric data for the RCW circuit. Therefore *Eq. 4.1* and *Eq. 4.2* can be written as:

$$I = Q - E \qquad (Eq. 4.3)$$

and

$$I\delta_I = Q\delta_Q - E\delta_E \qquad (Eq. 4.4)$$

All source waters I_x and associated isotopic signatures δ_{I_x} making up the total input to the reservoir (*i.e.* precipitation including rain and snow, tailings pore water, etc) are volume-weighted to estimate δ_I:

$$\delta_I = \sum \frac{I_x \delta_{I_x}}{I_x} \ [‰] \qquad (Eq. 4.5)$$

Combining *Eqs. 4.3 and 4.4* yields:

$$\frac{E}{I} = \frac{(\delta_I - \delta_L)}{(\delta_E - \delta_L)} \qquad (Eq. 4.6)$$

The isotopic composition of imported freshwater and OSPW are known from sampling; however, it is not possible to sample the evaporative flux *E*. Therefore, standard practice for estimating the isotopic signature of evaporated water δ_E in isotopic studies is by a linear resistance model developed by Craig and Gordon (1965), commonly referred to as the Craig and Gordon model (C-G model), and adapted by Gonfiantini (1986) as:

$$\delta_E = \left[\frac{\delta_L - \varepsilon^*}{\alpha^*} - h\delta_A - \varepsilon_k\right] \cdot \left[\frac{1}{1 - h - \frac{\varepsilon_k}{1000}}\right] [‰] \qquad (Eq. 4.7)$$

where *h* is the relative humidity of the air normalized to the surface temperature if data is available (Horita et al., 2008), α^* is the equilibrium fractionation factor at the liquid-air interface controlled by temperature *T* (Majoube, 1971). Here I use the empirical relationship developed by Horita et al., (1994) for ^{2}H as:

$$10^3 \ln \alpha_{L/V} \left({}^2H/{}^1H \right) = 1158.8(T^3/10^9) - 1620.1(T^2/10^6) + 794.84(T/10^3) - 161.04 + 2.9992(10^9/T^3) \qquad (Eq. 4.8)$$

and for ^{18}O:

$$10^3 \ln \alpha_{L/V} \left({}^{18}O/{}^{16}O \right) = -7.685 + 6.7123(10^3/T) - 1.6664(10^6/T^2) + 0.35041(10^9/T^3) \qquad (Eq. 4.9)$$

The equilibrium isotopic separation $\varepsilon^*$is calculated in permille based on $\varepsilon^* = (\alpha - 1) \cdot 10^3$ [‰], and the kinetic separation $\varepsilon_K$is controlled by the moisture deficit at the liquid-air interface $(1 - h)$ and the transport resistance of air based on relationships developed for frequently occurring conditions in nature by Majoube (1971) and Horita et al. (2008):

$$\varepsilon_K(^2H) = 12.5(1-h) \text{ and } \varepsilon_K(^{18}O) = 14.2(1-h)\ [‰] \qquad (Eq.4.10)$$

The final variable in the C-G model is the isotopic signature of the atmospheric water vapour (δ_A), which requires continuous measurements due to high diurnal variability (Bastrikov et al, 2014). Therefore, it is generally not possible to measure δ_A within most studies and is often estimated based on an assumed equilibrium relationship between the formation of precipitation and δ_A:

$$\delta_A = \frac{(\delta_P - \varepsilon^*)}{\alpha^*}\ [‰] \qquad (Eq.4.11)$$

where δ_P is the isotopic signature of precipitation.

Concern has arisen within the literature surrounding this technique for highly seasonal climates. As a result, various methods such as the use of an index-lake approach (Dincer, 1968; Gibson and Reid, 2014), a fitting coefficient to match observed evaporative enrichment of reservoirs (Bennet et al., 2008; Gibson and Reid, 2014), or the evaporative flux weighting of δ_A and exchange parameters has been proposed (Gibson et al., 2016b). However, most of these methods have been developed for scenarios where frequent measurements of δ_P are unavailable and an annual estimate of δ_P is used. Within this study I use *Eq. 4.11* to estimate δ_A as extensive work has been undertaken to characterize the seasonality of precipitation through frequent isotopic sampling of individual precipitation events at Mildred Lake Mine (see Chapter 3).

4.3.3.2 Recycle water circuit conceptual model

A conceptual model for the water and isotope mass balance of the RCW circuit is provided in *Fig. 4.3.* Multiple tailings ponds are all interconnected within the RCW circuit, with each pond acting as both storage and contributor of necessary clarified recycle water (*i.e.*, OSPW) for bitumen extraction. All tailings ponds feed clarified OSPW to a centralized location, the recycle pond that feeds recycle water to the extraction plant. Following use for extraction, the OSPW is then returned to tailings ponds through the hydrotransport of tailings in slurry form. Solids settle out of the slurry resulting in the expression of formerly bound pore water to the clarified water stores.

Volumes of clarified water within each active tailings pond making up the RCW circuit can vary greatly depending on tailings management operations; however, there is

approximately 200 Mm^3 of clarified water present within the RCW circuit at any given time (W. Zubot, personal communication. 2019). This volume is also the average annual volume of recycle water required for operations (W. Zubot, personal communication. 2019). Based on this operational information, I have implemented the assumption that the recycle water storage within the RCW circuit (*i.e.*, storage of clarified water stored in tailings ponds) is in a steady state. In other words, I am assuming that the clarified OSPW stored within the RCW circuit is being lost or consumed by evaporation and/ or mining operations at a similar rate it is being replenished through the expression of porewater during tailings settlement and the addition of meteoric waters.

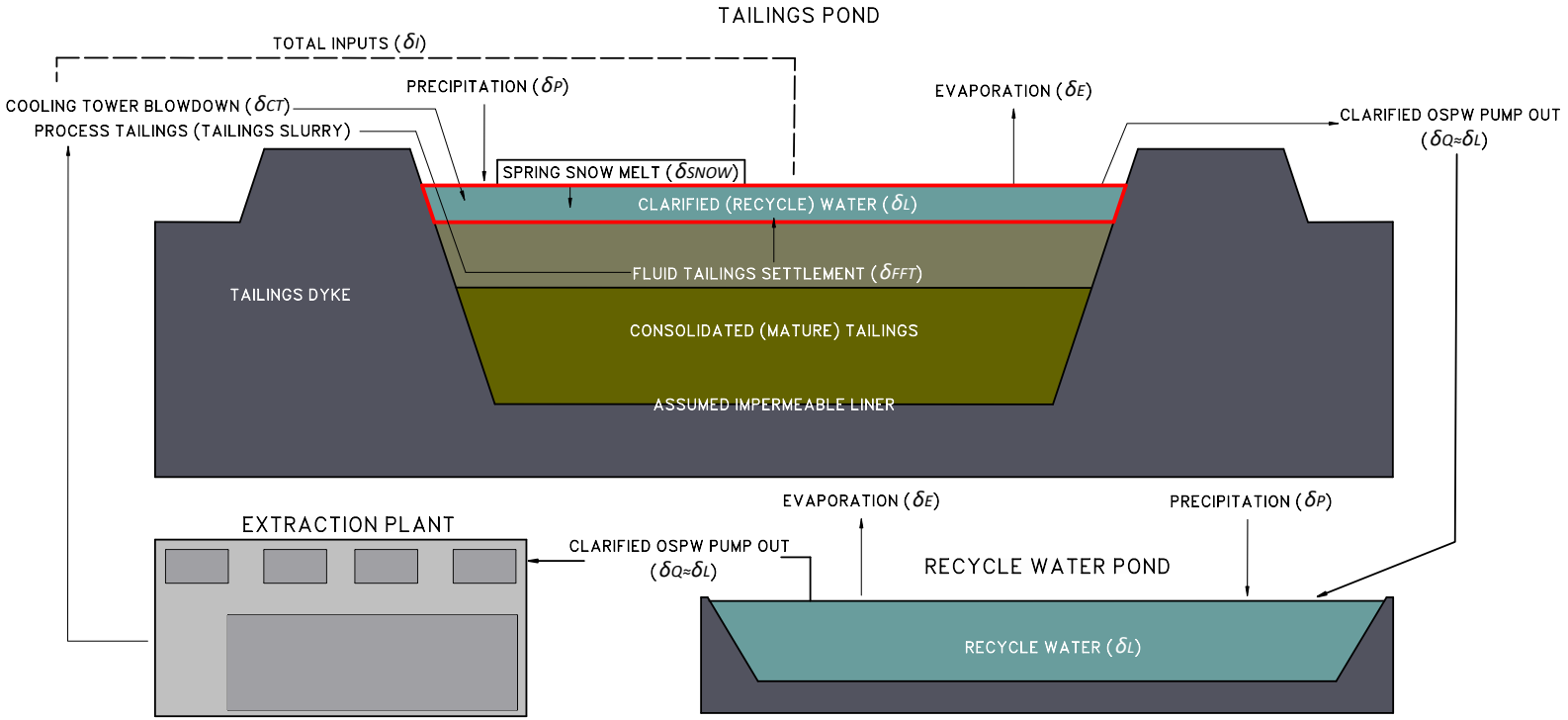

Figure 4.3 Conceptual model of the water and isotope mass balance of the recycle water circuit.

The interconnectivity between ponds and recycling nature of the circuit, in conjunction with high pumping rates to meet water demands, results in a relatively uniform isotopic signature of recycle water across each storage point within the RCW circuit. Isotope samples collected from the recycle pond are believed to act as proxy for the entire RCW circuit since all tailings ponds feed clarified water to it. This connectivity results in a mixed isotopic signature capturing hydrologic and operational processes from each tailings pond.

The isotopic seasonality of the RCW circuit was explored in depth in *Chapter 3* and found to exhibit isotopically steady state conditions at an annual time scale.

4.3.3.3 Isotope mass balance model — Evaporation/inflow ratio

The evaporation/inflow (E/I) ratio model is developed based on the assumption that the system is operating under steady state conditions. Following Gibson and Edwards (2002), *Eq. 4.6* and *Eq. 4.7* can be combined to obtain an expression to solve for the ratio of inflow lost to evaporation (E/I ratio) based on enrichment resultant of equilibrium and kinetic fractionation:

$$\frac{E}{I} = \frac{(\delta_L - \delta_I)}{m(\delta^* - \delta_L)} \qquad (Eq.\,4.12)$$

where *m* is the temporal enrichment slope (Welhan and Fritz, 1977; Allison and Leaney, 1982):

$$m = \frac{\left[h - \left(\varepsilon_K + \frac{\varepsilon^*}{\alpha^*}\right) \cdot 10^{-3}\right]}{(1 - h + \varepsilon_K \cdot 10^{-3})} \qquad (Eq.\,4.13)$$

and δ^* is the limiting isotopic composition a desiccating reservoir would approach as the volume approaches 0, and is atmospherically controlled by *T*, *h*, and δ_A (Gat and Levy, 1978, Gonfiantini, 1986):

$$\delta^* = \frac{\left(h\delta_A + \varepsilon_K + \frac{\varepsilon^*}{\alpha^*}\right)}{\left[h - \left(\varepsilon_K + \frac{\varepsilon^*}{\alpha^*}\right) \cdot 10^{-3}\right]} \text{ [‰]} \qquad (Eq.\,4.14)$$

By assuming the isotopic signature of our system (*i.e.* RCW circuit or Base Mine Lake) is equal to δ_I prior to any isotopically fractionating processes (*i.e.* evaporation) I use *Eq. 4.12* to estimate the amount of evaporation that has occurred by using the

evolution of the isotopic signature of the system. The further the observable signature of the system has enriched away from the volume-weighted input signature, the greater the volume of evaporative loss from the system. From *Eq. 4.12* an expression to solve for the E/I ratio can be obtained. This ratio is then supplemented with input volumes and tailings areas to estimate evaporation rates.

This E/I form of the isotope mass balance model is used to estimate annual evaporation from the RCW circuit during the open water period (May-Oct) over multiple years (2012-2014, 2016, and 2017), as well as three distinct seasonal periods for the year 2017.

To estimate annual evaporation, an integrated input signature δ_I to the RCW circuit was calculated from representative isotopic compositions developed in *Chapter 3* and using *Eq. 4.5*. The most enriched samples collected from the RCW circuit from the late summer and early fall periods of each year were set as δ_L.

To assess "seasonal" fluctuations in evaporative rates during the open water period I also calculated E/I ratios over three periods (May-June, July-August, and September-October) of the year 2017 using isotope samples collected from the recycle pond. Integrated input signatures and total input volumes were calculated for each distinct period. Climate parameters, and in turn fractionation factors, were also adjusted for the duration of each period by taking the period specific mean.

Tailings pond areas provided by SCL from 2016 (W. Zubot, personal communication. 2017) were used to calculate the total evaporative loss from the RCW circuit (Table A4.1).

4.3.3.4 Isotope mass balance — Gonfiantini model

The isotope mass balance model can be further simplified to a water body experiencing no inflow or outflow, from which water is solely removed by evaporation. This scenario is useful for providing an upper limit estimate of evaporation based on the observed enrichment within the ponds. The upper limit is established by attributing the entire isotopic shift observed in the RCW circuit during the open water period to evaporation while neglecting the effects of isotopically mixing processes. Gonfiantini (1986) outlined the following model, based on the Rayleigh distillation relationship, for this scenario:

$$\delta_f = \left(\delta_i - \frac{A}{B}\right) f^B + \frac{A}{B} \qquad (Eq.\,4.15)$$

where δ_i is the initial isotopic composition, δ_f is the final isotopic composition of the water body, f is the fraction of water remaining, and:

$$A = \frac{h\delta_A + \varepsilon_K + \frac{\varepsilon^*}{\alpha^*}}{1 - h + \frac{\varepsilon_K}{1000}} \qquad (Eq.\,4.16)$$

$$B = \frac{h - \frac{\varepsilon_K}{1000} - \left(\frac{\varepsilon^*}{\alpha^*}\right) \cdot 10^{-3}}{1 - h + \frac{\varepsilon_K}{1000}} \qquad (Eq.\,4.17)$$

The maximum value of enrichment ($\approx \delta^*$) the water body will attain as f approaches zero is expressed as A/B. The model assumes that evaporative conditions will remain unchanged (*i.e.*, h, δ_A, ε_K, ε^*, and α remain constant) during the model period.

Model parameters for RCW circuit isotope mass balance models

The following parameters are necessary for the isotope mass balance models of the RCW circuit and were calculated using the equations outlined in the preceding sections.

The fractionation factors and atmospheric parameters (*i.e.*, $\varepsilon^*, \varepsilon_K, m, \delta^*, \delta_A$) were all calculated at monthly time steps using the monthly means of each variable (*e.g.* temperature and relative humidity). Each parameter was then weighted by evaporation rates as suggested in Gibson (2002) to develop one integrated value for the open water period. These rates were calculated using the Penman open water equation for the open water months. Monthly means of temperature and humidity were also evaporation-weighted using the same method. The resulting model parameters for the isotope mass balance models are provided in *Table. 4.1*.

Table 4.1 Evaporation-weighted model parameters for isotope mass balance models of the recycle water circuit for each seasonal period and spanning the entire open water period (May-Oct).

	T [°C]	RH [%]	ε_{K18} [‰]	ε_{K2} [‰]	α_{18} -	α_{2} -	ε^{*}_{18} [‰]	ε^{*}_{2} [‰]	δ_{A18} [‰]	δ_{A2} [‰]	m_{18} -	m_{2} -	δ^{*}_{18} [‰]	δ^{*}_{2} [‰]
May-Jun	13.61	58	5.91	5.21	1.010375	1.092250	10.38	92.25	-25.21	-193.71	1.38	1.20	2.94	-45.19
Jul-Aug	17.54	67	4.73	4.16	1.010001	1.087281	10.00	87.28	-24.04	-188.98	1.93	1.73	-2.14	-71.39
Sept-Oct	7.40	74	3.75	3.30	1.011011	1.100810	11.01	100.81	-27.32	-210.04	2.76	2.45	-7.52	-93.15
May-Oct	14.82	63	5.20	4.57	1.010260	1.090770	10.26	90.77	-24.88	-192.88	1.74	1.54	-0.27	-60.89

A volume-weighted input signature δ_I was integrated over the open water period based on the estimated volumes of four contributing waters: cooling tower (CT) blowdown, direct rainfall on pond surface, snow melt on pond surface, and FFT pore water released during settlement. Tailings pond surface areas from 2016 were provided by SCL and were used to estimate the volume of direct precipitation as well as FFT settlement contribution. The total surface area of ponds making up the recycle water circuit in 2016 was 28.6 km^2. The average monthly rainfall and annual snow water equivalent amounts outlined in *Chapter 3* were used to calculate direct pond surface input totals of 8.38 Mm^3 and 1.52 Mm^3 of water added to the RCW circuit during the open water period. The total volume of cooling tower blowdown water was estimated to be 2.72 Mm^3 using the average monthly cooling tower blowdown data provided in *Chapter 3*. I was unable to obtain accurate reporting of tailings settlement rates at the tailings ponds within the RCW circuit during the study period. Therefore, the total volume of pore water released during settlement was estimated using a settlement rate of 0.2 m over the duration of the open water period and assumes the mudline represents 80% of the total surface area of the RCW, leading to a volumetric input of 4.58 Mm^3 (based on personal communications with D. Heisler, Syncrude). The total weighted isotopic signatures and associated volumes are presented in *Table. 4.2*. Overland runoff contributions were neglected in the calculations of δ_I because data regarding the contributing drainage area to the tailings ponds could not be obtained.

Table 4.2 Weighted isotopic inputs for each modelling period spanning the open water period (May-Oct) with respective volumetric contributions.

	May-Jun			Jul-Aug			Sept-Oct			Total open water period (May-Oct)		
	$\delta^{18}O$	$\delta^{2}H$	Volume	$\delta^{18}O$	$\delta^{2}H$	Volume	$\delta^{18}O$	$\delta^{2}H$	Volume	$\delta^{18}O$	$\delta^{2}H$	Volume
	[‰]	[‰]	Mm^3	[‰]	[‰]	Mm^3	[‰]	[‰]		[‰]	[‰]	Mm^3
Snow	-24.67	-191.04	1.52	-	-	-	-	-	-	-24.67	-191.04	1.52
Rain	-14.78	-119.19	2.98	-14.27	-117.88	3.41	-16.24	-128.04	1.99	-14.92	-120.75	8.38
CT Blowdown	-11.90	-108.49	0.88	-11.53	-106.33	0.94	-12.00	-109.07	0.90	-11.80	-107.94	2.72
FFT Settlement	-13.58	-117.89	1.52	-13.58	-117.89	1.52	-13.58	-117.89	1.52	-13.58	-117.89	4.56

4.3.3.5 Base Mine Lake isotope mass balance models

Base Mine Lake is currently part of ongoing monitoring studies due largely in part to being the first demonstration end pit lake within the Alberta Oil Sands Region (Risacher et al., 2018; Dompierre et al., 2017; Tedford et al., 2016; Lawrence et al., 2015). Water balance data collected by Dr. Sean Carey of McMaster University, in support of SCL and aforementioned ongoing studies, has been provided for this study. Interannual FFT settlement rates were calculated based on sonar surveys of the hard bottom and mudline at Base Mine Lake conducted by Barr Engineering in support of ongoing studies being performed for SCL. A conceptual isotope mass balance model is presented in *Fig. 4.4a.* The cumulative sums of each water balance parameter over the study period (2014-2017) are shown in *Fig. 4.4b*.

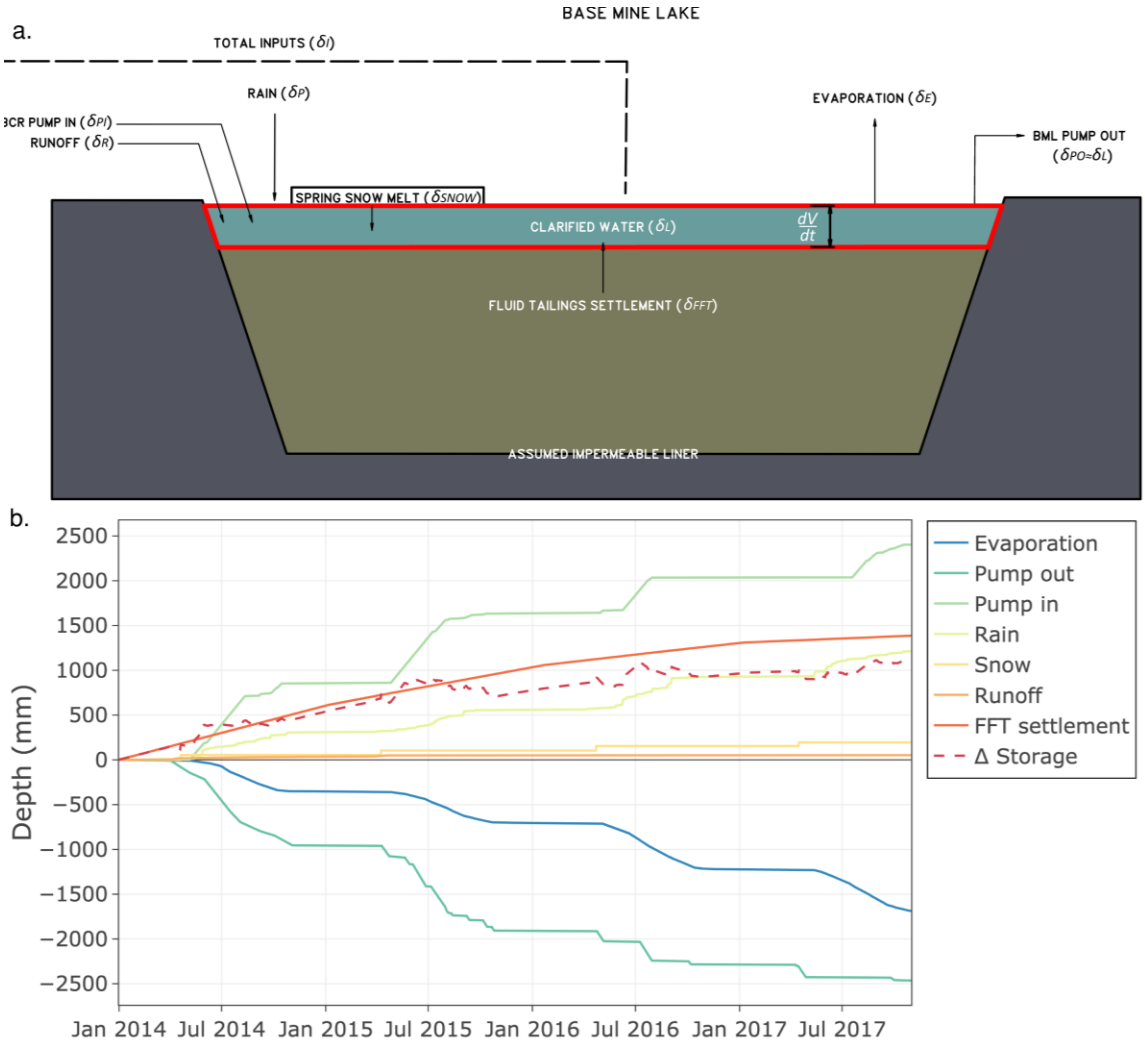

Figure 4.4 a.) Conceptual model of the water balance and isotope mass balance of Base Mine Lake. b.) Cumulative water balance for Base Mine Lake over the duration of the study period, as closed by Dr. Sean Carey (McMaster University).

Two scenarios implementing the isotope mass balance equation (*Eq. 4.2*) have been developed within this study specifically for BML. Both models utilize non steady state isotope mass balance techniques. One model solves for evaporation rates based on observed isotopic variations between sampling dates at BML, while the other attempts to recreate the observed seasonality of the isotopic signature of BML using daily water balance measurements.

Values of daily temperature and humidity necessary for the models were collected from a climate station located at Base Mine Lake. These values were used to calculate the fractionation factors outlined in the previous section.

Monthly volume-weighted means of δ_P have been developed in *Chapter 3* and were used to estimate δ_A for BML at a monthly time scale. This method involving the calculation of monthly δ_A was believed to capture the seasonality observed during the evaporative months that has posed issues in past studies of highly seasonal climates.

BML isotope mass balance evaporation scenario

The isotope mass balance model is used to quantify evaporation rates during the open water period by combining temporal isotopic observations of BML with daily water balance data. By substituting *Eq. 4.1* into *Eq. 4.2* and assuming $\delta_O = \delta_L$, the following expression can be used to solve for *E*:

$$E = -\frac{\left[V_i \cdot \frac{d\delta_L}{dt} - I(\delta_I - \delta_L)\right]}{(\delta_E - \delta_L)} \qquad (Eq.4.15)$$

This expression is used to calculate the total evaporation lost in *mm* depth between each date (generally bi-weekly to monthly) that a water sample was collected for isotope analysis. The equation is solved during each interval, while tracking changes in total volume with the following expression:

$$V_i = V_{i-1} + (I - PO - E) \qquad (Eq.4.16)$$

where *i* represents each time step between sampling events and *PO* is the water pumped out of BML to be returned to the RCW circuit.

An integrated flux-weighted input signature (δ_I) is calculated over the duration of this period using *Eq. 4.5*, where $I = P + PI + FFT + S + R$, with each parameter defined as *P* = rain; *FFT* = expressed pore water from fluid tailings settlement; *S* = snow; *R* =

runoff. Runoff inputs are included in the BML models because estimates of runoff to BMLwere provided by Dr. Carey.

The evaporation values calculated at each interval were then summed to give an annual evaporation rate in *mm* expressed as depth per year for the open water period of each respective year.

Evaporation rates at BML were also calculated using E/I ratios and the Gonfiantini model as outlined in *Sections 4.3.3.3 & 4.3.3.4*.

Model parameters for evaporation scenario

The following model parameters have been developed using similar techniques outlined in *Sec. 4.3.3.1.* Dr. Carey provided daily surface water temperatures for the duration of the study period. As a result, I was able to calculate relative humidity normalized to the surface water temperature to use for the calculation of m and δ^*. The constant model parameters listed in *Table. 4.3* were used for the BML E/I ratio model and Gonfiantini model.

Table 4.3 BML evaporation scenario parameters for E/I and Gonfiantini model.

Input	Value
T_{air} (°C)	13.95
$T_{surface}$ (°C)	15.93
RH (%)	65.41
RH_{norm} (%)	57.06
α_{18}, α_2	1.01017, 1.08957
ε^*_{18}, ε^*_2 [‰]	10.17, 89.57
ε_{K18}, ε_{K2} [‰]	6.10, 5.37
δ_{A18}, δ_{A2} [‰]	-25.24, -194.73
m_{18}, m_2	1.27, 1.11
δ^*_{18}, δ^*_2 [‰]	4.05, -54.13

The non steady state model involved a varying time step for each mass balance calculation determined by the time period between each observation of isotopic signature. As a result, the model parameters listed above were taken as the period-specific average based on the total days between each sampling event. This adjustment involved

calculating each parameter at a daily time step. The daily calculations were then averaged over the duration of the time period between each mass balance calculation. This was done in an attempt to capture the variance in fluctuating atmospheric conditions at the study site in unison with the daily water balance data.

Seasonality prediction scenario

Here I developed a numerical model to test the ability to replicate the measured isotopic evolution of ^{18}O and ^{2}H of BML over the 4-year period 2014-2017. Isotope samples were collected to represent the signatures of all water balance parameters with the exception of δ_E, which is estimated using the C-G model (*Eq. 4.7*). Initial isotopic composition for BML was passed to the model on day 1 and the resulting isotopic compositions on each subsequent day were calculated based on water balance and isotope mass balance fluxes by rearranging *Eqs. 4.1* & *4.2*, substituting *Eq. 4.7* for δ_E to obtain following expression:

$$\delta_{L_i} = \left(\delta_{L_{i-1}} \cdot V_{i-1} + I\delta_I + PO\delta_{L_{i-1}} - E \cdot \left[\left(\frac{\delta_{L_{i-1}} - \varepsilon_i^*}{\alpha_i^*} - h_i\delta_{A_{monthly\ ave.}}\right) \Big/ \left(1 - h_i - \varepsilon_{K_i} \cdot 10^{-3}\right)\right]\right) \cdot \frac{1}{V_i} \quad (Eq. 4.17)$$

where *i* represents the daily time step, the isotopic signature of the pump out water is assumed to equal BML signature of the previous day ($\delta_{PO} \approx \delta_{L_{i-1}}$). Daily changes in volume were calculated by simultaneously solving *Eq. 4.16* at each time step.

The model neglects to incorporate changes in surface area relating to declining or rising water levels, as this was not feasible to incorporate at a daily time step based on our data. I postulated this would not pose an issue as water levels are managed by operational pumping of freshwater to BML and removal to the RCW circuit to maintain consistent water levels. As a result, surface area should remain relatively constant. Changes in depth of the free water observed within the pond are primarily attributed to a lowering of the mudline (*i.e.* the free water and fluid fine tailings interface) as fluid fine tailings settle increasing the water depth from the surface to the mudline.

Model parameters for seasonality prediction scenario

An initial isotopic composition is set for the model on day 1 (where *i=1*; 1 January 2014) based on the previous fall isotope samples before freeze up - assuming this composition persists through winter. The isotopic composition of BML is then predicted each day based on the water balance fluxes and associated isotopic compositions. The isotopic signature of the FFT pore water released from settlement and the signature of snow/runoff are both assumed to be constant. Model parameters, assumptions, methods, and frequency of sampling are shown in *Table. 4.4*.

Table 4.4 Summary of model parameters for Base Mine Lake seasonality prediction model.

Parameter	Method	Frequency
T_{air}, $T_{surface}$	Met station, Direct measurement	Daily
RH	Met station, normalized to $T_{surface}$	Daily
Initial lake composition (δ_{Li})	Estimated based on Fall conditions	Once ($\delta^{18}O$ = -13.1, $\delta^{2}H$ = -115.7 [‰])
Atmospheric water vapour (δ_A)	Precipitation equilibrium model	Monthly
Rain (δ_{rain})	Observed	Monthly
Snow (δ_{snow})	Observed	Constant ($\delta^{18}O$ = -24.6, $\delta^{2}H$ = -190.9 [‰])
FFT (δ_{FFT})	Observed	Constant ($\delta^{18}O$ = -12.46, $\delta^{2}H$ = -112.80 [‰])
Pump in (δ_{PI})	Observed	Monthly mean
Pump out (δ_{PO})	Assumed = δ_L	Daily
Runoff (δ_{runoff})	Assumed = δ_{snow}	Constant
Evaporation (δ_E)	Craig-Gordon Model	Daily

Samples have been collected from three different locations on the lake at depth intervals ranging from the surface to the mudline. This presents a range of isotope values from samples collected on the same day. Since the model assumes well-mixed conditions at BML I assumed the calculated mean of all samples collected on the same day to be a representation of the homogenized composition of BML. It is noted that there is isotopic variation throughout the depth profile of BML and this may introduce a source of error to

calculations based on potential enriched or depleted “hot-spots”. Analysis of processes contributing to the evolution of isotopically distinct depth profiles within BML is beyond the scope of this study.

4.4 Results

4.4.1 Isotope characteristics of mine site waters

The isotope data collected from site waters at Mildred Lake Mine is presented in a dual isotope plot (*Fig. 4.4*). An initial local meteoric water line was published for Mildred Lake Mine $\delta^2H = 7.20 \cdot \delta^{18}O - 10.3$ [‰] by Baer et al., (2016). The LMWL has since been updated with new meteoric water samples in *Chapter 3* to $\delta^2H = 7.07 \cdot \delta^{18}O - 14.4$ [‰]. Individual rain samples collected on site ranged from -26.23 ‰ to -7.03 ‰ and -201.62 ‰ to -71.3‰ for ^{18}O and ^{2}H respectively. Snow surveys from an 8-year period (2009, 2012-2018) collected samples throughout the snowpack that ranged from -31.50 ‰ to -15.34 ‰ and -243.3 ‰ to -131.5 ‰, with a mean of -24.67 ‰ and -191.04 ‰ for ^{18}O and ^{2}H respectively. *Chapter 3* also undertook an extensive review of all meteoric water samples collected at the mine site and calculated the annual volume-weighted average of precipitation (including both rain and snow) to be -18.04 ‰ and -143.54 ‰ for ^{18}O and ^{2}H respectively. The volume-weighted average of precipitation during the open water season (May-October) was found to be -14.77 ‰ and -120.06 ‰ for ^{18}O and ^{2}H respectively.

Freshwater imported on-site originates from the Athabasca River, is then stored in Mildred Lake Reservoir that supplies upgrading and cooling processes, and finally any water that has not been chemically consumed or evaporated is released to the RCW circuit as cooling tower blowdown. Athabasca River samples were found to range from -20.18‰ to -16.55‰ and -158.1‰ to -133.8‰, with a mean of -17.93‰ and -142.81‰ for ^{18}O and ^{2}H respectively, based on a 12-year study performed by Gibson et al. (2016c). Mildred Lake Reservoir samples collected by Baer at al., (2016) ranged from -18.91‰ to -14.66‰ and -145.78‰ to -125.28‰, with a mean of -16.72‰ and -137.49‰ for ^{18}O and ^{2}H respectively over the years 2013-2015, and 2017. An investigation of the Mildred Lake Reservoir samples in *Chapter 3* found that the signature of the reservoir is

influenced by high site water demands resulting in low residence times; therefore, samples reflect those of the average Athabasca signature.

Four cooling towers operate at Mildred Lake Mine with varying internal and operational conditions. Observed cooling tower blowdown waters are more enriched in heavy isotopes than the freshwater samples due to evaporative fractionation under near-equilibrium conditions (Baer at al, 2016; *Chapter 3*). An evaporation line of $\delta^2H = 5.44 \cdot \delta^{18}O - 43.5$ [‰] was developed based on linear regression of the isotopic signatures over a two-year period (2016-2018). Individual samples ranged from -16.18‰ to -10.03‰ and -132.5‰ to -95.5‰, with a mean of -13.37‰ and -116.25‰ for ^{18}O and ^{2}H respectively. The evolution of cooling tower blowdown signatures was thoroughly investigated in *Chapter 3* and found to be largely influenced by internal operating conditions (*i.e.*, *T* and *RH*), as well as the number of cycles the water undergoes through the cooling circuit.

Samples have been collected from three perched ponds located on the reclaimed landscape South Bison Hills within the Mildred Lake Mine site for past studies from years spanning 2003-2012 (Baer et al., 2016; Hilderman 2011). The sampling program developed for this thesis project resumed bi-weekly sampling of the ponds for open water period over 2016-2018. The samples were used to develop a reference natural evaporation line of $\delta^2H = 5.19 \cdot \delta^{18}O - 58.0$ [‰] through linear regression analysis that was found to be in good agreement with the regional evaporation line $\delta^2H = 5.20 \cdot \delta^{18}O - 50.6$ [‰] developed by Gibson et al., (2015) based on sampling of 40 lakes located within a 200 km radius of Fort McMurray. Individual samples from the natural ponds ranged from -20.18‰ to -6.00‰ and -164.93‰ to -90.24‰, with a mean of -11.09‰ and -115.41‰ for ^{18}O and ^{2}H respectively. These three ponds displayed the largest isotopic range of surface waters observed on site.

Samples collected from the RCW circuit for this study consisted of individual sampling of two tailings ponds (MLSB and SWIP) composed of tailings and clarified OSPW, as well as the recycle pond. These three ponds were believed to be the most applicable proxies for the RCW circuit based on a detailed investigation of the seasonal cycles of the RCW circuit and individual tailings ponds found in *Chapter 3*. The samples were used to develop an evaporation line for the RCW circuit of $\delta^2H = 4.55 \cdot \delta^{18}O -$

55.85 [‰] through linear regression analysis. Individual samples ranged from -15.65‰ to -11.17‰ and -128.10‰ to -105.65‰, with a mean of -13.08‰ and -115.34‰ for ^{18}O and ^{2}H respectively. The RCW circuit appears to be operating under isotopically steady state conditions year over year with a maximum enrichment occurring in the late summer/early fall period generally ranging from -11‰ to -12‰ and -105‰ to -110‰ for ^{18}O and ^{2}H respectively. This enrichment is reset by spring, likely due to the mixing of expressed tailings pore water over winter while evaporation is not occurring, and the addition of depleted snow melt waters during the spring freshet.

Samples were collected from BML at three platforms within the lake, usually at depth intervals of 1 m from the water surface to the tailings mudline, as well as the pump out water from the lake. The samples were used to develop an evaporation line of $\delta^2 H = 4.11 \cdot \delta^{18} O - 62.27$ [‰] through linear regression analysis. The BML evaporation line exhibited the lowest slope of site waters. The individual samples collected ranged from -15.28‰ to -10.12‰ and -125.10‰ to -104.98‰, with a mean of -12.08‰ and -111.99‰ for ^{18}O and ^{2}H respectively. The isotopic signature of BML was similar to the RCW circuit, most likely due to the influence of pore water released during consolidation of fluid tailings. Seasonal sampling of BML has demonstrated progressive enrichment of the isotopic signature between 2014-2017 and is explored further in *Sec. 4.3.5*.

The feed line that transports tailings slurry to the tailings ponds following bitumen extraction were also sampled. These samples ranged from -14.82‰ to -11.75‰ and -124.10‰ to -106.90‰, with a mean of -13.58‰ and -117.89‰ for ^{18}O and ^{2}H respectively. The isotopic range of sampled fluid tailings was similar to waters collected from the RCW circuit. However, the mean of the samples was more depleted than the mean of the RCW circuit, likely due to the open water evaporative enrichment experienced from the tailings ponds.

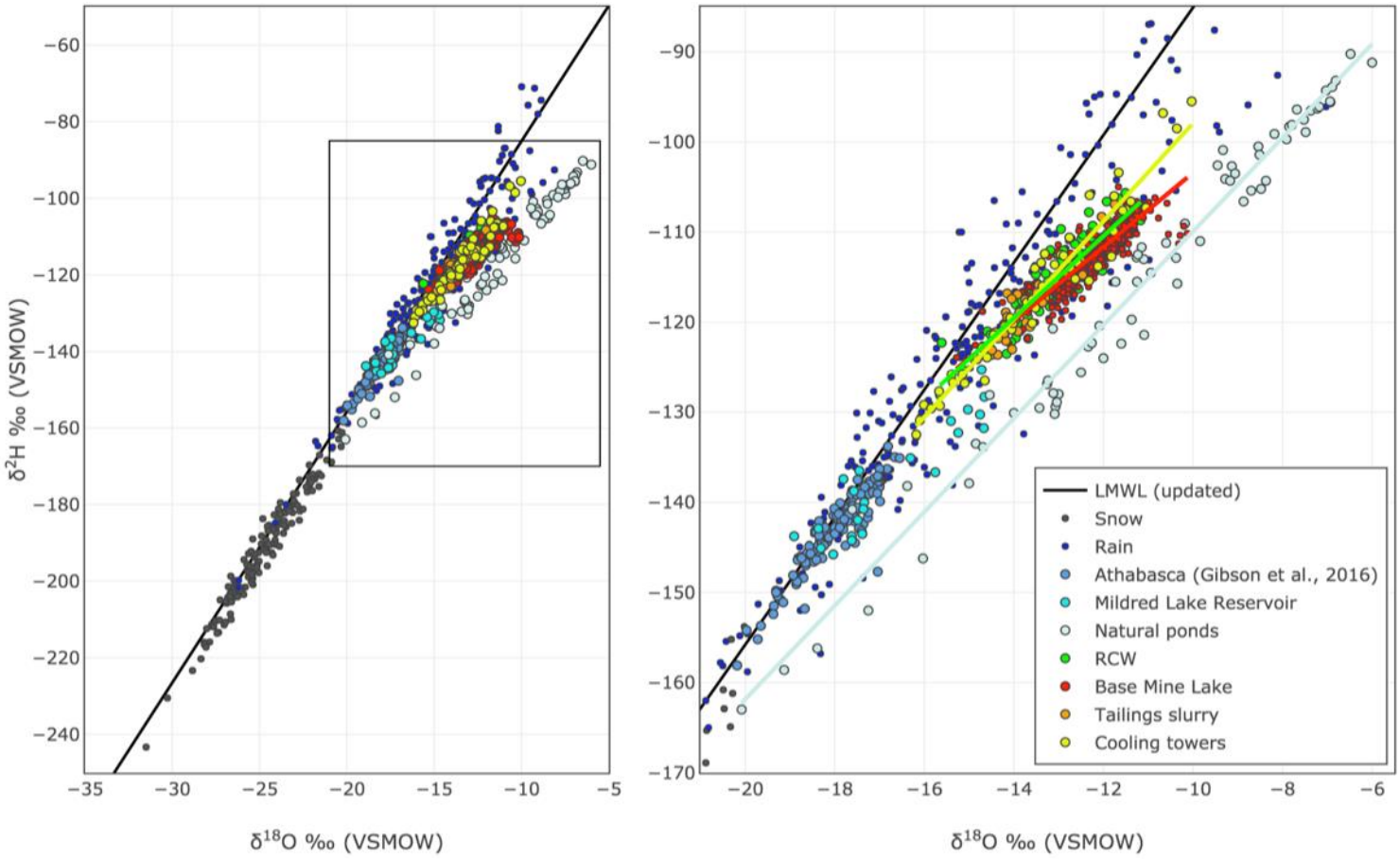

Figure 4.5 Dual isotope plot of site waters at Mildred Lake Mine site. Evaporation lines (solid lines on graph) are calculated based on regression analysis from cooling tower blowdown, recycle water circuit, Base Mine Lake, and natural ponds on site referenced by sample color.

4.4.2 Recycle water circuit — Evaporation/inflow ratios

Evaporation/inflow ratios from the open water period were calculated for the RCW circuit using the isotope mass balance developed in *Eq. 4.12.*

E/I ratios were calculated from three separate ponds (SWIP, MLSB, and Recycle Pond) within the RCW circuit using the most enriched δ-values observed from the late summer/early fall periods from the years 2012-2014, 2016, and 2017 shown in *Fig. 4.5b.*

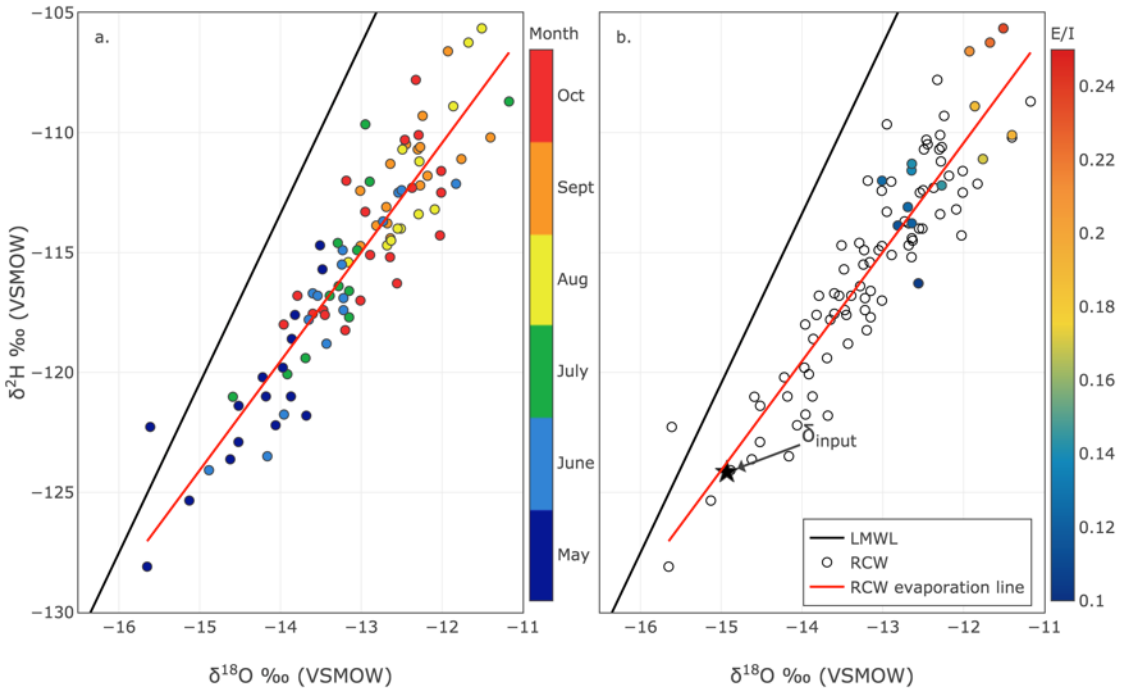

Figure 4.6 a.) Dual isotope plot $\delta^{18}O$-$\delta^{2}H$ of samples collected from the recycle water circuit during the open water period (May-Oct) over a 6-year period (2012-2017) sorted by month of collection. b.) The same plot showing the calculated evaporation/inflow ratios using the most enriched samples from the open water period of each year.

The results of the isotope mass balance model are presented in *Table. 4.5.* E/I ratios from all three ponds ranged from 0.09 to 0.18 using ^{18}O and 0.09 to 0.27 using ^{2}H as the tracers. These results suggest that less than 30% of the total inflow is being lost to open water evaporation from the RCW circuit.

The mean of E/I ratios calculated using ^{18}O and ^{2}H were supplemented with the total input volume presented earlier to calculate the total evaporation expressed as depth

of water (*mm*) using the total surface area of the RCW circuit. The recycle pond calculations resulted in the largest range of evaporation (67-133 mm) and the highest evaporation volume 133 mm, whereas SWIP displayed the lowest range (61-98 mm) and the lowest evaporation (61 mm) over all years.

E/I ratios were also calculated over three periods (May-June, July-Aug, and Sept-Oct) during the year 2017, using samples collected from the Recycle Pond. Results from these calculations are presented in Table 4.6. E/I ratios were found to range from 0.08 to 0.16 and 0.04 to 0.26 for ^{18}O and ^{2}H respectively. The highest evaporative period was found to be May-June (53 mm), while the lowest period was Jul-Aug (12 mm). The sum of the three periods (total open water period) was 98 mm. This value is slightly lower than the E/I ratio calculated from the recycle pond in 2017 over the entire evaporative period (111 mm; Table. 4.5).

Table 4.5 Results of recycle water circuit E/I calculations displaying evaporation rates both by depth (*mm yr^{-1}*) and volume (*Mm^3 yr^{-1}*).

		$\delta^{18}O$ [‰]		$\delta^{2}H$ [‰]		Mean E/I	RPD	Evaporation
	Year	Max	E/I	Max	E/I		[%]	[*mm yr^{-1}*]/[*Mm^3 yr^{-1}*]
Recycle Pond	2012	-11.51	0.17	-105.65	0.27	0.22	42.2	133/3.8
	2013	-12.64	0.11	-111.58	0.16	0.13	41.1	80/2.3
	2014	-12.81	0.10	-113.87	0.13	0.11	26.1	67/1.9
	2016	-12.64	0.11	-111.30	0.17	0.14	43.6	82/2.3
	2017	-11.40	0.18	-110.10	0.19	0.18	1.8	111/3.2
MLSB	2012	-11.67	0.16	-106.24	0.26	0.21	44.0	126/3.6
	2013	-11.93	0.15	-106.61	0.25	0.20	51.0	119/3.4
	2014	-13.01	0.09	-112.00	0.15	0.12	56.3	72/2.07
	2016	-12.69	0.10	-113.10	0.14	0.12	28.1	72/2.07
	2017	-11.86	0.15	-108.90	0.21	0.18	30.3	108/3.08
SWIP	2012	-	-	-	-	-	-	-
	2013	-12.00	0.11	-108.61	0.09	0.10	18.2	61/1.8
	2014	-12.64	0.11	-113.78	0.13	0.12	18.0	70/2.0
	2016	-12.27	0.13	-112.20	0.15	0.14	17.2	84/2.4
	2017	-11.76	0.16	-111.10	0.17	0.16	6.4	98/2.8

Table 4.6 E/I ratios calculated from the recycle pond over three evaporative periods in 2017.

Period	Input volume	$\delta^{18}O$ [‰]			$\delta^{2}H$ [‰]			Mean E/I	RPD	Evaporation
(2017)	[Mm^3]	Volume-weighted δ_I	Max	E/I	Volume-weighted δ_I	Max	E/I		[%]	[mm]/[Mm^3]
May-Jun	6.90	-16.32	-12.50	0.18	-133.32	-112.40	0.26	0.22	36	53/1.52
Jul-Aug	5.88	-13.65	-12.09	0.08	-116.04	-113.20	0.04	0.06	67	12/0.35
Sept-Oct	4.42	-14.45	-12.29	0.16	-120.66	-110.10	0.25	0.21	44	32/0.97
Total	17.20	-	-	-	-	-	-	-	-	98/2.78

I acknowledge there may be significant error associated with our means of estimating δ_I, due to the difficulty in obtaining accurate measurements of the large input volumes of water to the RCW circuit, which could be carried over to the calculated E/I ratios. I attempted to quantify this error by calculating the relative percent difference (RPD) between independent *E/I* ratios calculated using ^{18}O and ^{2}H. Following the rules of mass balance conserved within the steady state assumption, the evaporative fractionation will cause a linear enrichment of the RCW circuit away from δ_I. Therefore, the differences in *E/I* calculated using each tracer will represent samples that did not fall along the evaporation line originating from δ_I. This deviation may suggest inaccuracies in the input parameters used to calculate the weighted input signature.

The average calculated RPD of all years for each individual pond is 31.0%, 41.9%, and 14.9% from the recycle pond, MLSB, and SWIP respectively (*Table. 4.4*). The recycle pond had the lowest calculated RPD in 2017 across all three ponds, with ratios agreeing within 1.8%. MLSB had the highest RPD of all the calculations, with E/I ratios deviating by 56.3% in 2014.

The difference in RPDs between tailings ponds may be due to varying water balance conditions and dimensions of the ponds themselves. Surface area and in turn total volume will affect the degree of evaporative enrichment experienced, while variance amongst water balance inputs and outflows for each pond may also influence the individual slopes of each pond composing the RCW circuit. For example, a pond that is more influenced by rainfall and surface runoff may have a steeper slope reflecting the mixture of meteoric water and indicated by samples plotting closer to the LMWL.

The RPDs calculated for each of the three specific evaporative periods ranged from 36 to 67%, with the best agreement occurring in May-June, and the worst agreement occurring in July-Aug.

4.4.3 Recycle water circuit — Gonfiantini Model

Here we used the Gonfiantini model outlined in *Sec. 4.2.6* to estimate the evaporative loss from the RCW circuit over a five-year period. *Eq. 4.15* was rearranged to solve for *f* based on the observed minimum and maximum isotopic compositions of the RCW circuit throughout the duration of the open water evaporative period (May-Oct) for

each year. Samples collected from the recycle pond were selected for the calculations and assumed to be representative of the entire RCW circuit based on rationale outlined in *Chapter 3.* The model assumes no inflow or outflow from the system and therefore is not dependant on the isotopic compositions and volumes of water balance parameters, which have been identified as a potentially significant source of error in the *E/I* ratio calculations.

The results of the Gonfiantini model are presented in *Table. 4.7*. The fraction of water lost (*1-f*) was supplemented with the volume (200 Mm^3) and surface area (28.6 Mm^2) of the RCW circuit to estimate the total evaporation lost during the open water period and expressed as total depth of evaporation (*mm*). The volume and area of the RCW circuit were assumed to be constant throughout the duration of the study period based on limited data available for all years.

Table 4.7 Estimates of evaporative loss from the recycle water circuit based on observed isotopic enrichment of the recycle pond and calculated using the Gonfiantini model.

	$\delta^{18}O$ [‰]			$\delta^{2}H$ [‰]			Mean *f*	RPD	Evaporation
Year	Max	Min	*f*	Max	Min	*f*		[%]	*[mm yr^{-1}]*
2012	-11.51	-12.90	0.93	-105.65	-112.04	0.91	0.92	2.22	561
2013	-12.64	-15.65	0.87	-115.19	-128.10	0.86	0.87	1.54	931
2014	-12.81	-15.61	0.88	-113.87	-122.27	0.90	0.89	2.12	757
2016	-12.64	-13.47	0.96	-111.30	-117.60	0.92	0.94	4.30	418
2017	-11.40	-14.22	0.87	-110.10	-120.20	0.88	0.87	0.85	892

Independent values of *f* were calculated using ^{18}O and ^{2}H. The average of the two *f* values was then used to calculate the estimated evaporation lost from the RCW circuit. The annual evaporation rates ranged from 418 mm yr^{-1} in 2016 to 931 mm yr^{-1} in 2013, with an average annual rate of 712 mm yr^{-1}. This range is much larger than those estimated using the Penman combination method for the years 2012 to 2017 (373 – 513 mm yr^{-1}) and by eddy covariance for 2014 to 2017 (351 – 518 mm yr^{-1}). The evaporation rates from the Gonfiantini model are also substantially higher than those predicted using the *E/I* ratios in *Sec. 4.4.2*.

Eq. 4.15 was also used to predict an evaporation line for the RCW circuit by calculating δ_f for ^{18}O and ^{2}H using a range of values for f between 1 and 0. Linear regression was then used to calculate the evaporation line $\delta^2 H = 4.46 \cdot \delta^{18} O - 61.57$ [‰] which is in good agreement with the evaporation line $\delta^2 H = 4.55 \cdot \delta^{18} O - 55.85$ [‰] developed by regression analysis of the samples collected from the RCW circuit. The agreement between the modelled slope using *Eq. 4.15* and the slope developed based on regression analysis of samples collected is used to attest to the suitability of the atmospheric parameters outlined in *Sec. 4.3.3.4;* as the slope of the evaporation line is largely controlled by these variables.

The RPD was calculated between *f* values of ^{18}O and ^{2}H tracers. The RPDs ranged from 0.85% in 2017 to 4.30% in 2016 and showed much better agreement between the two isotope tracers for this model when compared to the E/I model. This agreement signifies that the evaporation line developed by *Eq. 4.15* accurately captured the minimum and maximum isotopic compositions observed for each year from the recycle pond.

4.4.4 Base Mine Lake

The largest input to BML is freshwater pumped in from Beaver Creek Reservoir (BCR) located in close proximity to the end pit lake. A seasonal pattern can be observed in the BCR isotope data collected as *Pump in* water to BML, as seen in *Fig. 4.7*. Spring depletion is attributed to the spring freshet that adds isotopically depleted waters as snow and ice melt - both directly at the thawing reservoir surface and as surface runoff. Evaporative enrichment throughout the open water period results in the accumulation of ^{18}O and ^{2}H within the reservoir.

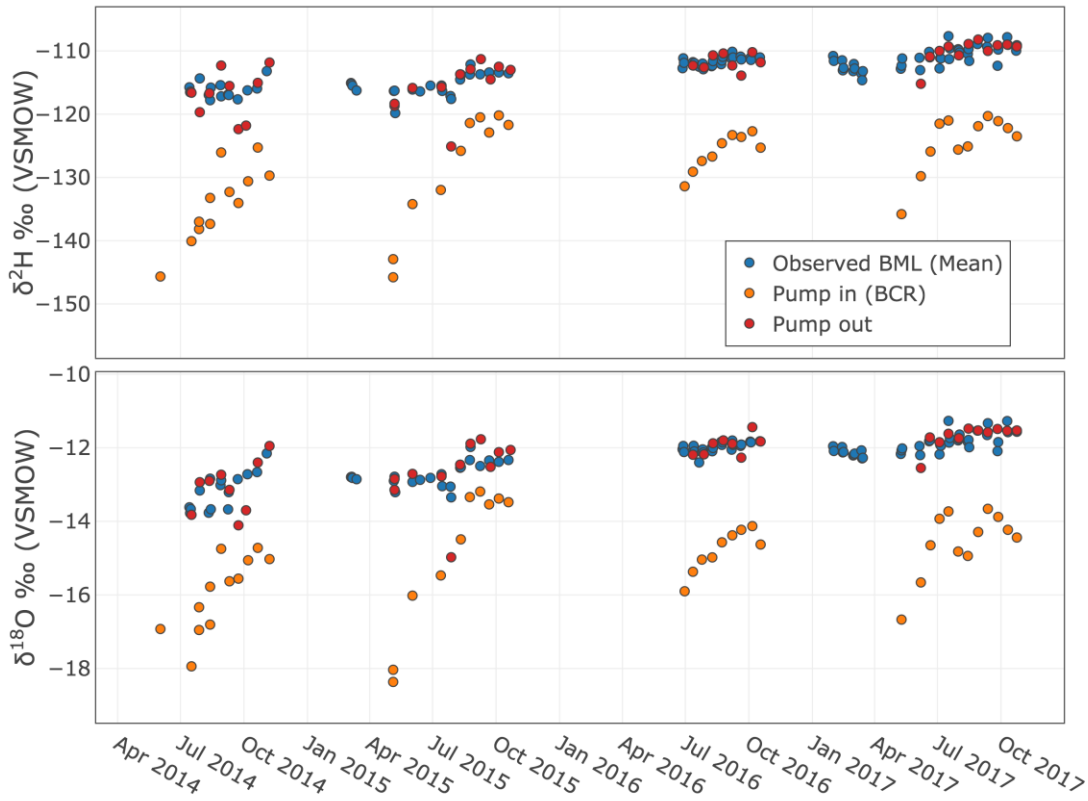

Figure 4.7 Temporal variations of ^{18}O and ^{2}H for *pump in* from BCR, *pump out* from BML to the RCW, and the mean of the observed isotopic signatures collected from three platforms at Base Mine Lake.

The BML signatures in *Fig. 4.7* display temporal enrichment both seasonally and interannually. However, the seasonal enrichment is muted when compared to the BCR samples, with BCR enrichment up to an order of magnitude higher than BML, as shown in *Table.* 4.8. This muted enrichment suggests that one or more water balance parameters at BML are acting as a buffer to the range of isotopic fluctuations observed at BCR.

Table 4.8 Summary of annual Base Mine Lake and Beaver Creek Reservoir isotopic signatures, where n = number of days sampled each year. Annual enrichment is calculated based on maximum and minimum signatures from each year.

		δ^2H [‰]					$\delta^{18}O$ [‰]				
Year	n	Mean	STD	Min	Max	Enrichment	Mean	STD	Min	Max	Enrichment
Base Mine Lake											
2014	17	-116.15	1.16	-117.79	-113.20	4.59	-13.16	0.47	-13.78	-12.15	1.01
2015	22	-115.33	1.74	-119.83	-112.14	7.69	-12.72	0.33	-13.35	-11.98	0.74
2016	24	-111.69	0.69	-112.90	-110.13	2.77	-11.99	0.14	-12.40	-11.80	0.19
2017	39	-111.03	1.72	-114.63	-107.67	6.97	-11.89	0.27	-12.29	-11.27	0.62
Beaver Creek Reservoir											
2014	12	-134.12	5.90	-145.66	-125.28	20.38	-15.96	1.03	-17.94	-14.72	3.22
2015	10	-128.74	9.54	-145.78	-120.20	25.58	-14.93	1.97	-18.36	-13.19	5.17
2016	9	-126.01	2.91	-131.40	-122.70	8.70	-14.80	0.58	-15.90	-14.13	1.77
2017	12	-124.48	4.50	-135.80	-120.30	15.50	-14.58	0.88	-16.67	-13.66	3.01

I postulate that the primary mechanism of this isotopic buffering effect is the addition of pore water released from fluid fine tailings (FFT) during settlement to the overall storage. Interval sampling to assess the isotopic signature of FFT was performed by Dompierre et al., 2017 over the years 2012, 2014, and 2015. Samples were collected from the water surface to depths up to 47 m below the surface establishing an isotopic profile throughout the water column extending to the original depth of the open pit mine (*i.e.* depth of tailings backfill). Based on these samples the average isotopic signatures of FFT were calculated to be -12.46‰ and -112.80‰ for ^{18}O and ^{2}H respectively. The temporal BML signatures seem to fluctuate closely to these averages rather than the water pumped in from BCR.

The following sections have been developed to assess the feasibility of isotope tracer techniques for estimating evaporation at BML. The previous models applied to the RCW (E/I ratios, Gonfiantini model) are applied to BML, as well as a non steady state isotope mass balance model incorporating the daily water balance data provided by Dr. Carey.

4.4.4.1 Base Mine Lake Evaporation/Inflow Ratios

Here I implement the E/I isotope mass balance model to BML. Our E/I ratio assessment of BML differs from the RCW circuit because I have high-level water balance data available to create a more accurate integrated input signature. Total volume of inflow *I*, expressed as depth of water (*mm* yr^{-1}), and the volume-weighted input signature δ_I for each year are provided in *Table. 4.9*.

E/I ratios calculated for the period 2014-2017 at BML are presented in *Table. 4.9*. The E/I ratios ranged from 0.13 (2014) to 0.22 (2017) using ^{18}O and 0.09 (2015) to 0.13 (2017) using ^{2}H as tracers, with the mean of the ratios ranging from 0.11 (2015) to 0.18 (2017).

Table 4.9. Results of Base Mine Lake Evaporation/Inflow ratio calculations

	$\delta^{18}O$ [‰]			$\delta^{2}H$ [‰]			Mean E/I	RPD	Inflow	Evaporation
Year	Max	δ_I	E/I	Max	δ_I	E/I		[%]	[*mm yr*$^{-1}$]	[*mm yr*$^{-1}$]
2014	-12.15	-14.85	0.13	-109.41	-126.36	0.12	0.13	8.5	1821	228
2015	-11.78	-14.52	0.14	-111.37	-124.77	0.09	0.11	41.1	1520	172
2016	-11.69	-14.67	0.15	-109.60	-123.77	0.10	0.13	40.1	1082	135
2017	-10.85	-14.95	0.22	-106.20	-125.10	0.13	0.18	52.7	773	136

Calculated RPDs were similar to those calculated from the *E/I* ratios of the RCW circuit. BML RPDs ranged from 8.5% to 52.7%, whereas the RPDs from the RCW ranged from 1.8% to 56.3%. As discussed in *Sec. 4.3.3* the large range of RPDs may reflect inaccuracies in the integrated weighted inflow signature or may be due in part to inaccuracies in the atmospheric exchange parameters. Regardless, it allows for quantification of the range of error associated with evaporation calculations using the E/I ratio method for each individual tracer.

4.4.4.2 Base Mine Lake Gonfiantini model

Results of the Gonfiantini model calculated over a four-year period are presented in *Table. 4.10*. Here the total fraction of volume remaining (*f*) ranged from 0.92 – 0.97 and 0.91 – 0.96 for ^{18}O and ^{2}H respectively, with the average *f* calculated from the two tracers ranging from 0.92 – 0.97. The average *f* values were used to calculate the annual evaporation rate based on the fraction lost ($1-f_{mean}$) and expressed as *mm* depth based on annual volumes of BML. The BML volumes were adjusted based on the change in storage calculated from the water balance provided by Dr. Carey.

Table 4.10 Estimates of evaporative loss from Base Mine Lake based on observed isotopic enrichment and calculated using the Gonfiantini model.

	$\delta^{18}O$ [‰]			$\delta^{2}H$ [‰]				RPD	Average Volume	Evaporation
Year	Max	Min	*f*	Max	Min	*f*	Mean *f*	[%]	[*mm*]	[*mm yr*$^{-1}$]
2014	-12.15	-13.78	0.92	-113.20	-117.79	0.94	0.93	2.2	9300	651
2015	-11.78	-13.21	0.93	-112.14	-119.83	0.91	0.92	2.2	9740	779
2016	-11.69	-12.40	0.97	-110.13	-112.60	0.96	0.97	1.0	9911	347
2017	-10.85	-12.19	0.95	-107.67	-113.70	0.91	0.93	4.3	10000	700

Evaporation rates from 2014-2017 ranged from 347 to 779 mm yr^{-1}, with an average rate of 619 mm yr^{-1}. Again, this range is higher than both those calculated by the Penman combination method and eddy covariance methods (*Table. 4.2*).

The Gonfiantini model does not consider inflows or outflows from Base Mine Lake and therefore attributes all enrichment directly to evaporation. As discussed in *Sec. 4.4.3*, it is expected that pore water released from FFT settlement is contributing to the overall enrichment of BML free water in addition to evaporation. I believe expressed porewater is influencing enrichment because the average isotopic signature of FFT is contained within the range of observed seasonal isotopic composition of BML.

The Gonfiantini model was also used to predict the evaporation line of BML using *Eq. 4.15.* The resultant evaporation line was found to be $\delta^2H = 3.96 \cdot \delta^{18}O - 64.58$ [‰], which is in good agreement with the evaporation line developed by regression analysis of samples collected $\delta^2H = 4.11 \cdot \delta^{18}O - 62.27$ [‰]. As discussed in *Sec. 4.4.3* this indicates the suitability of the atmospheric exchange parameters developed for the BML models, as they could be used in the reproduction of the observed slope with reasonable accuracy.

4.4.4.3 Base Mine Lake isotope mass balance model (non steady state)

The BML non steady state isotope mass balance model developed in *Sec. 4.3.3.5* was used to estimate annual evaporation rates during the open water period for each year (Table 4.11). The lowest values of *E* were calculated in 2017 as 210 and 307 mm yr^{-1} for ^{18}O and ^{2}H respectively, with an average of 259 mm yr^{-1}. The highest values of *E* were calculated as 447 mm yr^{-1} in 2014 (^{18}O tracer) and 684 mm yr^{-1} in 2015 (^{2}H tracer). Annual evaporation estimates calculated using each tracer resulted in discrepancy between the tracers. The highest range of E between the tracers occurred in 2015 with annual *E* estimated to be 407 mm and 684 mm using ^{18}O and ^{2}H respectively.

Table 4.11 Estimates of annual evaporation rates using the non steady state isotope mass balance model.

Evaporation (*E*)				
Year	^{18}O	^{2}H	Mean	RPD
	[*mm yr^{-1}*]	[*mm yr^{-1}*]	[*mm yr^{-1}*]	[*%*]
2014	447	318	382	34
2015	407	684	545	51
2016	444	599	522	30
2017	210	307	259	37

4.4.4.4 Base Mine Lake seasonality prediction model

All hydrologic and climatic aspects of Base Mine Lake are highly monitored. This available data provides the opportunity to utilize a non steady state isotope mass balance approach to predict isotopic evolution at a daily timescale and in turn attempt to reproduce observed seasonality interannually. *Eq. 4.16,* as developed in *Sec. 4.3.3.5*, was used here to solve for the daily isotopic composition based on observed isotopic signatures and monitoring data of water balance fluxes.

The purpose of the seasonality model was to replicate the enrichment observed during the evaporative period. From a water balance perspective, evaporation is the only fractionating process; therefore, observed enrichment could be used to predict evaporation rates. Results of the model are shown in *Fig. 4.9.*

The isotope mass balance model was ran using ^{18}O and ^{2}H as independent tracers. When ^{18}O was used as the tracer the model results were in good agreement with the observed mean compositions collected throughout 2014-2017. Accuracy of the model appears to decrease when ^{2}H is used as the tracer. The ^{2}H scenario resulted in limited enrichment during the open water period for both 2014 and 2015.

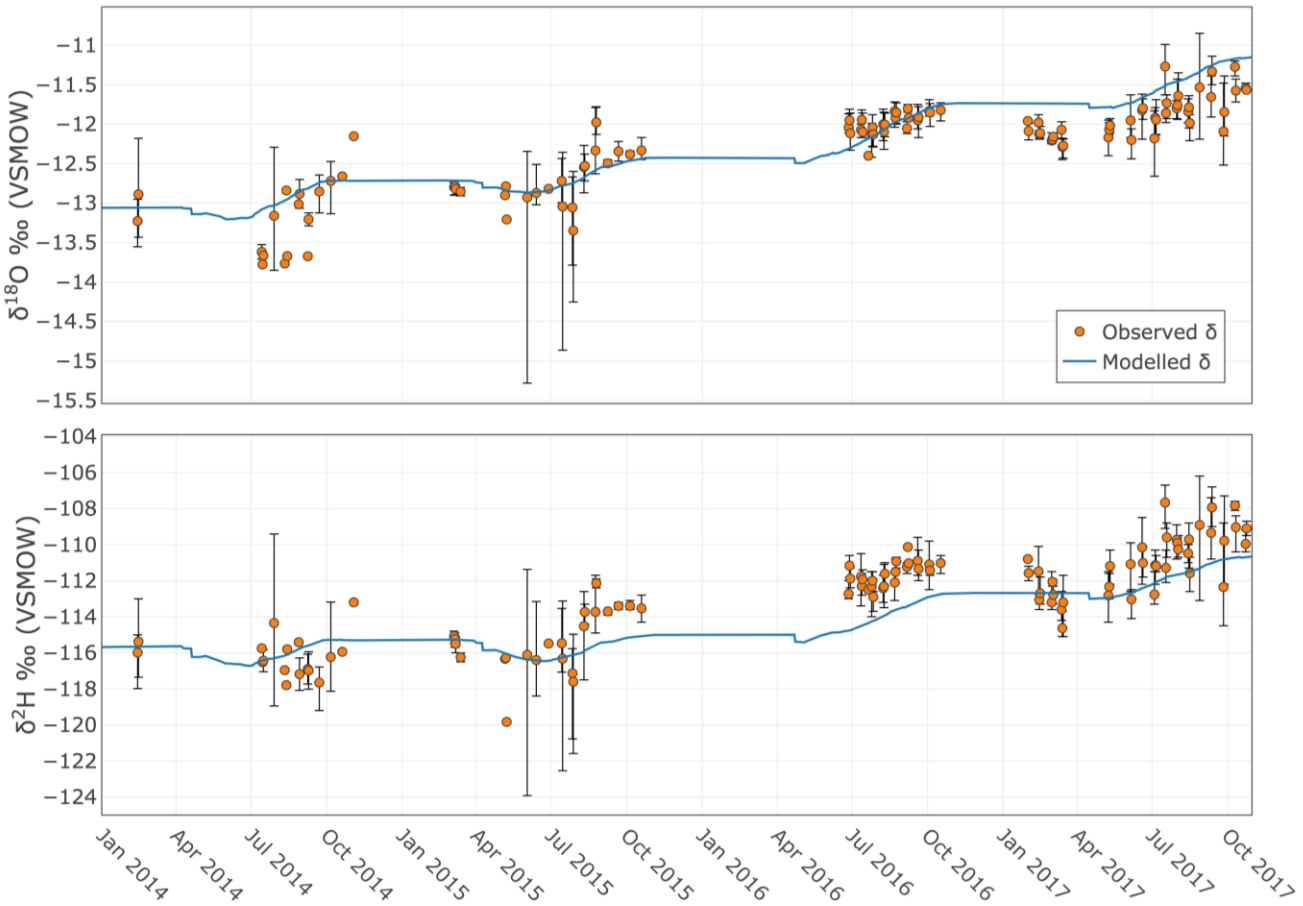

Figure 4.8 Output of the seasonality prediction model developed for Base Mine Lake. Circles represent the calculated mean isotopic composition based on three monitoring stations on Base Mine Lake. Error bars indicate the maximum and minimum observed values from the sampling date.

4.4.4.5 Base Mine Lake seasonality model sensitivity analysis

Errors associated with the measurement of water balance components are difficult to assess due to the techniques associated with them. An estimate of the % error associated with each flux which are provided in *Table. 4.12 (from Dr. S. Carey, pers. Comm).*

.

Table 4.12 Estimates of error associated with Base Mine Lake water balance fluxes (S. Carey, pers. Comm.).

Parameter	% Error (+/-)
Pump in/out (*PI/PO)*	15
Evaporation (*E*)	15-20
Precipitation (*P*)	15
Runoff (*R*)	20
Expressed pore-water (FFT)	10

I tested the sensitivity of the BML seasonality model to each water balance parameter by inducing a ±10% shift within each independant parameter. The results of the sensitivity anlysis are shown in *Fig. 4.9.*

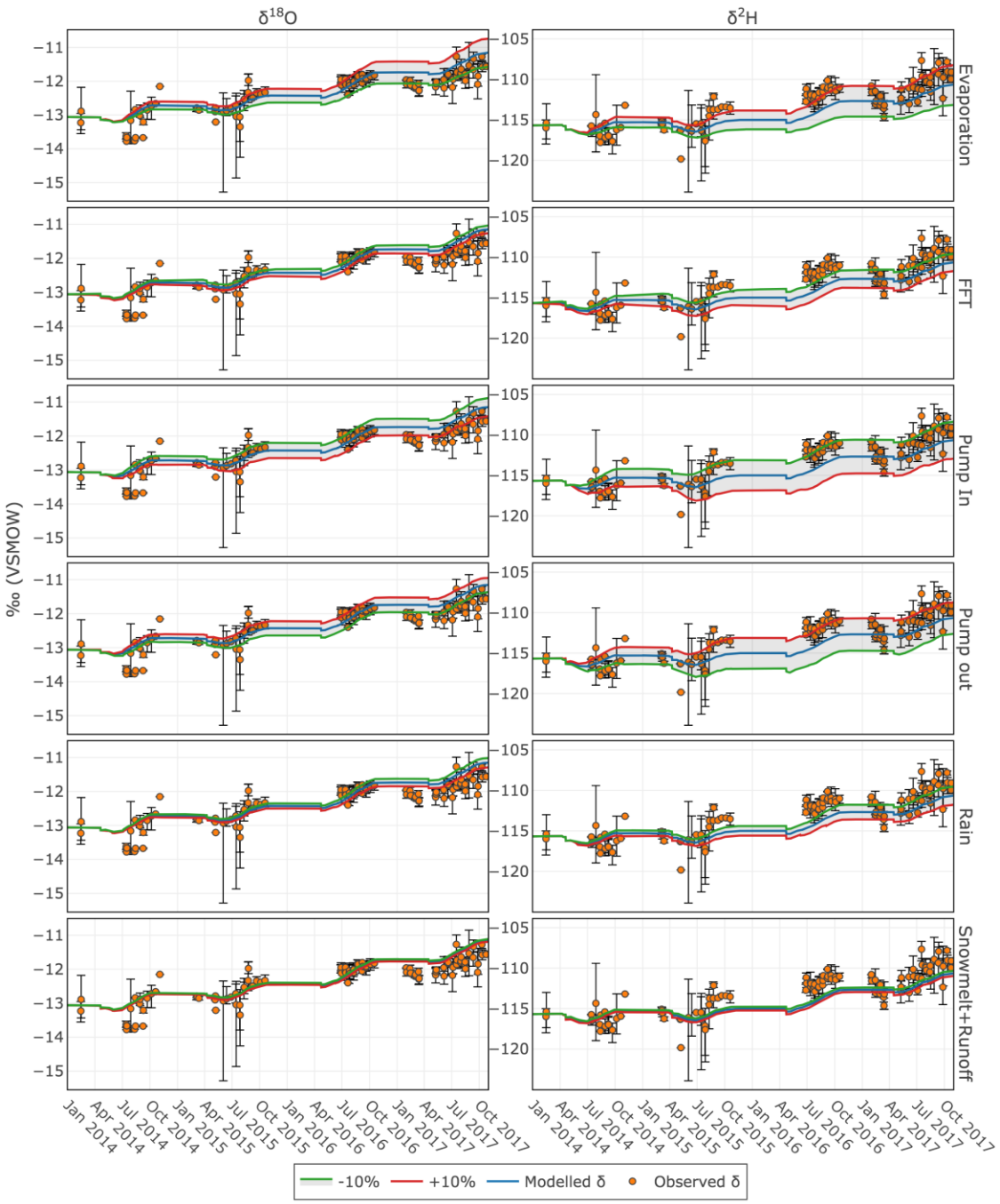

Figure 4.9 Sensitivity analysis of the BML seasonality model to each water balance parameter. A ±10% shift was applied to each parameter.

In *Fig. 4.4* I show that *PI*, *PO*, and *E* are the largest contributors to the water balance — so it is not overly surprising that the ±10% shifts in volume for each had the largest effect on the seasonality model. However, the magnitude of the effects of *PI* and *PO* shifts were relatively constant through 2015, 2016 and 2017 as seen in the temporal plots (*Fig. 4.4*), while the effects of *E* amplified through each year. This observation may

suggest that there is an error in the atmospheric parameters of the C-G model, which results in deviation from the original model propagating the longer the model is ran. Shifts in the amount of snowmelt/runoff to BML had very little effect on the model, which is in line with our temporal observations that BML is continuously enriching year over year within our study period. Other water balance parameters such as the expression of enriched tailings pore water (*FFT*) are likely acting as a buffer to the addition of depleted waters. Contrary to the limited effects of freshwater additions via meteoric water, when *PI* is adjusted, I did see substantial changes to the model. The volumetric shift in *PI* and associated seasonal isotopic signatures of the BCR source water seems to be enough to overpower the buffering effects of *FFT*. The model showed a low degree of sensitivity to shifts in rain volume, which is again likely due to greater volume of other water balance parameters. There was also a low degree of sensitivity to shifts in *FFT* contribution, which is likely because the signature of *FFT* pore water is already similar to the overall isotopic signature of BML.

Each water balance parameter was tested using both ^{18}O and ^{2}H as the tracers. It would appear that ^{2}H is more sensitive to errors associated with measurements of water balance fluxes than ^{18}O and may not be an ideal tracer for isotope mass balance models when using an individual tracer.

4.5 Discussion

4.5.1 E/I ratios

Bennett et al., (2008) studied 50 lakes located in Northern Alberta found that the fraction of input water lost to evaporation ranged from 8% to 75% compared to our values of 11% to 22% from the RCW circuit. Low E/I ratios are characteristic of high throughflow systems with short residence time (Bennet et al., 2008; Gibson et al., 2002). These findings are consistent with hydrological knowledge of the tailings ponds where it is expected that high pumping rates associated with site water demands (200 $Mm^3\ yr^{-1}$) result in short residence times of each tailings pond.

An E/I ratio of 1 indicates that the inflow volume is balanced by evaporation, with values above 1 indicating volumetric loss from the reservoir. Here I calculated E/I ratios much lower than 1 (*e.g.*, 0.22 or 22% of inflow lost to evaporation). By design the RCW

circuit operates as a closed system with no outflows to the surrounding environment (assuming there is no leakage from the tailings ponds). In order to maintain steady state mass balance, the remaining 78% of inflow must be accounted for. From an operational perspective this outflow is likely "free" recycle water becoming entrained within tailings since the RCW circuit operates as a closed system, with the exception of evaporation. It is also likely that current OSPW stores making up the RCW circuit are increasing in volume as tailings ponds grow in size or new pits are created. I was unable to assess this growth in stored OSPW within our model due to the steady state assumptions. Annual bathymetric surveys would provide more accurate volumes of free water within each tailings management facility and would greatly improve the accuracy of isotope mass balance techniques for the RCW circuit.

When the 2017 E/I isotope mass balance model for the recycle pond was implemented over three distinct periods (May-June, July-Aug, Sept-Oct) the mean E/I ratios were found to be the highest in May-June (0.22) and lowest in July-Aug (0.06). May-June also displayed the best agreement (36% relative percent difference) of E/I ratios calculated independently using ^{18}O and ^{2}H, while July-Aug had the worst agreement (67% relative percent difference). Intuitively, it should be expected that the prime summer months (July-Aug) would exhibit the highest evaporation. However, the E/I model works by estimating evaporation through the observed degree of enrichment away from the total input signature. Within our model I used a new integrated total input signature for each period. For the case of Jul-Aug, there was the smallest difference in the total input signature and most isotopically enriched samples collected from the recycle pond and therefore the smallest E/I ratio. Based on this observation, the model is likely best implemented over the entire open water period rather than at smaller time scales. A more accurate form of the model could likely be developed with observations of changes in free water storage from the tailings ponds/RCW circuit.

SCL was unable to provide surface water temperatures for the recycle pond and tailings ponds. As a result, relative humidity could not be normalized to the surface water temperature for use in the C-G model to predict δ_E and calculations of periodic kinetic enrichment factors. This is not uncommon in isotope mass balance studies due to difficulties in collecting such data (Horita et al., 2008). Nevertheless, this can become an

issue in highly seasonal climates when the average of climate parameters is being used. In this case, some daily occurrences of relative humidity near 100% and air temperatures near or below 0°C (common scenarios in late September and October), are likely causing inaccurate representation of the fractionation occurring—primarily in ^{2}H.

4.5.2 BML isotope mass balance models

The observed isotopic composition of BML was found to be similar to the isotopic composition of the RCW circuit despite the mixing of imported freshwater from BCR to BML. Annual mean E/I ratios calculated at BML were 0.11 to 0.18, which is similar to the range of 0.11 to 0.22 from the RCW circuit. These concurrent ranges may indicate that similar physical or chemical processes associated with the storage and management of tailings (*e.g.* evolution of chemical composition or bitumen mats persisting at the water surface) are influencing the evaporation rates within the tailings ponds and the end pit lake. The restriction of surface evaporation by bitumen mats on the surface of both BML and tailings ponds could explain the low rates of evaporation predicted by the E/I ratios.

The annual mean evaporation rates calculated from BML using the isotope mass balance model differed by 6% to 36% when compared to the Penman combination method and 1% to 57% when compared to eddy covariance.

Here I note that the annual cumulative sums of the evaporation rates calculated over each sampling interval appear to be a good estimate of *E* when compared to the Penman and eddy covariance methods. However, the actual evaporation rates calculated between each sampling interval fluctuate over a large range as shown in *Fig. 4.10*, including many periods of large negative evaporation rates. Many of these period specific evaporation rates do not make sense based on the measured physical water balance parameters.

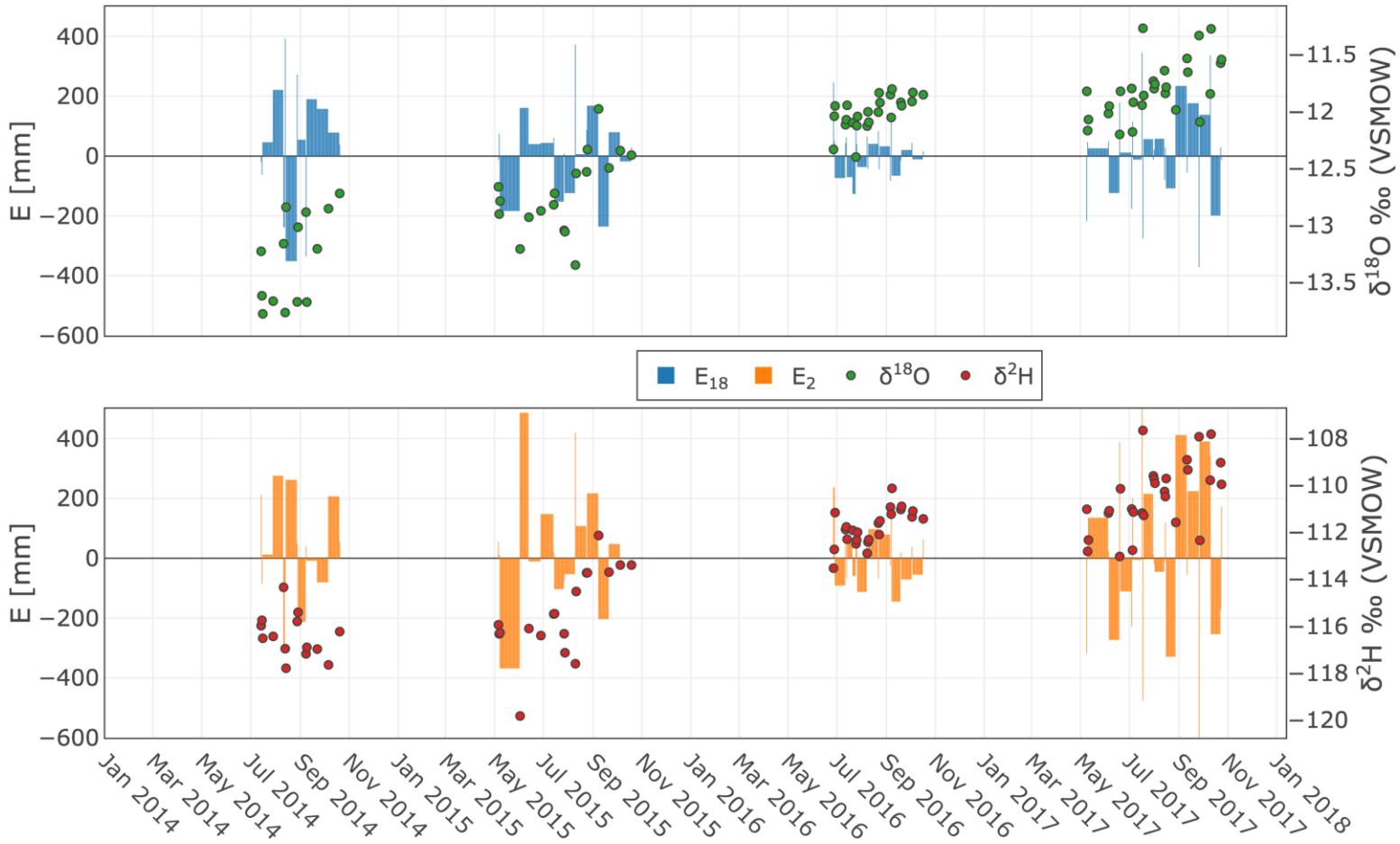

Figure 4.10 Evaporation at BML calculated at each time interval using the non steady state isotope mass balance. Bars represent the total evaporation between each interval and circles are the observed isotopic signatures. Only samples collected between May and October inclusively were used for calculations. E_{18} and E_2 represent evaporation rates calculated with each respective tracer.

There are intervals within the observations where the isotopic signature of the samples collected from BML experience depletion rather than enrichment during the open water period. If the water balance parameters provided do not accurately capture a mixing scenario that would cause this depletion, then the model will return a negative evaporation value to maintain mass balance.

The BML seasonality prediction model was used to reproduce the observed seasonal and interannual isotopic evolution of BML by implementing daily water balance data to estimate isotopic mixing and fractionation. The model results showed good agreement with the observed isotopic evolution when ^{18}O was used as the tracer, but accuracy decreased with ^{2}H as the tracer. The model also appeared to not accurately capture input of depleted waters during the spring freshet in 2014 and 2017. Observed isotopic depletion in the model is solely a result of mixing processes (*i.e.*, non-fractionating) so when the model is under predicting these portions of the observed data it may indicate errors in the water balance data (*e.g.*, underestimating snowmelt/runoff contributions or pump in volumes from BCR). The model does well matching the observed data for the rest of the time period, following good agreement with the degree of enrichment each year — the main purpose of the model.

The poor performance of ^{2}H as a tracer is consistent with findings reported by Gibson et al., (1996), who found low accuracy when using ^{2}H as an isotope mass balance tracer for short time periods. The study recommended that ^{2}H not be used for intervals of less than 50 days. The magnitude of enrichment during 2014 and 2015 was almost identical during the open water period, with 2015 under-predicting the observed enrichment. In 2016 the model did not match any of the observed data although the slope of enrichment is similar to that of the observed data. In 2017 the model began to match the lower end of the observed isotopic composition, but again the degree of enrichment was not representative of the observed data.

Inaccuracies between the modelled results and observed results when using ^{2}H as a tracer may be due in part to errors associated with the water balance flux measurements—such as inaccurate accounting of isotopic signatures of isolated precipitation events. The underestimation of the observed enrichment of the model may

also have been due to a discrepancy in the calculated atmospheric exchange parameters for ^{18}O and ^{2}H used for the Craig and Gordon linear resistance model, which estimates the fractionation associated with evaporation. The fact that ^{18}O fits well and ^{2}H does not may also be due to an inaccurate representation of ^{2}H fractionation at the boundary layer of air-water surface, possibly as a result of salinity, persisting bitumen molecules, or other chemicals associated with tailings waste.

One example of chemical reactions that may potentially influence the isotopic composition of BML is the influence of methane gas bubbles released from the FFT. Methane (CH_4) is released year-round, but during winter will become trapped below the ice and partially dissolve in the underlying water. Dissolved oxygen (O_2) present under the ice can react with CH_4 and become converted to carbon dioxide (CO_2) via microbial processes, with the C coming from CH_4 and the O coming from O_2. The CO_2 will then incorporate a water molecule via hydration to form carbonic acid (H_2CO_3) in the reaction $CO_2 + H_2O \Rightarrow H_2CO_3$. The pH observed at BML is approximately 8.3. At this level, the H_2CO_3 loses one proton to solution by the following acid dissociation reaction $H_2CO_3 \Rightarrow H^+ + HCO_3^-$. It is possible that there may be fractionation of ^{18}O and/ or ^{2}H during this process influencing the isotopic signature of BML over the winter period.

The effects of the water chemistry of OSPW on isotope fractionation are beyond the scope of this study — but provide an interesting area for future research.

4.5.3 Comparison of isotope mass balance evaporation rates with Penman combination and eddy covariance

Part of this study was to compare the evaporation fluxes estimated by traditional methods (*i.e.* Penman combination method and eddy covariance towers) with those calculated using isotope mass balance models. As discussed in *Sec. 4.3.3.3* the E/I ratios can only be used to calculate the amount of total inflow to the reservoir lost through evaporation. This is an imporant parameter to quantify from water management perspectives, but the evaporation rates calculated using this method cannot be directly compared with the Penman and EC rates as these represent the total evaporative loss from each system. However, none of the E/I ratios from either the RCW circuit or BML

resulted in evaporative losses greater than those from any other method, which suggests, theoretically, that the model is "working", by returning only the fraction of inflow lost to evaporation rather than total evaporation.

Annual evaporation results from the Penman combination, EC, and isotope mass balance models (Gonfiantini and non-steady state) are presented in *Table. 4.13.* The Penman combination and EC evaporation rates were found to differ from each other by up to 29% interannually.

The Penman combination and EC evaporation rates displayed less variation interannually than the isotope mass balance models from RCW circuit and BML, with the ranges equal to 373 to 460 mm yr^{-1} and 351 to 518 mm yr^{-1} for Penman combination and EC respectively. The high variability in our model results when compared to the Penman and EC results suggests the influence of the ever-changing operational mine water circuit and water management procedures on evaporation rates. It is interesting to note that the EC rates are lower than those estimated using the Penman method for 2014 and 2015 but are higher in 2016 and 2017. It is possible that clarification of the lake by alum dosing in the fall of 2016, as well as ongoing efforts to clean up bitumen mats may be affecting evaporation rates measured by the EC towers.

Table 4.13 Comparison of annual evaporation rates calculated by Penman combination, eddy covariance, Gonfiantini model (RCW and BML), and non-steady isotope mass balance model (BML).

			RCW			BML					
Year	Penman combination	Eddy covariance	Gonfiantini	RPD (Penman)	RPD (Eddy covariance)	isotope mass balance	RPD (Penman)	RPD (Eddy covariance)	Gonfiantini	RPD (Penman)	RPD (Eddy covariance)
Units	[mm yr^{-1}]	[mm yr^{-1}]	[mm yr^{-1}]	[%]	[%]	[mm yr^{-1}]	[%]	[%]	[mm yr^{-1}]	[%]	[%]
2012	513	-	561	9	-	-	-	-	-	-	-
2013	471	-	931	66	-	-	-	-	-	-	-
2014	405	352	757	61	53	382	6	8	651	47	60
2015	460	351	-	-	69	545	17	43	779	52	76
2016	385	518	418	8	50	522	30	1	347	10	40
2017	373	466	892	82	35	259	36	57	700	61	40
Average	434	422	689	50	52	427	22	27	619	42	54

The results of the Gonfiantini models from each system (RCW circuit and BML) displayed good agreement between the two systems, with relative RPDs ranging from 10 to 24 %. These results correspond to similar degrees of seasonal and interannnual isotopic enrichment and depletion since the total enrichment is the basis of this model without considering the influence of inputs to the system. The over-prediction of evaporation by the Gonfiantini model suggests that evaporation is not the only contributor to isotopic enrichment.

Tailings ponds are more dynamic than natural systems, and mining processes such as cooling tower operations, bitumen extraction, and expressed pore water during tailings settlement could also be contributing to overall enrichment of the tailings ponds. Mixing of these process-affected waters with current water stores would need to be further explored and will require a better understanding of volumes associated with these waters. Tailings settlement rates are a large unknown within the water balance of tailings ponds and further work to quantify settlement rates and subsequent volume of expressed porewater would greatly improve the isotope mass balance models.

The Gonfiantini model can be used as a first order approximation of the upper limit of evaporative losses from engineered systems. An isotopic framework can easily be developed by calculating an evaporation line for the mine site using measured atmospheric parameters and limited isotopic data necessary for the Gonfiantini model. Isotopic signatures can then be collected from the various site-wide water bodies and referenced to the evaporation line. Where the samples plot along the evaporation line can be compared to volumetric losses that would result in that degree of enrichment. However, the limitation of the Gonfiantini model is that it attributes all enrichment to evaporation.

4.6 Concluding remarks

This work is a starting point for isotope mass balance techniques to be utilized for estimating evaporation rates from tailings ponds and closure landscapes within the oil sands region. I have expanded upon the initial isotopic characterization work by Baer et al., (2016) and the recent work presented in *Chapter 3*, which characterized the unique isotopic signatures of site-wide mine waters sources and the seasonal and interannual isotopic trends of said waters. I hypothesized that isotope mass balance techniques could

be used to quantify evaporative losses from the RCW circuit based on the observable temporal enrichment of the isotopic signature of the RCW circuit throughout the open water period of each year.

Our application of traditional isotope mass balance techniques that are generally applied to natural systems and applying them to an engineered system (*i.e.* operational mine site) shows potential for an "in-situ" method for estimating evaporation from site-wide water bodies. Our work has shown that such systems may have various factors affecting evaporation rates not found in natural systems (*e.g.* high salinity, bitumen mats, chemicals associated with bitumen extraction). Because traditional methods of estimating evaporation (*e.g.* Penman combination equation and eddy covariance) generally rely on climatic parameters to predict evaporation they may not provide accurate representation of tailings management facilities and closure landscapes that have been built using mining waste.

The forms of the isotope mass balance model implemented within this study were chosen for the RCW circuit based on the data available from Syncrude and findings outlined in *Chapter 3*. E/I ratios were calculated to estimate the amount of input water lost to evaporation from the RCW and BML and were found to be in agreement with previous studies of natural lakes performed within the region.

Quantifying evaporative losses would be useful at the industry level for site wide water management purposes. Better understanding of water losses across the site will lead to more efficient water usage and import for operational purposes. Predicting the amount of water gained and stored on site allows for better design of management facilities as well. The E/I model requires an accurate understanding of the volumes of input waters to the system. This study was not able to obtain high quality data for these parameters and therefore the methods and results of the model should be interpreted as a proof of concept, as there is likely large error in the calculations associated with the volumes of the input parameters.

The Base Mine Lake non steady state isotope mass balance model and seasonality predictive model demonstrate how isotope mass balance models can be implemented with high frequency water balance data. Evaporation rates from the non steady state isotope mass balance model were in good agreement with those predicted by the Penman

and EC methods. However, there was a large variation of calculated evaporation rates between each time interval that would need to be further explored to fully develop the method for industry use. ^{18}O appears to be a more accurate tracer than ^{2}H based on the results of the seasonality predictive model, these findings are in agreement with a previous study performed by Gibson et al., (1996).

The historic effects of mining processes appear to be preserved in the isotopic signature of fluid tailings. Based on the results of the isotope mass balance models it appears that pore water released from tailings settlement may be acting as a buffer to meteoric water inputs to the RCW circuit and BML, but also contributing to the overall temporal enrichment. Future work should be conducted to further understanding of the influence of tailings pore water on the overall isotopic composition of site-wide water bodies. There is the opportunity to quantify the effects of fluid tailings settlement through winter monitoring of isotopic compositions of the RCW circuit and BML when they are ice covered and evaporative enrichment is not occuring.

4.7 References

Allison, G. B., & Leaney, F. W. (1982). Estimation of isotopic exchange parameters, using constant-feed pans. *Journal of Hydrology*, *55*, 151-161.

Baer, T., Barbour, S. L., & Gibson, J. J. (2016). The stable isotopes of site wide waters at an oil sands mine in northern Alberta, Canada. *Journal of Hydrology*, *541*, 1155-1164.

Barbour, S. L., Hendry, M. J., & Carey, S. K. (2016). High-resolution profiling of the stable isotopes of water in unsaturated coal waste rock. *Journal of Hydrology*, *534*, 616-629.

Bastrikov, V., Steen-Larsen, H. C., Masson-Delmotte, V., Gribanov, K., Cattani, O., Jouzel, J., & Zakharov, V. (2014). Continuous measurements of atmospheric water vapour isotopes in western Siberia (Kourovka). *Atmospheric Measurement Techniques*, *7*(6), 1763-1776.

Bennett, K. E., Gibson, J. J., & McEachern, P. M. (2008). Water-yield estimates for critical loadings assessment: comparisons of gauging methods versus an isotopic approach. *Canadian Journal of Fisheries and Aquatic Sciences*, *65*(1), 83-99.

Craig, H. (1961). Isotopic variations in meteoric waters. *Science*, *133*(3465), 1702-1703.

Craig, H., & Gordon, L.I. (1965). Deuterium and oxygen 18 variations in the ocean and marine atmosphere. In *Stable Isotopes in Oceanographic Studies and Paleotemperatures,* E. Tongiorgi (Ed.) pp. 9-130, Laboratorio di Geologia Nucleare, Pisa.

Coplen, T. B. (1996). New guidelines for reporting stable hydrogen, carbon, and oxygen isotope-ratio data. *Geochimica et Cosmochimica Acta*, *60*(17), 3359-3360.

COSIA Water EPA (2019). 2018 Water Research Report. Canada's Oil Sands Innovation Alliance. https://www.cosia.ca/sites/default/files/attachments/COSIA%20Annual%20Report%202018_WATER_FINAL%20Nov%2021_0.pdf

Dansgaard, W. (1964). Stable isotopes in precipitation. *Tellus*, *16*(4), 436-468.

Dincer, T. (1968). The use of oxygen 18 and deuterium concentrations in the water balance of lakes. *Water Resources Research*, *4*(6), 1289-1306.

Dompierre, K. A., & Barbour, S. L. (2016a). Characterization of physical mass transport through oil sands fluid fine tailings in an end pit lake: a multi-tracer study. *Journal of contaminant hydrology*, *189*, 12-26.

Dompierre, K. A., Barbour, S. L., North, R. L., Carey, S. K., & Lindsay, M. B. (2017). Chemical mass transport between fluid fine tailings and the overlying water cover of an oil sands end pit lake. *Water Resources Research*, *53*(6), 4725-4740.

Gammons, C. H., Duaime, T. E., Parker, S. R., Poulson, S. R., & Kennelly, P. (2010). Geochemistry and stable isotope investigation of acid mine drainage associated with abandoned coal mines in central Montana, USA. *Chemical Geology*, *269*(1-2), 100-112.

Gat, J. R., & Levy, Y. (1978). Isotope hydrology of inland sabkhas in the Bardawil area, Sinai. *Limnology and Oceanography*, *23*(5), 841-850.

Gibson, J, Edwards, TWD, & Prowse, T. (1996). Development and validation of an isotopic method for estimating lake evaporation. Hydrological Processes, 10(10), 1369-1382.

Gibson, J. J., Edwards, T. W. D., Bursey, G. G., & Prowse, T. D. (1993). Estimating Evaporation Using Stable Isotopes: Quantitative Results and Sensitivity Analysis for Two Catchments in Northern Canada: Paper presented at the 9th Northern Res. Basin Symposium/Workshop (Whitehorse/Dawson/Inuvik, Canada-August 1992). *Hydrology Research*, *24*(2-3), 79-94.

Gibson, J. J., Reid, R., & Spence, C. (1998). A six-year isotopic record of lake evaporation at a mine site in the Canadian subarctic: results and validation. *Hydrological Processes*, *12*(10-11), 1779-1792.

Gibson, J. J. (2002). Short-term evaporation and water budget comparisons in shallow Arctic lakes using non-steady isotope mass balance. *Journal of Hydrology*, *264*(1-4), 242-261.

Gibson, J. J., & Edwards, T. W. D. (2002). Regional water balance trends and evaporation-transpiration partitioning from a stable isotope survey of lakes in northern Canada. *Global Biogeochemical Cycles*, *16*(2), 10-1.

Gibson, J. J. (2002). A new conceptual model for predicting isotopic enrichment of lakes in seasonal climates. *Pages News*, *10*(2), 10-11.

Gibson, J. J., Birks, S. J., Moncur, M., Yi, Y., Tattrie, K., Jasechko, S., ... & Eby, P. (2011). Isotopic and geochemical tracers for fingerprinting process-affected waters in the oil sands industry: A pilot study. *Oil Sands Research and Information Network*, 1-120.

Gibson, J. J., & Reid, R. (2014). Water balance along a chain of tundra lakes: A 20-year isotopic perspective. *Journal of Hydrology*, *519*, 2148-2164.

Gibson, J. J., Birks, S. J., Yi, Y., & Vitt, D. (2015). Runoff to boreal lakes linked to land cover, watershed morphology and permafrost thaw: a 9-year isotope mass balance assessment. *Hydrological Processes*, *29*(18), 3848-3861.

Gibson, J. J., Birks, S. J., Yi, Y., Moncur, M. C., & McEachern, P. M. (2016a). Stable isotope mass balance of fifty lakes in central Alberta: Assessing the role of water balance parameters in determining trophic status and lake level. *Journal of Hydrology: Regional Studies*, *6*, 13-25.

Gibson, J. J., Birks, S. J., & Yi, Y. (2016b). Stable isotope mass balance of lakes: a contemporary perspective. *Quaternary Science Reviews*, *131*, 316-328.

Gibson, J. J., Yi, Y., & Birks, S. J. (2016c). Isotope-based partitioning of streamflow in the oil sands region, northern Alberta: Towards a monitoring strategy for assessing flow sources and water quality controls. *Journal of Hydrology: Regional Studies*, *5*, 131-148.

Ghomshei, M. M., & Allen, D. M. (2000). Hydrochemical and stable isotope assessment of tailings pond leakage, Nickel Plate Mine, British Columbia. *Environmental Geology*, *39*(8).

Gonfiantini, R. (1986). Environmental isotopes in lake studies. *Handbook of environmental isotope geochemistry*, *2*, 113-168.

Hilderman, J. (2011). Net percolation as a function of topographic variation in a reclamation cover over a saline-sodic overburdern dump. M, Sc. Thesis Department

Civil, Geological, and Environmental Engineering. University of Saskatchewan, Saskatoon, Saskatchewan.

Horita, J., Rozanski, K., & Cohen, S. (2008). Isotope effects in the evaporation of water: a status report of the Craig–Gordon model. *Isotopes in environmental and health studies*, *44*(1), 23-49.

Horita, J., & Wesolowski, D. J. (1994). Liquid-vapor fractionation of oxygen and hydrogen isotopes of water from the freezing to the critical temperature. *Geochimica et Cosmochimica Acta*, *58*(16), 3425-3437.

Huang, M., Hilderman, J. N., & Barbour, L. (2015). Transport of stable isotopes of water and sulphate within reclaimed oil sands saline–sodic mine overburden. *Journal of Hydrology*, *529*, 1550-1561.

Ingraham, N. L., Johnson, R. J., & Broadbent, R. (1994). Facility-altered stable isotopic ratios of power generation cooling wastewater: opportunity for tracing leakages. *Environmental science & technology*, *28*(11), 1983-1986.

Lawrence, G. A., Tedford, E. W., & Pieters, R. (2015). Suspended solids in an end pit lake: potential mixing mechanisms. *Canadian Journal of Civil Engineering*, *43*(3), 211-217.

Majoube, M. (1971). Oxygen-18 and deuterium fractionation between water and steam (in French). *Journal de Chimie Physique et de Physico-Chimie Biologique*, *68*, 1423-1436.

McMahon, T. A., Peel, M. C., Lowe, L., Srikanthan, R., & McVicar, T. R. (2013). Estimating actual, potential, reference crop and pan evaporation using standard meteorological data: a pragmatic synthesis. *Hydrology and Earth System Sciences*, *17*(4), 1331-1363.

McMahon, T. A., Finlayson, B. L., & Peel, M. C. (2016). Historical developments of models for estimating evaporation using standard meteorological data. *Wiley Interdisciplinary Reviews: Water*, *3*(6), 788-818.

Risacher, F. F., Morris, P. K., Arriaga, D., Goad, C., Nelson, T. C., Slater, G. F., & Warren, L. A. (2018). The interplay of methane and ammonia as key oxygen consuming constituents in early stage development of Base Mine Lake, the first demonstration oil sands pit lake. *Applied Geochemistry*, *93*, 49-59.

Tedford, E., Pieters, R., & Lawrence, G. Under ice processes in Base Mine Lake. In *Citation for published version: Wain, D & Bryant, L (eds) 2016, Proceedings of the 19th International Workshop on Physical Processes in Natural Waters: PPNW2016, Bath, UK, 12-15 July 2016. Department of Architecture and Civil Engineering, University of Bath, Bath, UK.* (p. 86).

Tondu, J. M. E., Turner, K. W., Wolfe, B. B., Hall, R. I., Edwards, T. W. D., & McDonald, I. (2013). Using water isotope tracers to develop the hydrological component of a long-term aquatic ecosystem monitoring program for a northern lake-rich landscape. *Arctic, antarctic, and alpine research*, *45*(4), 594-614.

Turner, K. W., Wolfe, B. B., & Edwards, T. W. (2010). Characterizing the role of hydrological processes on lake water balances in the Old Crow Flats, Yukon Territory, Canada, using water isotope tracers. *Journal of Hydrology*, *386*(1-4), 103-117.

Turner, K. W., Wolfe, B. B., Edwards, T. W., Lantz, T. C., Hall, R. I., & Larocque, G. (2014). Controls on water balance of shallow thermokarst lakes and their relations with catchment characteristics: a multi-year, landscape-scale assessment based

on water isotope tracers and remote sensing in Old Crow Flats, Yukon (Canada). *Global change biology*, *20*(5), 1585-1603.

Welhan, J. A., & Fritz, P. (1977). Evaporation pan isotopic behavior as an index of isotopic evaporation conditions. *Geochimica et Cosmochimica Acta*, *41*(5), 682-686.

Zimmermann, U., & Ehhalt, D. H. (1970). Stable isotopes in study of water balance of Lake Neusiedl, Austria. *Isotope hydrology*, 129-138.

Zuber, A. (1983). On the environmental isotope method for determining the water balance components of some lakes. *Journal of Hydrology*, *61*(4), 409-427.

4.8 Appendix A

Table A4.1 Individual tailings pond surface areas of the RCW circuit (provided by Syncrude)

SCL Tailings Pond ID	Fluid Pond Surface Area
	(km^2)
East In-Pit (EIP)	1.1
Mildred Lake Settling Basin (MLSB)	5.7
Base Mine Lake (BML)*	7.8
Southwest In-Pit (SWIP)	3.4
Southwest Sand Storage Facility (SWSS)	14.9
North Mine South Pond East (NMSP-E)	1.5
North Mine South Pond West (NMSP-W)	2

*BML not included in total RCW circuit surface area

Chapter 5: Conclusions and recommendations

The rapid development of the northern Alberta oil sands region over the past several decades has led to environmental concerns surrounding water demands in support of operations, and the future planning of remediation and/ or disposal of the massive inventory of oil sands process affected waters (OSPW) currently being stored. For example, Syncrude Canada Ltd. (SCL) currently requires the import of 2 m^3 of freshwater for every 1 m^3 of crude oil produced. No policy exists for the treatment and release of oil sands process affected water to the surrounding environment, which has led to the storage of 1.7 Gm^3 of OSPW since the start of operations over 40 years ago. In an effort to mitigate imported water demands, SCL operates a recycle water (RCW) circuit that supplies approximately 80% of water demands for mining operations through the reuse of 200 Mm^3 of OSPW annually. These volumes highlight the importance of improving both water use efficiency and the accuracy of quantifying water balance parameters of site wide waters.

The purpose of this work was to demonstrate the use of stable isotopes of water (^{18}O and ^{2}H) as tracers to provide new techniques for improving management and usage of site wide waters at an oil sands mine site, as well as future planning for remediation and release of OSPW to the surrounding environment following mine closure. In order to accomplish this work, I first developed a high frequency isotope-sampling program of site wide waters that built upon the initial sampling program conducted by Baer et al., (2016). These data were used to characterize the seasonal and interannual patterns observed within the RCW circuit. Following the characterization of temporal isotopic signatures of the RCW, I applied isotope mixing and mass balance models using ^{18}O and ^{2}H as tracers to assess the impacts of varying water balance parameters contributing to the observed trends. Isotope mass balance models were specifically developed to quantify evaporative flux, the primary mechanism for water loss from the RCW circuit. Two isotope mass balance models were also developed specifically for Base Mine Lake (BML), the first end pit lake within the oil sands region. Both models were paired with daily water balance data collected as part of ongoing studies at BML. I showed the ability of ^{18}O and ^{2}H to provide insight on mining operations such as efficiency of cooling

towers and tailings management, and water management such as evaporative loss from the RCW circuit and inputs of meteoric water volumes to the RCW circuit. I also provided a model utilizing isotope tracers to assess the accuracy of water balance flux measurements of a closure landscape.

Our conclusions are in two parts. Part one (*Chapter 3*) of this study undertook a characterization of the OSPW signature of the RCW circuit including seasonal and interannual patterns. An in-depth analysis of potential mechanisms contributing to the isotopic signature of the RCW circuit was conducted to explain this unique signature. Seasonal depletion associated with the spring freshet and systematic enrichment throughout the open water season was observed within the RCW circuit. On an interannual scale the RCW circuit appears to be in an isotopic steady state, with consistent degrees of depletion and enrichment between years. I found that new mechanisms not previously assessed within the literature are also contributing to the isotopic evolution of the RCW circuit such as expressed pore water from fluid tailings settlement and fractionation during ice formation, in addition to cooling tower blowdown and open water evaporation initially proposed by Baer et al., (2016).

Part two of this study (*Chapter 4*) adapted isotope mass balance techniques frequently used to assess the water balance of natural bodies of water (*e.g.,* lakes and ponds) within isotope hydrology literature. Two primary isotope mass balance models were used to assess evaporative losses from the RCW circuit and compared to evaporation rates estimated by the Penman combination equation and eddy covariance (EC) towers.

The first isotope mass balance model was used to calculate the ratio of inflow to a reservoir lost as evaporation (E/I ratio). Within the literature this method relies on the assumption that the mean-weighted isotopic signature of precipitation, often estimated as the intersection between the local evaporation line and the local meteoric water line, is an accurate estimation of total inflow signature to the reservoir. Although this may hold true for most natural systems, it does not apply to an engineered system such as the RCW circuit that experiences inflows from various sources (*e.g.,* cooling tower blowdown, expressed pore water, and river import) in addition to meteoric water. Therefore, I calculated mean flux-weighted inflow signatures based on observed isotopic signatures of

inflow waters and estimates of corresponding volumes based on insight provided by SCL personnel. Average E/I ratios ranged from 0.11 to 0.22 and were found to be on the low end of those calculated from studies performed within the region (Gibson and Reid, 2014; Gibson et al., 2016). These ratios are characteristic of systems with high throughflow and low residence time (Bennet et al., 2008; Gibson et al., 2002), which accurately describes the RCW circuit.

The second isotope mass balance model was based on work done by Gonfiantini (1986), which estimates the fraction of a body of water lost to evaporation based on minimum and maximum observed isotopic signatures. This method does not account for isotopic changes associated with inflows or outflows and attributes all enrichment to evaporation. Annual evaporation rates calculated from the RCW circuit ranged from 418 to 931 mm yr^{-1} over a five-year period. The evaporation rates were higher than those predicted by the Penman combination equation and EC towers. These findings agree with our observations that other mechanisms are influencing the enrichment of the RCW circuit in addition to evaporative enrichment.

Part two also included an isotopic assessment of BML. Seasonal enrichment of BML was found to be highly muted when compared to the isotopic composition of Beaver Creek Reservoir, which is used to supply freshwater to BML. This muted enrichment is attributed to the buffering of the BML isotopic signature by expressed fluid tailings pore water. BML was also observed to be systematically enriching interannually based on samples collected from 2014-2017. A non steady state isotope mass balance model was developed based on daily water balance data available and isotopic signatures of water balance fluxes either directly measured or modelled. The model was used to calculate the evaporative flux associated with isotopic shifts occurring between the time intervals of each isotopic observation at BML. The annual sums of the interval evaporation rates were found to be in good agreement with those predicted by the Penman combination and EC methods over a four-year period, with the exception of 2014. The non steady state isotope mass balance model was also adapted to predict the isotopic signature of BML based on daily water balance fluxes. The model found good agreement when ^{18}O was used as a tracer, but accuracy decreased when ^{2}H was the tracer, which is consistent with results found by Gibson et al., (1996).

Several specific opportunities for future research relating to the application of stable isotopes of water as tracers at oil sands mine sites arose throughout the course of this research. Within *Chapter 3* I proposed a model for using ^{18}O and ^{2}H to assess the efficiency of cooling towers. The model used a closed-system fractionation relationship between fraction of water lost as evaporation and the isotopic signature of blowdown. This relationship was used to correlate the observed isotopic signatures of cooling tower blowdown with cycles of concentration (COC), a parameter currently used by SCL to monitor efficiency of cooling towers. The findings of the model demonstrated that evaporative fractionation occurring within the cooling towers is largely controlled by internal operating conditions (*i.e.*, temperature and humidity) and may be influenced by climatic parameters on site. The relationship between COC and isotopic signatures of blowdown could be improved with monitoring of the internal conditions reflecting the shifts associated with climatic seasonality.

Pore water expressed during tailings settlement was identified as a key mechanism influencing the evolution of the isotopic signature at both the RCW circuit and BML. Therefore, future work to assess the contribution of tailings pore water on the RCW circuit could greatly improve isotope mass balance models for estimating evaporation. It is difficult to assess the contribution of pore water during the open water period when evaporation is influencing isotopic enrichment of the tailings ponds. However, assessments performed during the winter when evaporation is shut down due to ice cover may provide opportunity to better quantify the influence of isotopic tailings pore water compositions on the overall OSPW signature. This ice-covered scenario could then be used to provide crucial estimates of tailings settlement rates if the volume of expressed porewater was calculated using isotope mass balance modelling. Tailings settlement rates within the RCW circuit are not well quantified and could not be provided by SCL for the purpose of this study.

Stable isotopes of O and H are treated as near ideal tracers for hydrologic studies based on their conservative nature and resistance to biogeochemical mechanisms affecting fractionation at near surface conditions. However, our assessment at BML suggests isotopic evolution may be influenced by the chemical composition of OSPW. One such process may be the influence of ^{2}H fractionation during the production of CO_2

from methane released from fluid fine tailings. The influence of the chemical composition and reactions occurring within OSPW on isotopic fractionation provides an interesting area of future research.

Based on a review of current literature this study provides the first application of isotope mass balance modelling techniques at an oil sands mine site, including the first characterization of seasonal and interannual evolution of isotopic signatures of an operational recycle water circuit at an oil sands mine site. Within the work I define primary mechanisms contributing to the evolution of the isotopic signature of the RCW circuit not previously defined within the literature. Overall, this work provides the foundation for the development of isotope tracer techniques to be developed for industry applications as additional tools for monitoring the water balance of site wide waters. The work is also useful for tracking the evolution of closure landscapes, such as end pit lakes, as they transition from process-affect waters to freshwater chemical compositions.

5.1 References

Baer, T., Barbour, S. L., & Gibson, J. J. (2016). The stable isotopes of site wide waters at an oil sands mine in northern Alberta, Canada. *Journal of Hydrology*, *541*, 1155-1164.

Bennett, K. E., Gibson, J. J., & McEachern, P. M. (2008). Water-yield estimates for critical loadings assessment: comparisons of gauging methods versus an isotopic approach. *Canadian Journal of Fisheries and Aquatic Sciences*, *65*(1), 83-99.

Gibson, J, Edwards, TWD, & Prowse, T. (1996). Development and validation of an isotopic method for estimating lake evaporation. Hydrological Processes, 10(10), 1369-1382.

Gibson, J. J. (2002). Short-term evaporation and water budget comparisons in shallow Arctic lakes using non-steady isotope mass balance. *Journal of Hydrology*, *264*(1-4), 242-261.

Gibson, J. J., & Reid, R. (2014). Water balance along a chain of tundra lakes: A 20-year isotopic perspective. Journal of Hydrology, 519, 2148-2164.

Gibson, J. J., Birks, S. J., Yi, Y., Moncur, M. C., & McEachern, P. M. (2016). Stable isotope mass balance of fifty lakes in central Alberta: Assessing the role of water balance parameters in determining trophic status and lake level. Journal of Hydrology: Regional Studies, 6, 13-25.

Gonfiantini, R. (1986). Environmental isotopes in lake studies. *Handbook of environmental isotope geochemistry*, *2*, 113-168.